Supplementary Information

Highly multiplexed profiling of single-cell effector functions reveals deep functional heterogeneity in response to pathogenic ligands

Yao Lu[1,8], Qiong Xue[1,8], Markus R. Eisele[1,2], Endah Sulistijo[1], Kara Brower[3], Lin Han[1], El-ad David Amir[4], Dana Pe'er[4], Kathryn Miller-Jensen[1,5,6 *] & Rong Fan[1,6,7 *]

[1] Department of Biomedical Engineering, Yale University, New Haven, CT 06520, USA
[2] Institute for System Dynamics, University of Stuttgart, Stuttgart, Germany
[3] Isoplexis, New Haven, CT 06511, USA
[4] Department of Biological Sciences, Columbia University, New York, New York, USA.
[5] Department of Molecular, Cellular and Developmental Biology, Yale University, New Haven, CT 06520, USA
[6] Yale Comprehensive Cancer Center, New Haven, CT 06520, USA
[7] Yale Stem Cell Center, Yale School of Medicine, New Haven, CT 06520, USA
[8] These authors contributed equally to this work.

All correspondence should be addressed to KMJ (kathryn.miller-jensen@yale.edu) and RF (rong.fan@yale.edu)

List of Supporting Information Documents

Fig. S1 . **Microchamber array chip.** **a**, Picture of the assembly of a complete single cell secretomic analysis device. **b**, Specifications of the microchamber array chip. It indicates the number of microchambers per chip and the dimensions of microchambers. **c**. Stitched phase contrast image showing the while microchip and the select region with a block of microchambers loaded with U937-derived macrophage cells.

Fig. S2 **Antibody barcode chip for 42-plex protein detection in single cells. a.** Representative scanned image with three colors showing protein detection with the antibody barcode array. **b**, Scanned fluorescence images showing three channels (blue, green and red) separately. **c**, Organization of 42 antibodies used in this study: For detection antibodies, 42 antibodies are categorized into 3 equal groups based on their detection colors: 488blue, 532green, 635red (biotin conjugated, to react with streptavidin APC for red color detection). For

Fig. S3 Spectral compensation between blue (Alexa fluor 488) and green (Alexa fluor 532) channels. a, Alexa fluor 488 conjugate was spotted onto poly-l-lysine glass slide and imaged with the microarray scanner using both blue and green channels. Due to spectral overlap between Alexa fluor 488 and 532 dyes, fluorescence signals in both blue channel (real signal) and green channel (crosstalk) would be detected. The blue channel signal and green channel signal showed consistent correlation between each other (R=99%) and compensation equation can thus be extracted; **b**; correlation between real signal from 532 channel and overlap from 488 channel for Alexa fluor 532 conjugate. Similarly, Alexa fluor 532 was spotted on a glass slide and imaged with both channels to quantify spectral overlap and describe the compensation equation. The algorithms were initially designed for spectral overlap compensation in multicolore flow cytometric analysis.

Fig. S4 Standard titration curves for all proteins. The titration curves were obtained using recombinant proteins. These curves have been fit with a 4PL curve, which is standard for ELISA. Fluorescence intensity represents the original photon counts averaged from 16 spots for each protein.

Fig. S5 Cross-reactivity check for all proteins. Most of the antibodies used in this study are monoclonal antibodies to ensure good specificity and reduced cross reactivity. The test was conducted by spiking a single antigen (recombinant protein) in a solution applied to a full capture antibody microarray containing all 42 capture antibodies, followed by detection with a mixture of all detection Abs. Some antibodies showed relatively weak signals such as MMP-2, IL-29, which are probably caused by low reactivity of recombinant proteins.

Fig. S6 Flow chart depicting the procedure and timeline for preparing U937 derived macrophages and performing single-cell protein secretion profiling. The differentiation was conducted in a conventional cell culture dish. The differentiated cells were the trypsinized and resuspended to prepare for single-cell secretion assay. Single-cell suspension was devised into two portions. One was direct loaded to microchip and the other was added with LPS to inducate TLR4 activation, which is a well characterized process and results in the secretion of a large panel of cytokines. Thus, it serves as an excellent model system to test the new technology platform – single-cell, 42-plex protein secretion profiling.

Fig. S7 Surface antigen expression confirms successful differentiation of U937 monocytes to macrophages. There scatter plots show flow cytometric analysis of cell surface markers CD11b and CD14 in the U937 cells treated by PMA (50 ng/mL) for 48 hr.

Fig. S8 Population level protein secretion profile. Protein secretion was measured on U937 derived macrophage cells at the population level using a conventional micro titer plate (cell density ~10^6/mL). Both non-stimulated and LPS stimulated cells were measured.

Fig. S9 Vertical scatter plots showing cytokine secretion levels and frequency in all single cells and for all protein measured. It includes complete single-cell cytokine vertical scatter plots showing in Fig. 2B. The plots compare single-cell protein secretion at the basal level (blue dots) and upon LPS stimulation (red dots). The dashed line marks the “gate” defined as (zero-cell data average + 2 STDV). The data were shifted vertically to match the “gates” obtained from two microchips.

Fig. S10 Comparison between the microchip data and the flow cytometric ICS data. The major secreted proteins identified by single-cell microchip experiments were measured using both methods. The raw data for fraction of cytokine-secreting cells in both basal and LPS stimulated cells was compared. The correlation between ICS and our assay is moderate due to several reasons. (1) The microchip assay measures the amount of protein secreted by a cell, whereas ICS measures the protein synthesized but trapped inside a cell, representing a different biological process. (2) We used a sandwich immunoassay, which requires two different epitopes of a protein being recognized to give rise to a positive signal and thus provides higher or more stringent specificity than intracellular staining. (3) Our microchip assay eliminates paracrine-induced amplification of protein secretion all the way in the beginning, which is different from the standard ICS assay. Thus, detection threshold for a protein secreting cell differs substantially using these two methods. However, we observed that the response to LPS stimulation measured by the increase in the fraction of cells secreting a given cytokine exhibits good correlation between the two methods (Fig. 2d).

Fig. S11 Cell viability assay. The cells were stained with Calcein AM (Life technologies, USA) before loading into PDMS microwells. Then they were imaged at 0, 4, 8, 12and 19hr. One column was randomly chosen and quantified (220 microchannels, around 350 cells in total). The cells showing positive green fluorescence signal were scored as viable. The result showed that 90% of the cells were still alive after 19 hr incubation.. Considering the dye may be toxic to cells and cells were imaged at non-tissue culture environment for 1 hr in each imaging (5 hr in total), the cell viability is estimated higher than 90%.

Fig. S12 Cell hypoxia assay. Hypoxia test of U937 macrophage cells after 24 hr incubation in enclosed PDMS microwells with hypoxia fluorescence probe LOX-1 (SCIVAX, USA). The results showed that less than 1 % (2 cells positive out of 351 cells) of cells enclosed showed positive with hypoxia fluorescence dye, which indicates excellent oxygen permeability of PDMS can ensure cells be cultured in normoxia condition all through single cell experiment.

Fig. S13 Effect of substrate mechanical property on protein secretion. Comparison of U937 populational protein secretion profiles cultured on the polystyrene surface in a 96 well plate vs. a standard PDMS elastomer surface (prepolymer:initiator = 10:1). PDMS is nontoxic, biocompatible, transparent elastomer and has been widely used in biological and biomedical research. Polystyrene is a routine material used in conventional well pate experiment. The results indicate the U937 macrophage cells exhibited very similar protein secretion patterns and intensity on both substrates. The protein secretion profiles measured in cells cultured on two different substrates showed highly correlated with each ($R>0.99$ and 0.94 in basal and LPS stimulated protein secretion tests, respectively)..

Fig. S14. Heatmap showing MIF-secreting population is largely anti-correlated with proinflammatory cytokine-secreting populations. The plot is from the data shown in Figure 2a and apparently MIF is anti-correlated with LPS activation.

Fig. S15. viSNE maps showing the high-dimensional clustering of single cells (U937-derived macrophages) at the basal level and stimulated with different TLR ligands. It shows viSNE structure maps for U937 derived macrophage cells at the basal state and under the stimulation of different TLR ligands(basal, TLR4 by LPS, TLR1/2 by PAM3, TLR3 by poly IC).

Fig. S16 Protein distribution in the viSNE maps of U937-derived macrophages at the basal level and stimulated with different TLR ligands. Cytokine functions in all subpopulations identified by the viSNE analysis for U937 derived macrophage cells under the stimulation of different TLR ligands (basal, TLR4 by LPS, TLR1/2 by PAM3, TLR3 by poly IC). The figures are arranged in the following sequence: combined (top) vs basal (middle left) vs LPS stimulated (middle right) vs PAM3 stimulated (bottom left) vs poly IC stimulated (bottom right).

Fig. S17 Single-cell polyfunctionality in response to LPS stimulation. It shows poly-functionality analysis of U937 macrophage (control and LPS stimulated), in which a wide variety of single cell poly-functionality was observed and U937 derived macrophage cells showed more poly-functionality upon LPS stimulation.

Figure S18. Correlation analysis indicates increased co-secretion of multiple cytokines in U937-derived macrophages in response to LPS stimulation. Upper panel: basal cells. Lower panel: LPS stimulated cells.

Fig. S19 Heatmap summarizing the frequency (%) of proteins-secreting cells in the whole population. U937-derived macrophage cells at the basal level and the cells stimulated by LPS, PAM3 or polyIC were measured for all 42 cytokines. The frequency of cells secreting a given cytokine is shown as the color intensity.

Fig. S20 Principle Component Analysis of the samples in a triplicate basal vs. LPS treatment experiment. Six independent single-cell protein secretion experiments were conducted on U937-derived macrophages. Three were measured in the basal condition (control_t1, 2, and 3) and three were measured on the macrophage cells treated by LPS for 20 hr.

Fig. S21. viSNE maps for primary macrophage cells derived from a healthy donor. viSNE structure maps showing primary macrophage under the stimulation of different TLR ligands(basal, TLR4 by LPS, TLR2 by PAM3, TLR3 by poly IC).

Fig. S22. Protein distribution in the viSNE maps for primary macrophages derived from a healthy donor. Cytokine functions in all primary macrophage subpopulations identified by the viSNE analysis. U937 derived macrophage under the stimulation of different TLR ligands (basal, TLR4 by LPS, TLR2 by PAM3, TLR3 by poly IC).

Table S1: Summary of antibodies (name, clone, company, catalog) used in this study.

Table S2: List of all proteins (full name and their functions in human physiology) incorporated in the microchip platform.

Table S3: Statistical analysis of protein signals detected from single U937-derived macrophage cells (basal vs LPS stimulation).

a

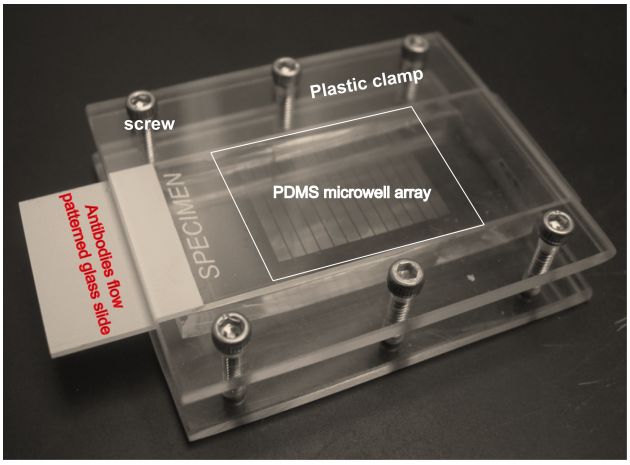

b

Device Design Parameters

- Microarray chamber array area: 2cm x 3cm
- Each block has 426 micro-chambers and 13 Blocks total
- Total number of micro-chambers per chip: 5538
- Microchamber dimensions:
- 20μm x 17μm x 1.8mm (WxHxL)

c

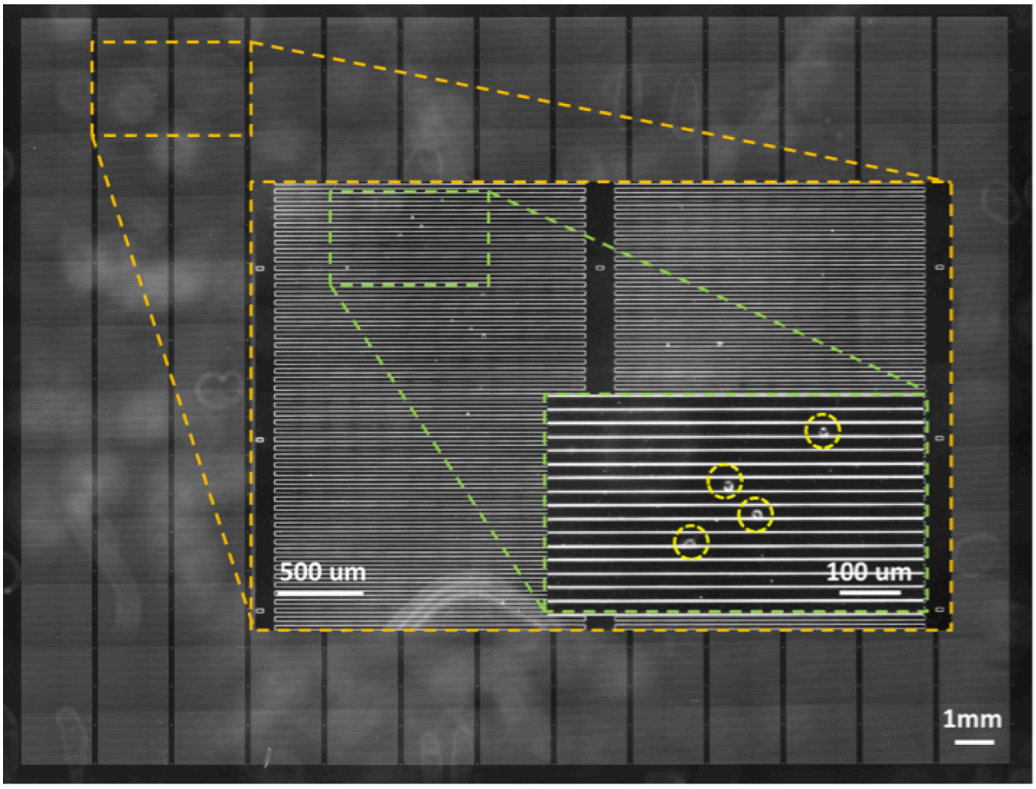

Fig.S1 . **Microchamber array chip.** **a**, Picture of the assembly of a complete single cell secretomic analysis device. **b**, Specifications of the microchamber array chip. It indicates the number of microchambers per chip and the dimensions of microchambers. **c**. Stitched phase contrast image showing the while microchip and the select region with a block of microchambers loaded with U937-derived macrophage cells.

a

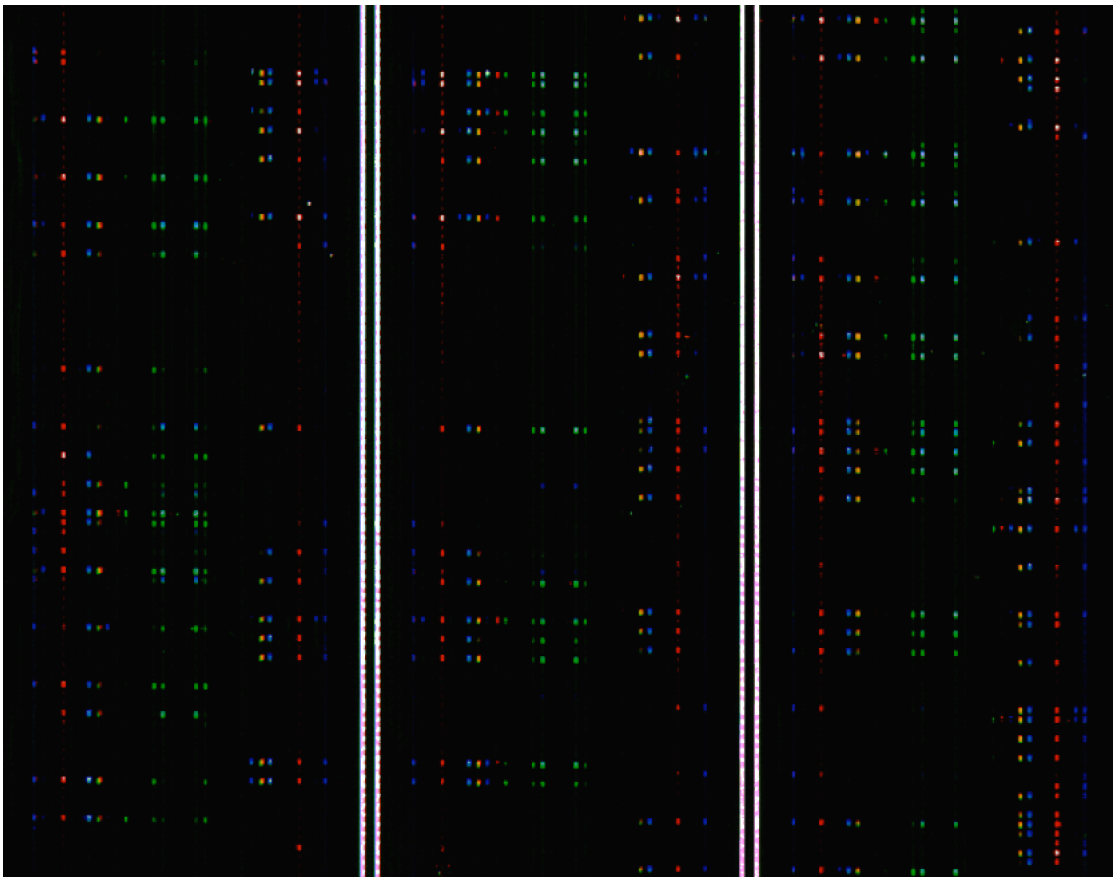

b

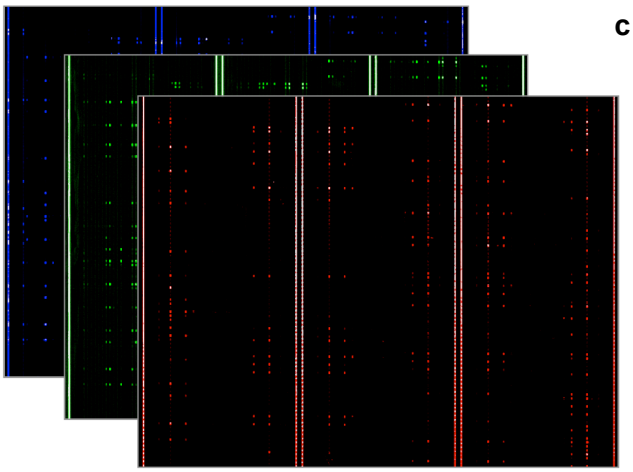

c

Capture \ Detection	488 color	532 color	635 color
1	IL-1a	IL-17A	IL-2
2	IL-1b	MCP-1	MIP-1a
3	IL-3	Rantes	TGF-a
4	IL-4	TNF-a	TGF-b
5	IL-5	TNF-b	G-CSF
6	IL-6	IL-22	IFN-g
7	IL-7	MIP-1b	GMCSF
8	IL-8	SCF	IL-9
9	IL-10	M-CSF	IL-23
0	IL-12	EGF	MMP-2
11	IL-13	HGF	MMP-9
12	IL-15	NGF-b	IL-27
13	IL-1RA	PDGF	IL-29
14	MIF	VEGF	TSLP
15	488-BSA	532-BSA	635-BSA

Fig.S2 Antibody barcode chip for 42-plex protein detection in single cells. a. Representative scanned image with three colors showing protein detection with the antibody barcode array. **b**, Scanned fluorescence images showing three channels (blue, green and red) separately. **c**, Organization of 42 antibodies used in this study: For detection antibodies, 42 antibodies are categorized into 3 equal groups based on their detection colors: 488blue, 532green, 635red (biotin conjugated, to react with streptavidin APC for red color detection). For capture antibodies, they are organized into 14 mixed groups: each has one individual capture antibody corresponding to blue, green, red detection antibodies respectively.

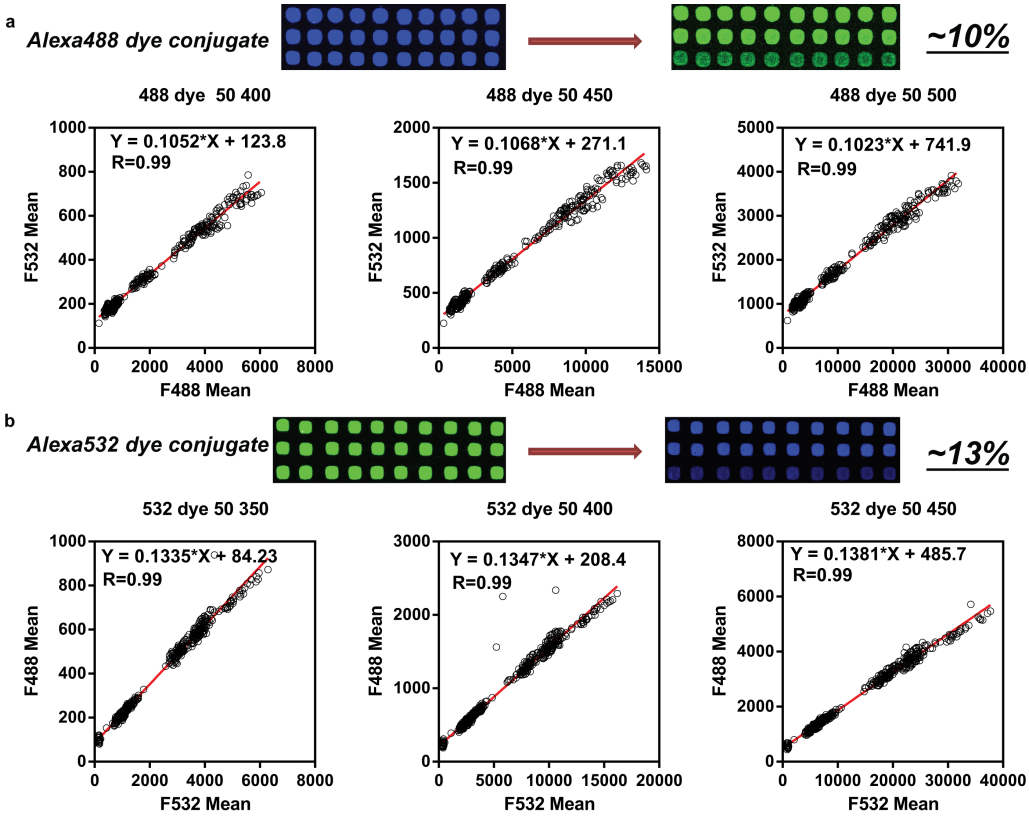

Fig. S3 Spectral compensation between blue (Alexa fluor 488) and green (Alexa fluor 532) channels. a, Alexa fluor 488 conjugate was spotted onto poly-l-lysine glass slide and imaged with the microarray scanner using both blue and green channels. Due to spectral overlap between Alexa fluor 488 and 532 dyes, fluorescence signals in both blue channel (real signal) and green channel (crosstalk) would be detected. The blue channel signal and green channel signal showed consistent correlation between each other (R=99%) and compensation equation can thus be extracted; **b**; correlation between real signal from 532 channel and overlap from 488 channel for Alexa fluor 532 conjugate. Similarly, Alexa fluor 532 was spotted on a glass slide and imaged with both channels to quantify spectral overlap and describe the compensation equation. The algorithms were initially designed for spectral overlap compensation in multicolore flow cytometric analysis.

(1) $\boldsymbol{F488 = T488 + T532 * a + A}$

(2) $\boldsymbol{F532 = T532 + T488 * b + A}$

The true signal from each channel can be calculated with formula (3) and (4) respectively:

(3) $\boldsymbol{T488 = [F488 - A - (F532 - B) * a]/(1 - ab)}$

(4) $\boldsymbol{T532 = [F532 - B - (F488 - A) * b]/(1 - ab)}$

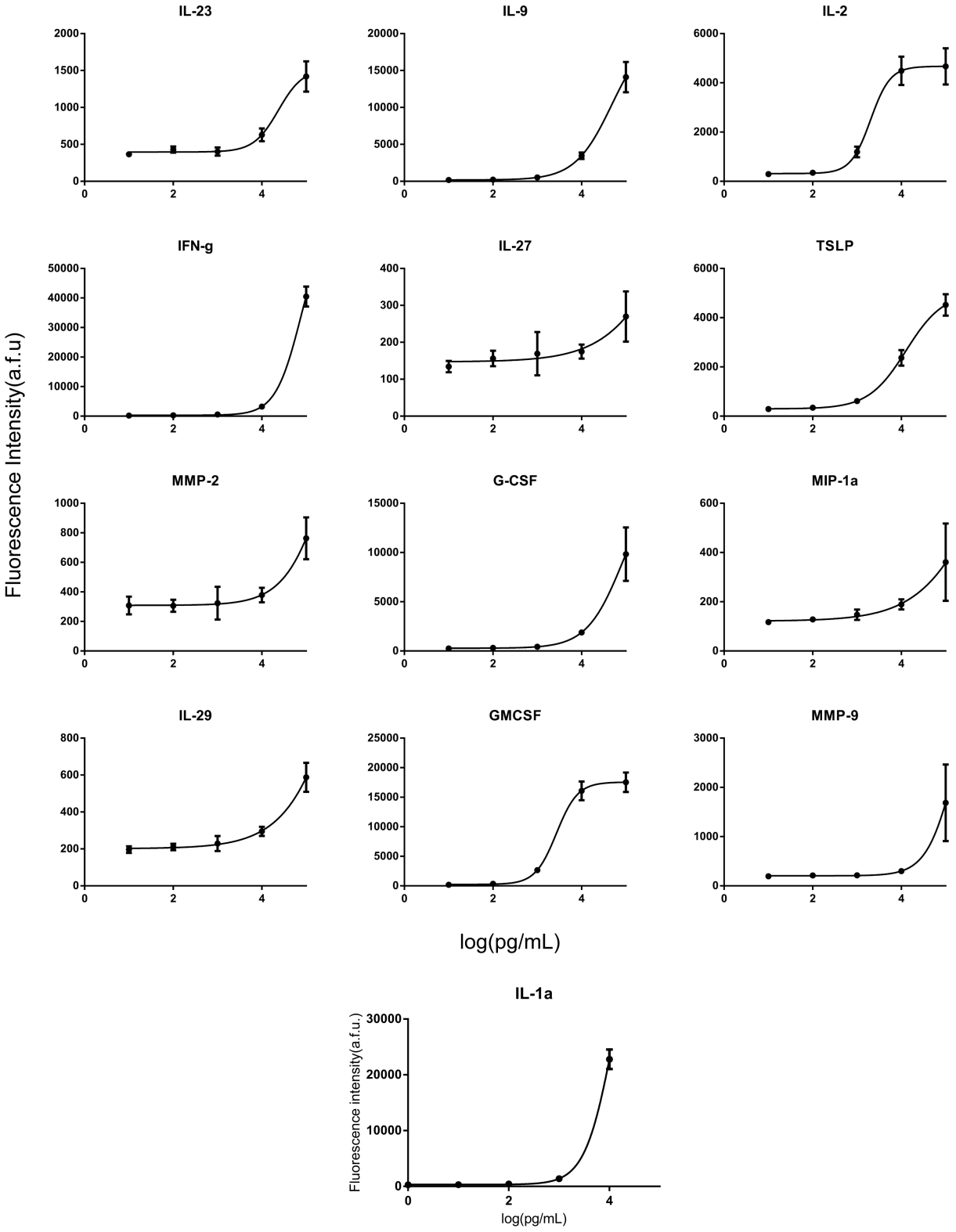
IL-23
IL-9
IL-2
IFN-g
IL-27
TSLP
MMP-2
G-CSF
MIP-1a
IL-29
GMCSF
MMP-9
Fluorescence Intensity(a.f.u)
log(pg/mL)
IL-1a
Fluorescence intensity(a.f.u.)
log(pg/mL)

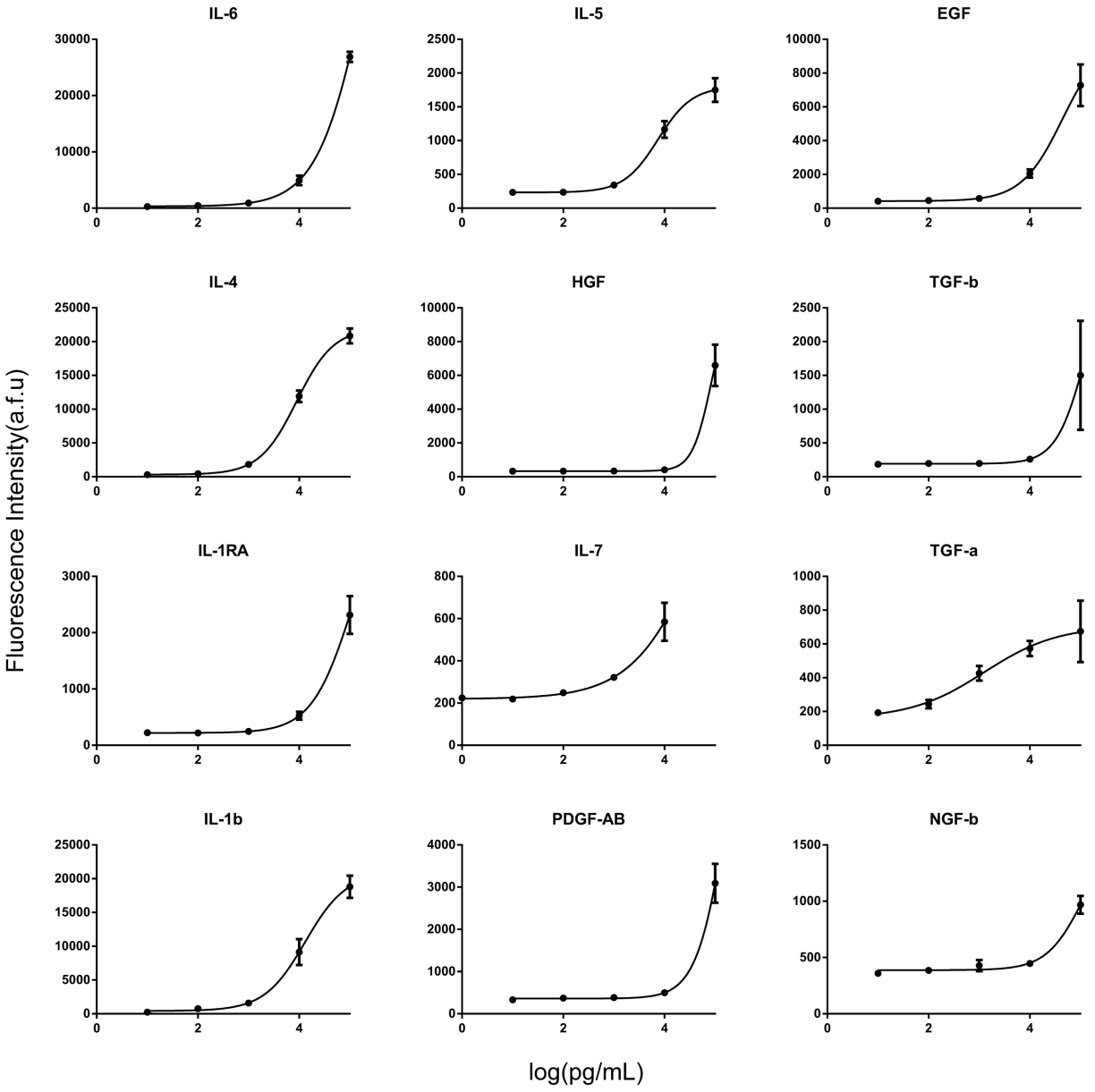
IL-6
IL-5
EGF
IL-4
HGF
TGF-b
IL-1RA
IL-7
TGF-a
IL-1b
PDGF-AB
NGF-b
Fluorescence Intensity(a.f.u)
log(pg/mL)

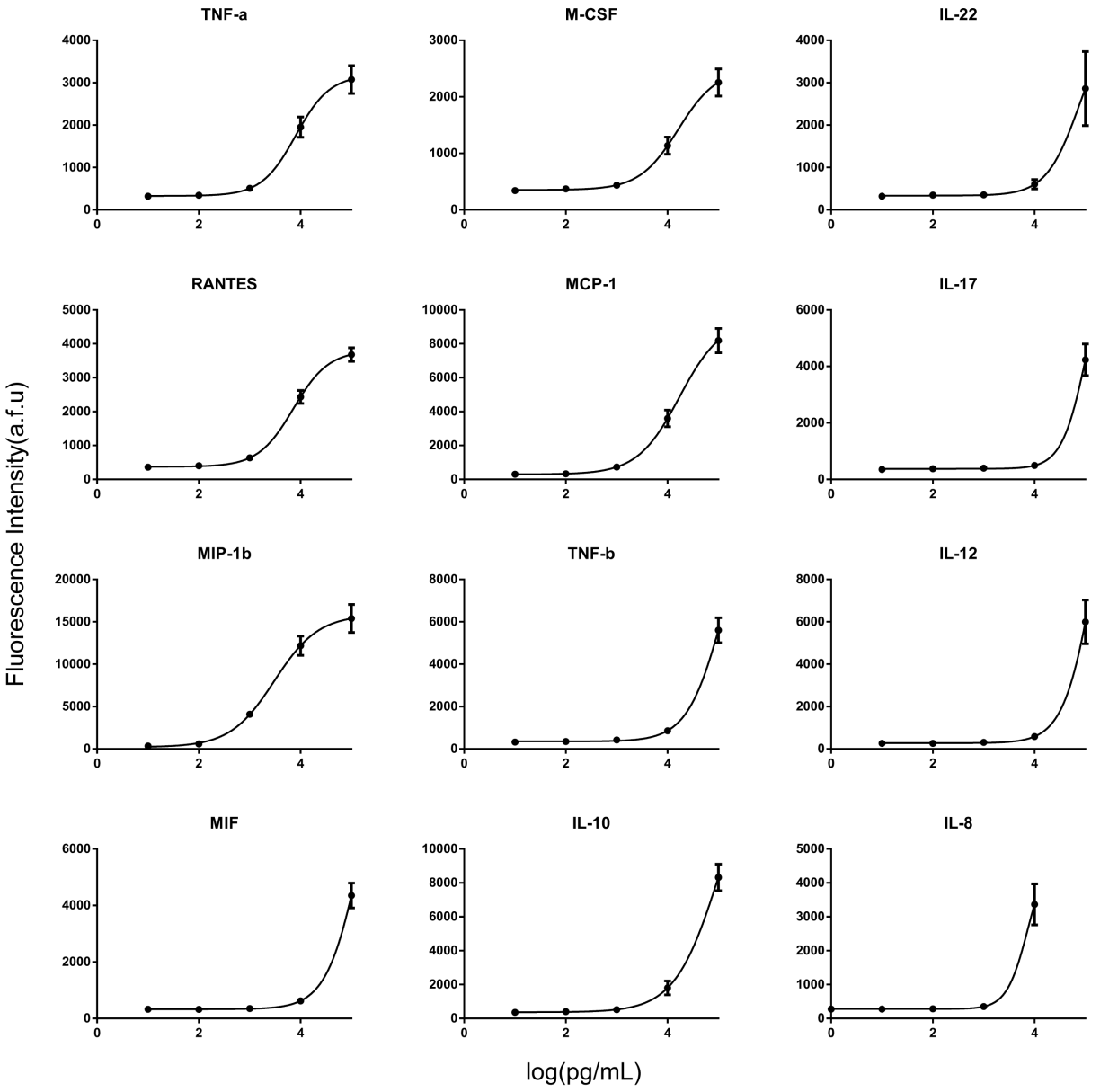

Fig. S4 Standard titration curves. The titration curves were obtained using recombinant proteins. These curves have been fit with a 4PL curve, which is standard for ELISA. Fluorescence intensity represents the original photon counts averaged from 16 spots for each protein.

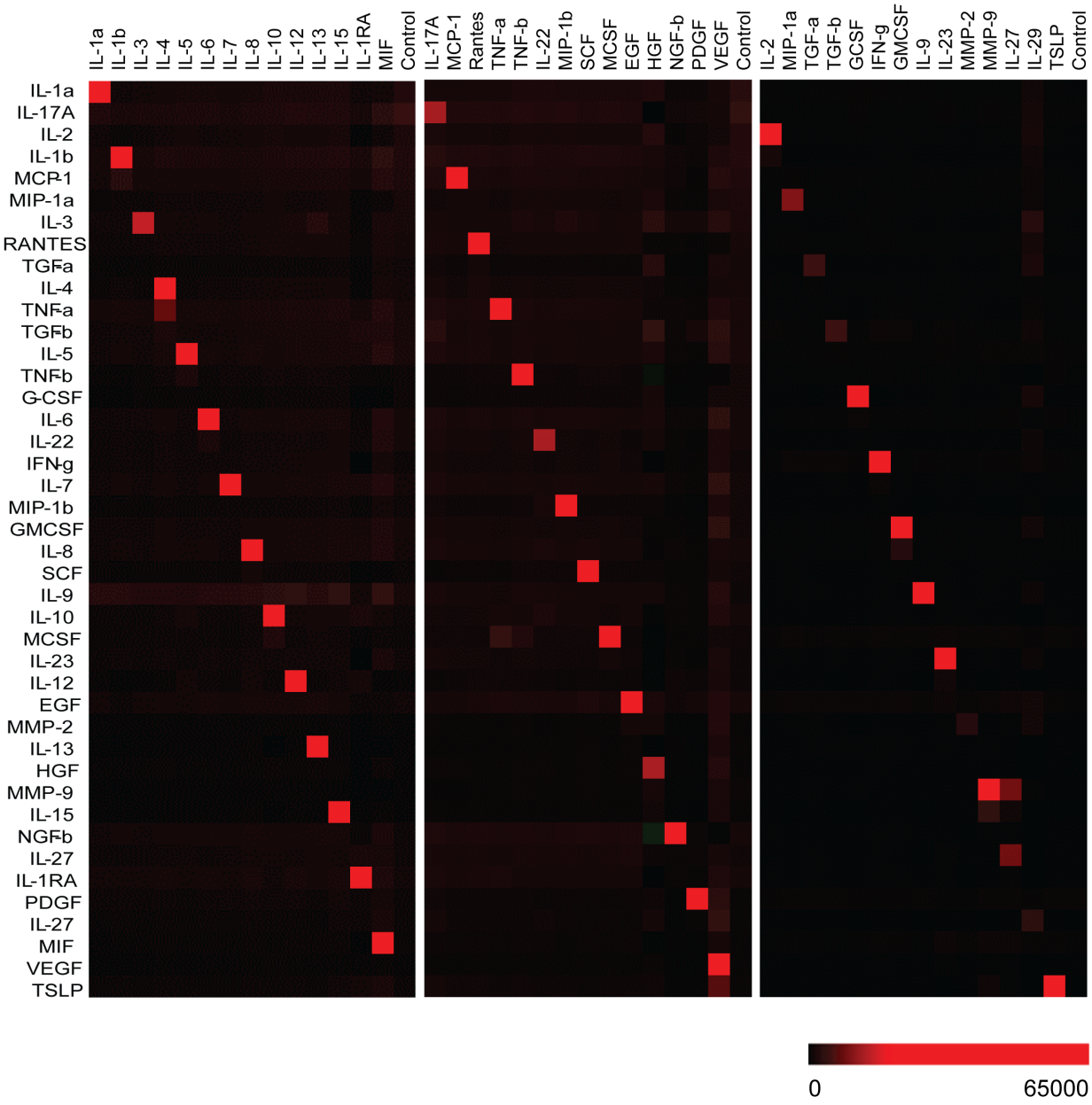

Fig. S5 Cross-reactivity check for all 42 proteins. Most of the antibodies used in this study are monoclonal antibodies to ensure good specificity and reduced cross reactivity. The test was conducted by spiking a single antigen (recombinant protein) in a solution applied to a full capture antibody microarray containing all 42 capture antibodies, followed by detection with a mixture of all detection Abs. Some antibodies showed relatively weak signals such as MMP-2, IL-29, which are probably caused by low reactivity of recombinant proteins.

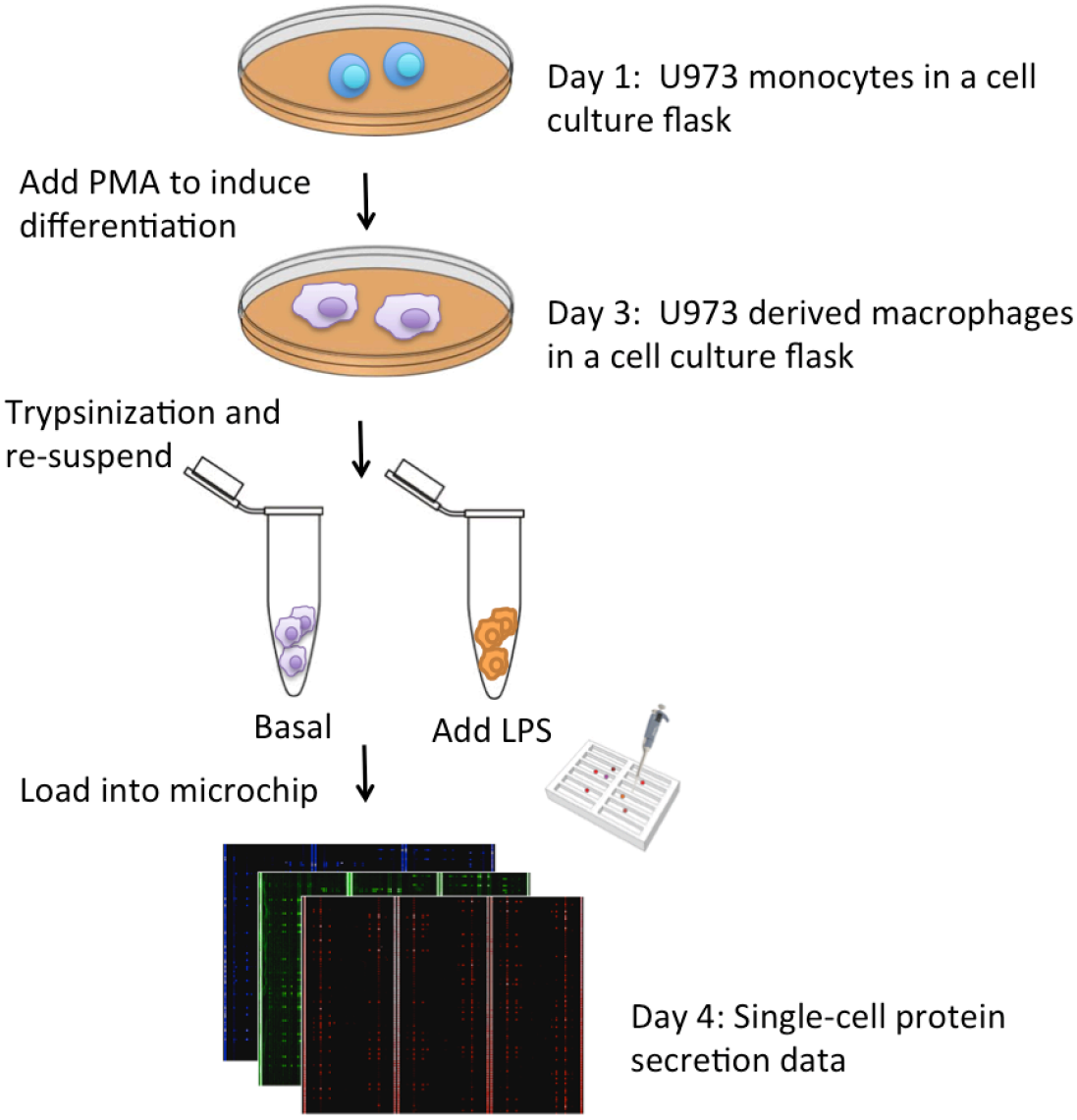

Fig. S6 Flow chart depicting the procedure and timeline for preparing U937 derived macrophages and performing single-cell protein secretion profiling. The differentiation was conducted in a conventional cell culture dish. The differentiated cells were the trypsinized and resuspended to prepare for single-cell secretion assay. Single-cell suspension was devised into two portions. One was direct loaded to microchip and the other was added with LPS to inducate TLR4 activation, which is a well characterized process and results in the secretion of a large panel of cytokines. Thus, it serves as an excellent model system to test the new technology platform – single-cell, 42-plex protein secretion profiling.

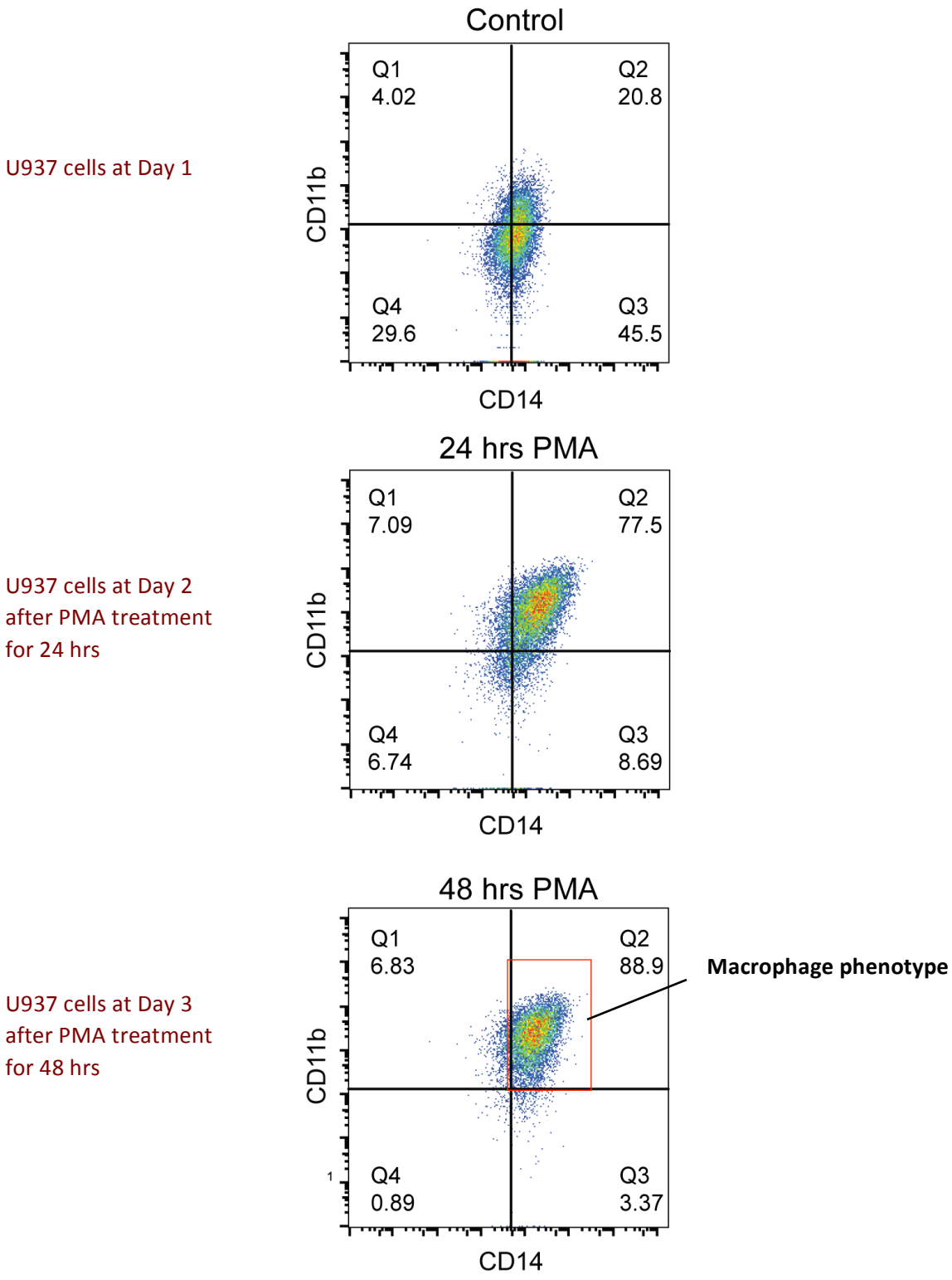

Fig. S7 Surface antigen expression confirms successful differentiation of U937 monocytes to macrophages. There scatter plots show flow cytometric analysis of cell surface markers CD11b and CD14 in the U937 cells treated by PMA (50 ng/mL) for 48 hr.

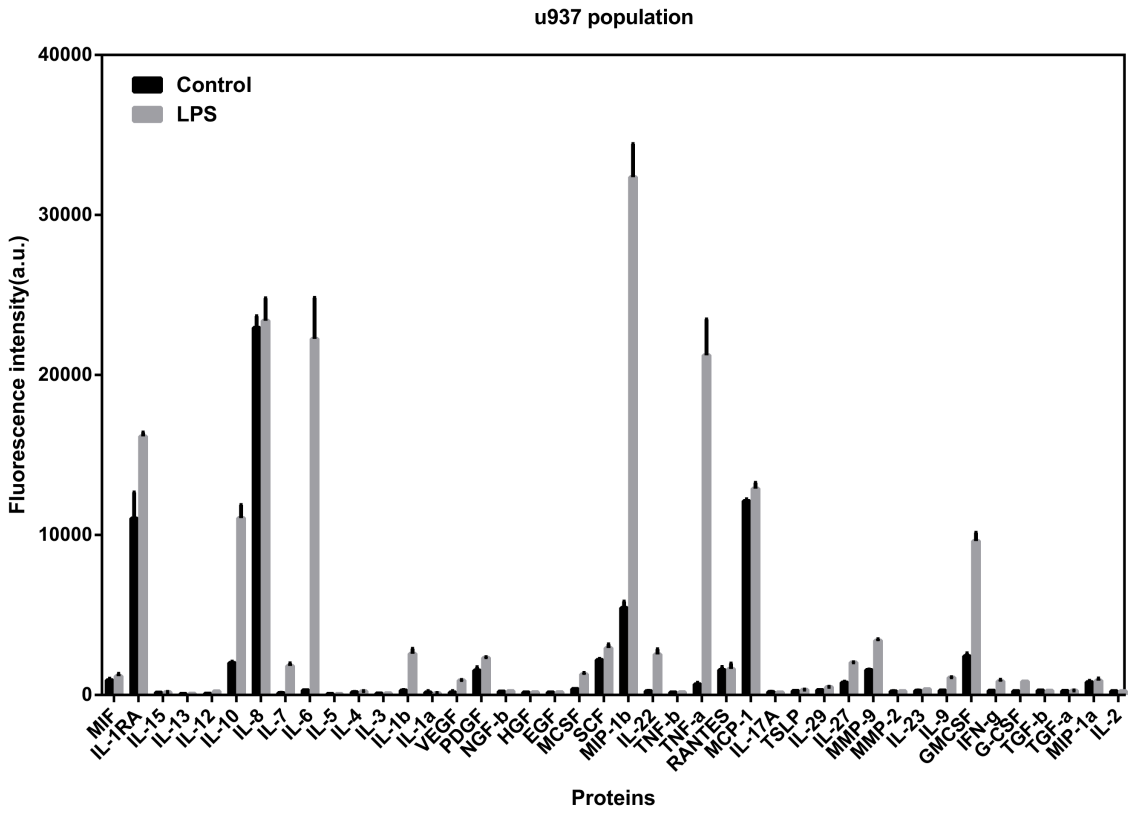

Fig. S8 Population level protein secretion profile. Protein secretion was measured on U937 derived macrophage cells at the population level using a conventional micro titer plate (cell density ~10^6/mL). Both non-stimulated and LPS stimulated cells were measured.

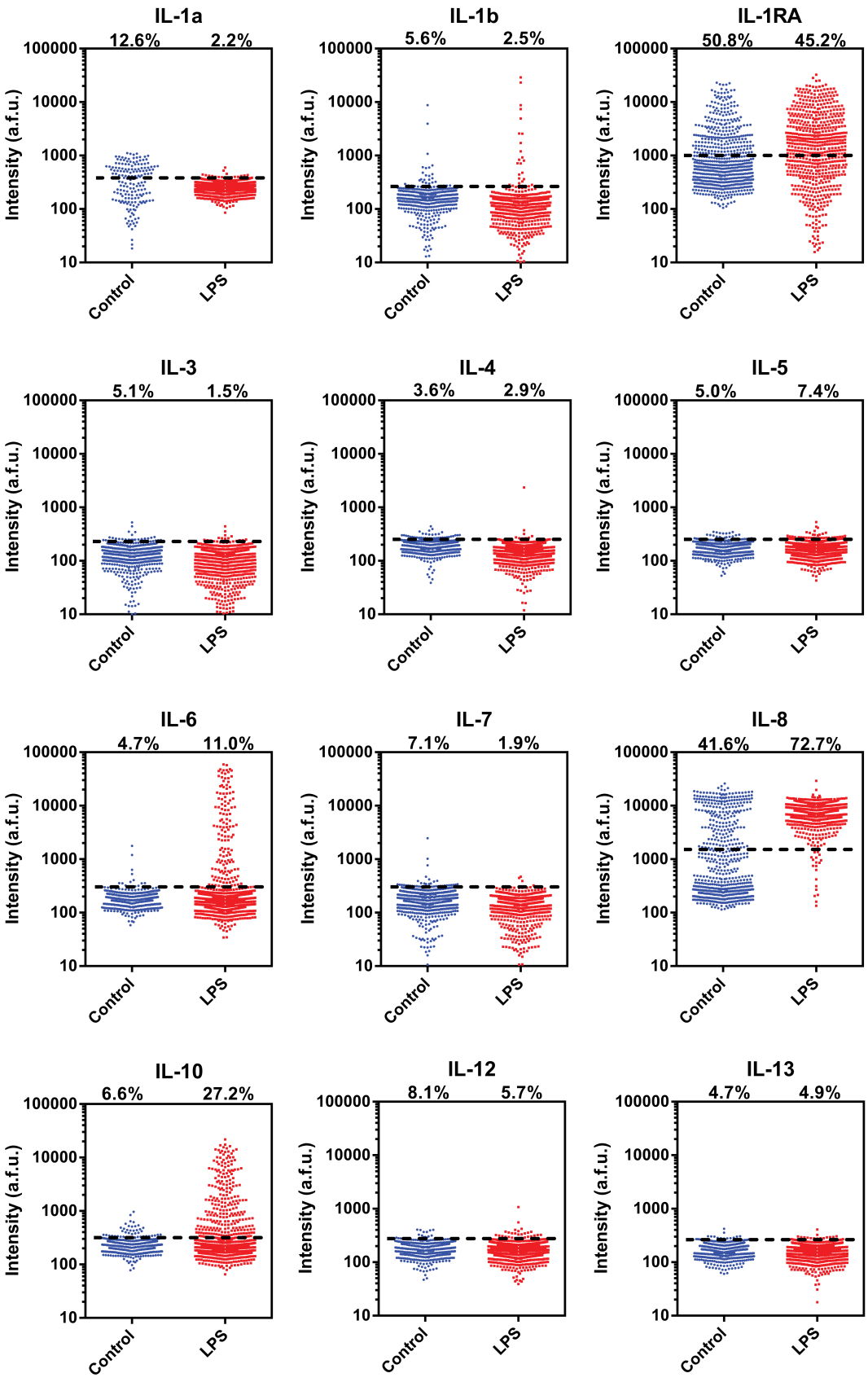
IL-1a
12.6%
2.2%
IL-1b
5.6%
2.5%
IL-1RA
50.8%
45.2%
IL-3
5.1%
1.5%
IL-4
3.6%
2.9%
IL-5
5.0%
7.4%
IL-6
4.7%
11.0%
IL-7
7.1%
1.9%
IL-8
41.6%
72.7%
IL-10
6.6%
27.2%
IL-12
8.1%
5.7%
IL-13
4.7%
4.9%
Intensity (a.f.u.)
100000
10000
1000
100
10
Control
LPS

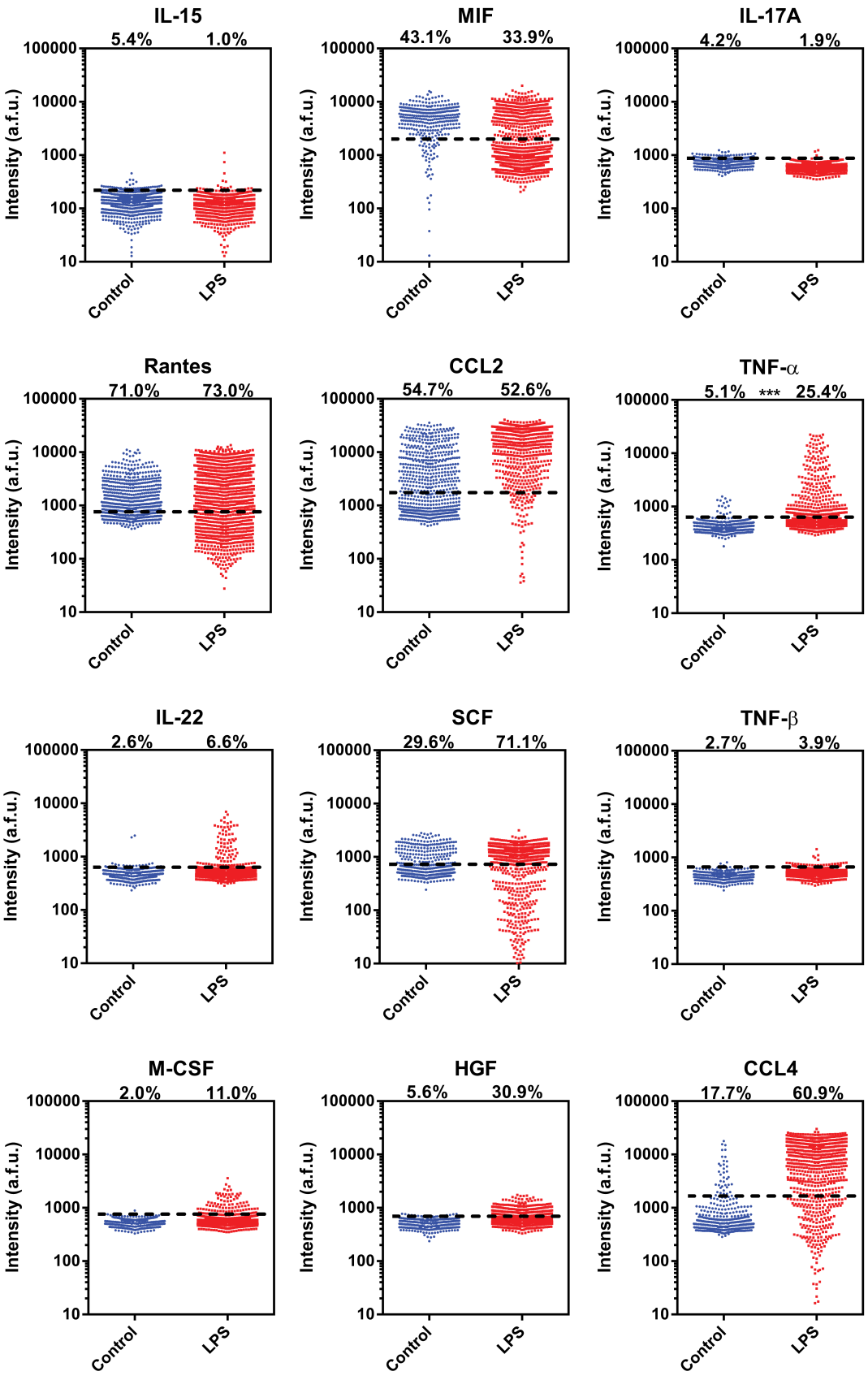
IL-15
5.4%
1.0%
MIF
43.1%
33.9%
IL-17A
4.2%
1.9%
Rantes
71.0%
73.0%
CCL2
54.7%
52.6%
TNF-α
5.1%
***
25.4%
IL-22
2.6%
6.6%
SCF
29.6%
71.1%
TNF-β
2.7%
3.9%
M-CSF
2.0%
11.0%
HGF
5.6%
30.9%
CCL4
17.7%
60.9%
Intensity (a.f.u.)
100000
10000
1000
100
10
Control
LPS

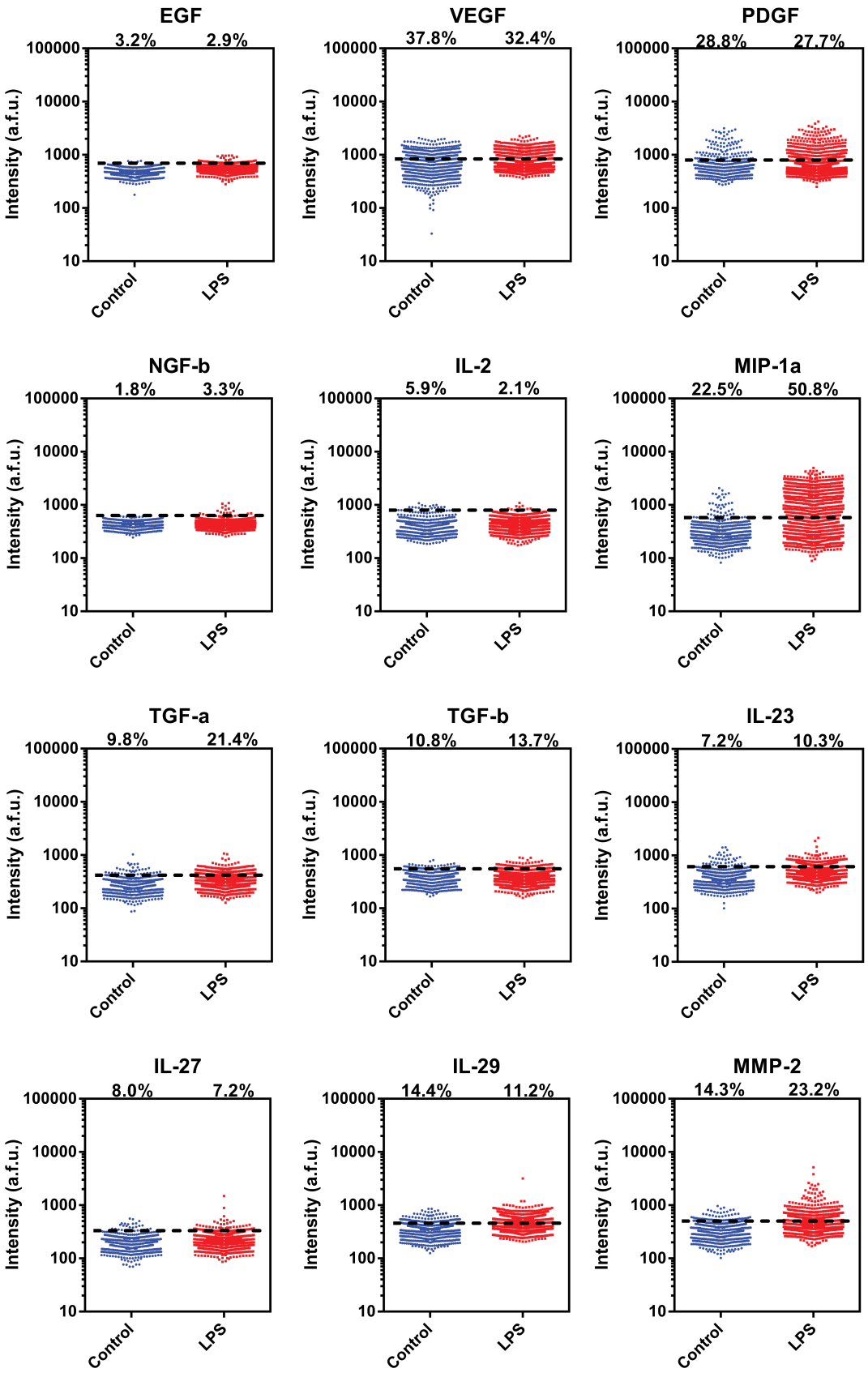
EGF
3.2%
2.9%
VEGF
37.8%
32.4%
PDGF
28.8%
27.7%
NGF-b
1.8%
3.3%
IL-2
5.9%
2.1%
MIP-1a
22.5%
50.8%
TGF-a
9.8%
21.4%
TGF-b
10.8%
13.7%
IL-23
7.2%
10.3%
IL-27
8.0%
7.2%
IL-29
14.4%
11.2%
MMP-2
14.3%
23.2%
Intensity (a.f.u.)
100000
10000
1000
100
10
Control
LPS

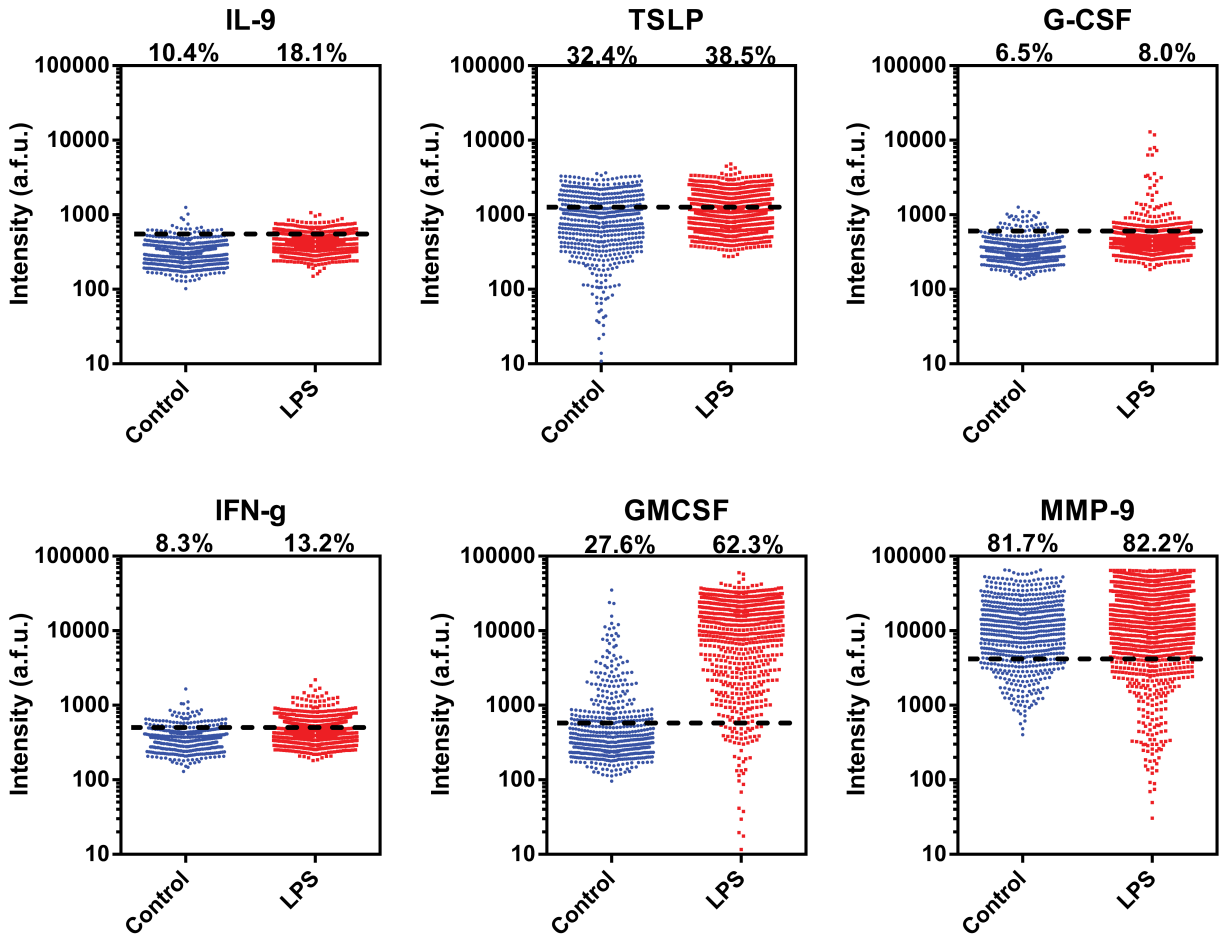

Fig. S9 Vertical scatter plots showing cytokine secretion levels and frequency in all single cells and for all protein measured. It includes complete single-cell cytokine vertical scatter plots showing in Fig. 2B. The plots compare single-cell protein secretion at the basal level (blue dots) and upon LPS stimulation (red dots). The dashed line marks the "gate" defined as (zero-cell data average + 2 STDV). The data were shifted vertically to match the "gates" obtained from two microchips.

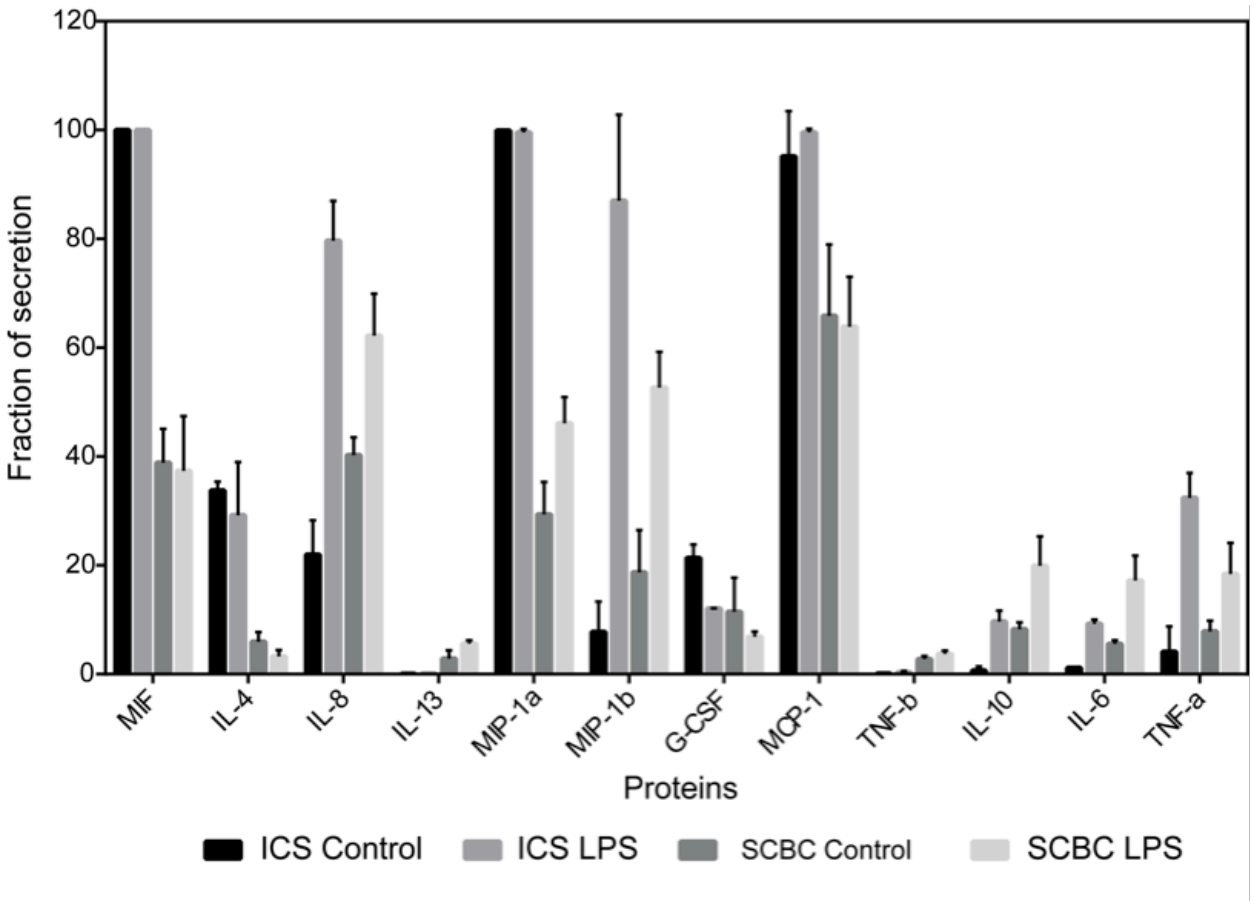

Fig. S10 Comparison between the microchip data and the flow cytometric ICS data. The major secreted proteins identified by single-cell microchip experiments were measured using both methods. The raw data for fraction of cytokine-secreting cells in both basal and LPS stimulated cells was compared. The correlation between ICS and our assay is moderate due to several reasons. (1) The microchip assay measures the amount of protein secreted by a cell, whereas ICS measures the protein synthesized but trapped inside a cell, representing a different biological process. (2) We used a sandwich immunoassay, which requires two different epitopes of a protein being recognized to give rise to a positive signal and thus provides higher or more stringent specificity than intracellular staining. (3) Our microchip assay eliminates paracrine-induced amplification of protein secretion all the way in the beginning, which is different from the standard ICS assay. Thus, detection threshold for a protein secreting cell differs substantially using these two methods. However, we observed that the response to LPS stimulation measured by the increase in the fraction of cells secreting a given cytokine exhibits good correlation between the two methods (Fig. 2d).

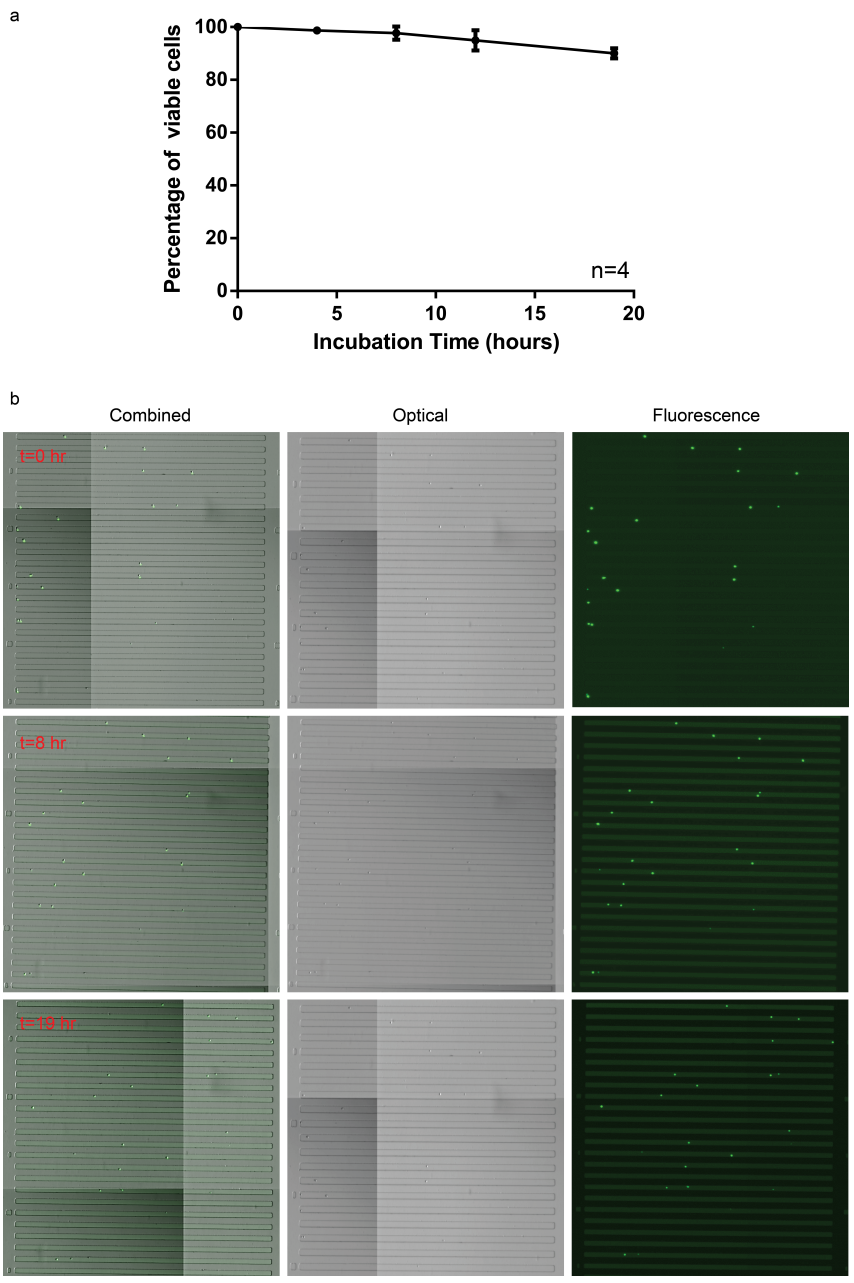

Fig. S11 Cell viability assay. The cells were stained with Calcein AM (Life technologies, USA) before loading into PDMS microwells. Then they were imaged at 0, 4, 8, 12and 19hr. One column was randomly chosen and quantified (220 microchannels, around 350 cells in total). The cells showing positive green fluorescence signal were scored as viable. The result showed that 90% of the cells were still alive after 19 hr incubation.. Considering the dye may be toxic to cells and cells were imaged at non-tissue culture environment for 1 hr in each imaging (5 hr in total), the cell viability is estimated higher than 90%.

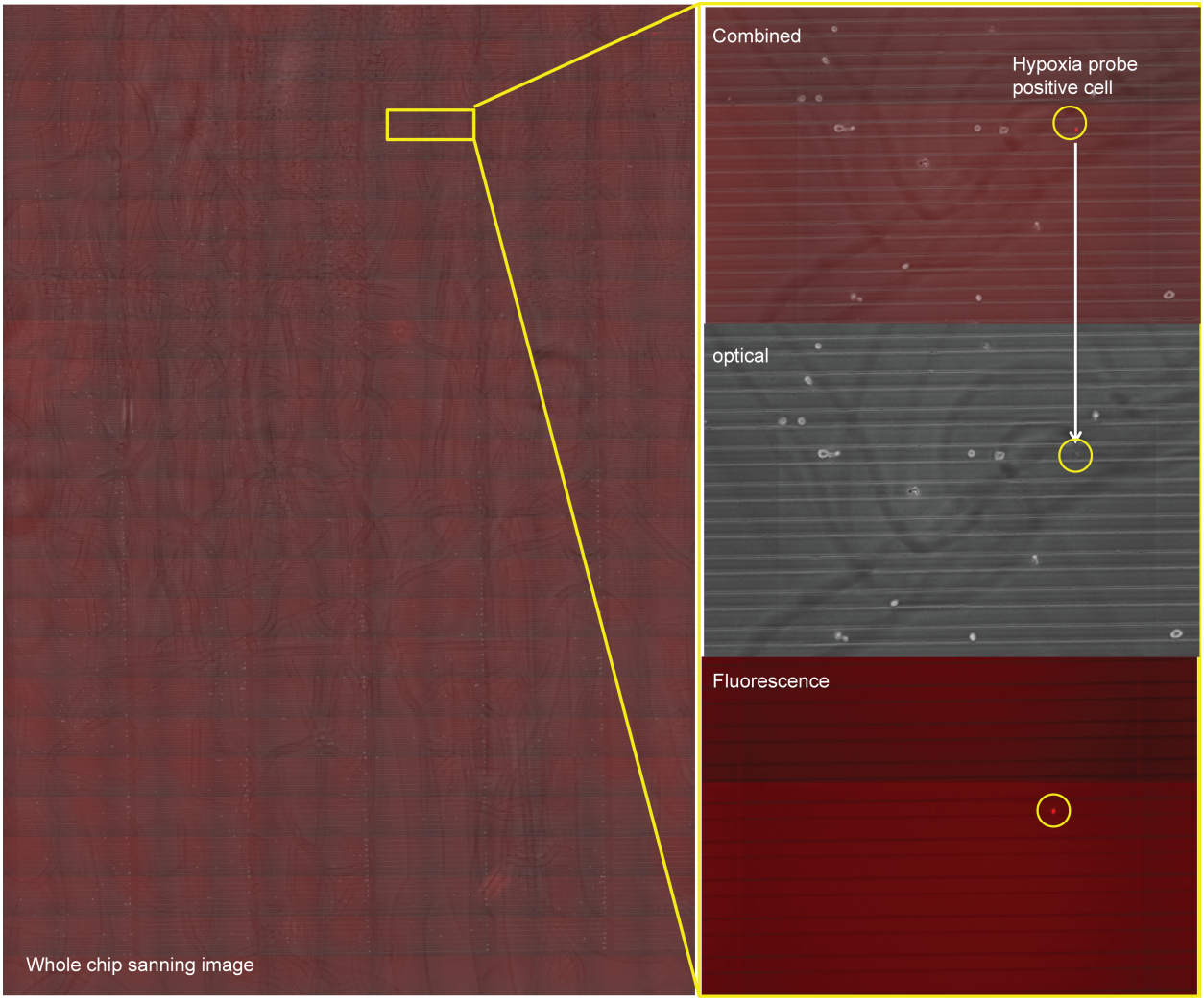

Fig. S12 Cell hypoxia assay. Hypoxia test of U937 macrophage cells after 24 hr incubation in enclosed PDMS microwells with hypoxia fluorescence probe LOX-1 (SCIVAX, USA). The results showed that less than 1 % (2 cells positive out of 351 cells) of cells enclosed showed positive with hypoxia fluorescence dye, which indicates excellent oxygen permeability of PDMS can ensure cells be cultured in normoxia condition all through single cell experiment.

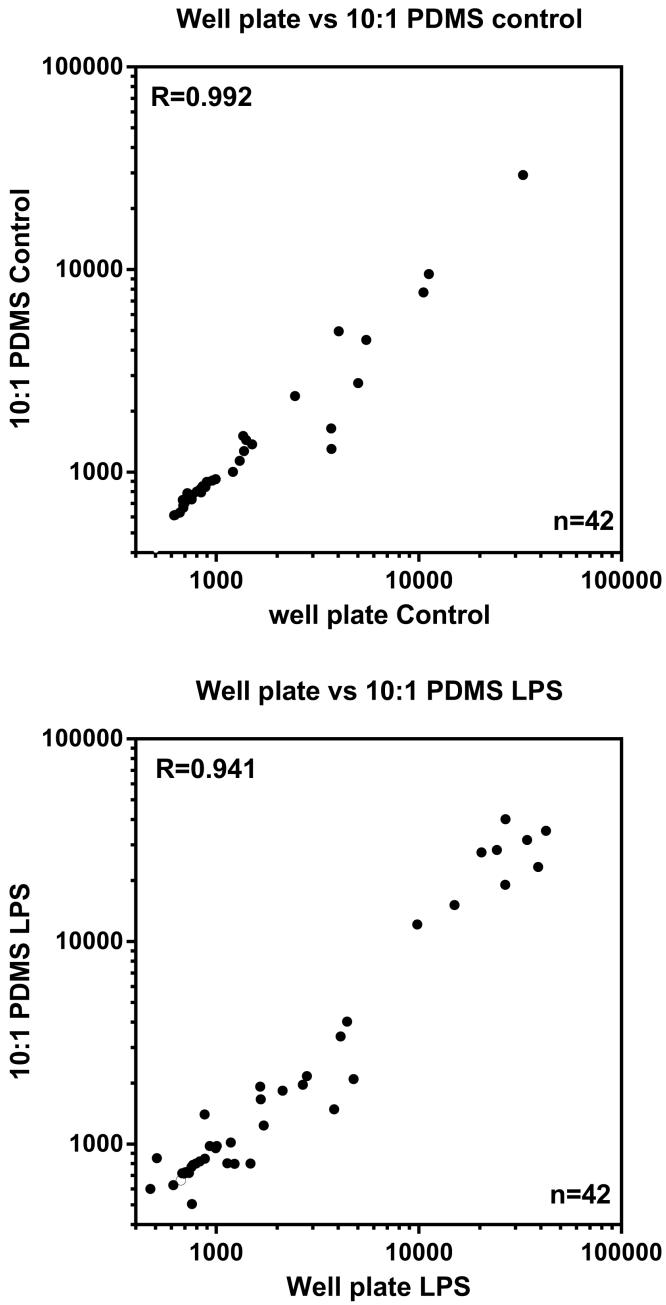

Fig. S13 Effect of substrate mechanical property on protein secretion. Comparison of U937 populational protein secretion profiles cultured on the polystyrene surface in a 96 well plate vs. a standard PDMS elastomer surface (prepolymer:initiator = 10:1). PDMS is nontoxic, biocompatible, transparent elastomer and has been widely used in biological and biomedical research. Polystyrene is a routine material used in conventional well pate experiment. The results indicate the U937 macrophage cells exhibited very similar protein secretion patterns and intensity on both substrates. The protein secretion profiles measured in cells cultured on two different substrates showed highly correlated with each other (R>0.99 and 0.94 in basal and LPS stimulated protein secretion tests, respecrtively).

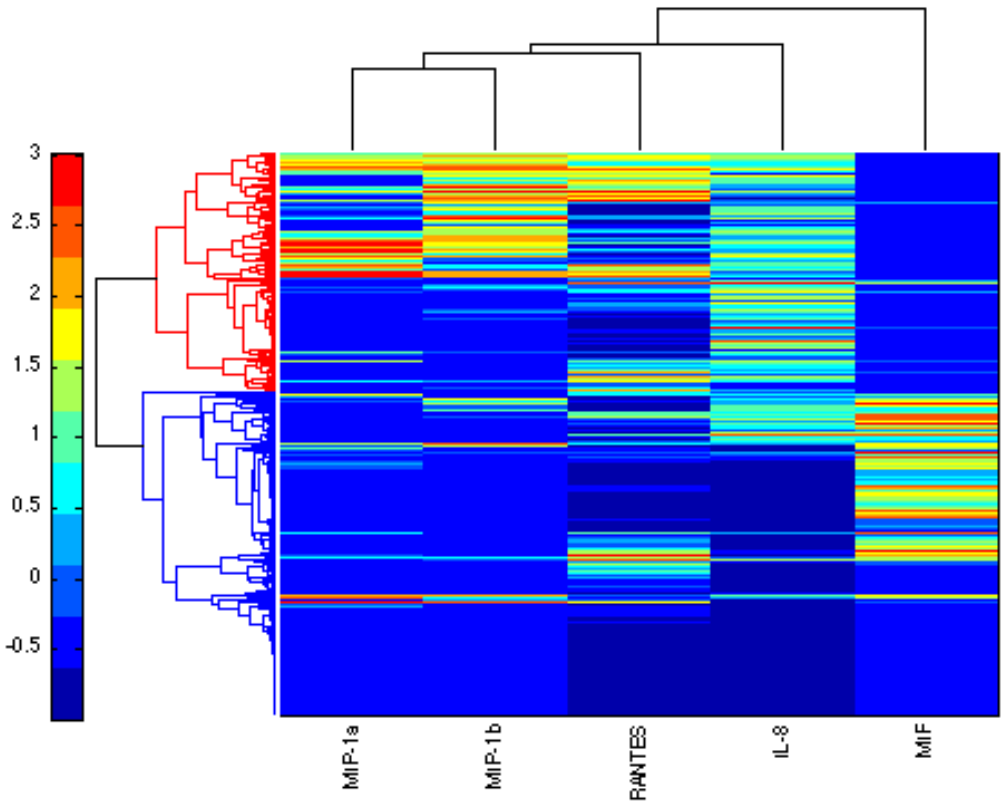

Fig. S14. Heatmap showing MIF-secreting population is largely anti-correlated with proinflammatory cytokine-secreting populations. The plot is from the data shown in Figure 2a and apparently MIF is anti-correlated with LPS activation.

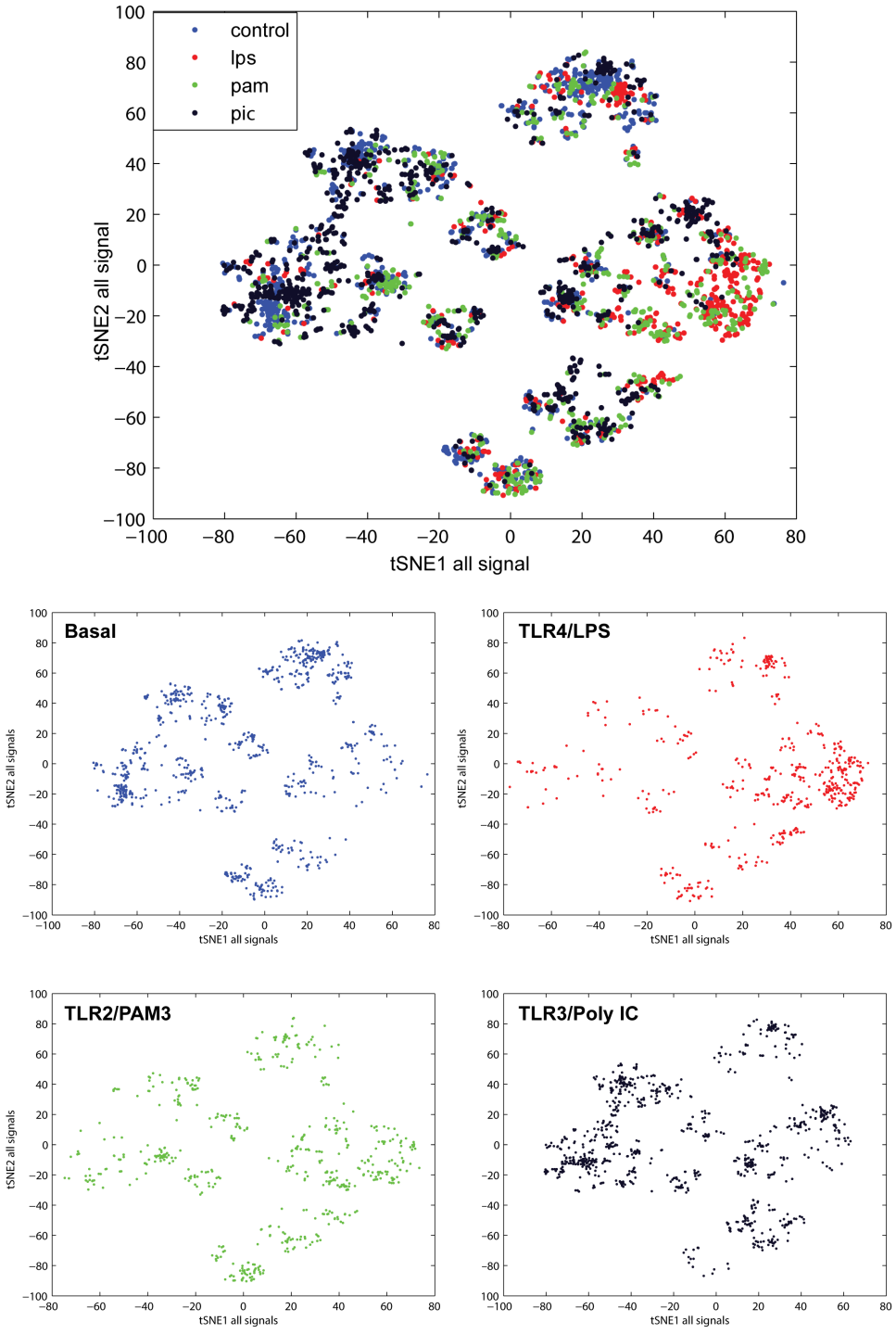

Fig. S15. viSNE maps showing the high-dimensional clustering of single cells (U937-derived macrophages) at the basal level and stimulated with different TLR ligands. It shows viSNE structure maps for U937 derived macrophage cells at the basal state and under the stimulation of different TLR ligands(basal, TLR4 by LPS, TLR1/2 by PAM3, TLR3 by poly IC).

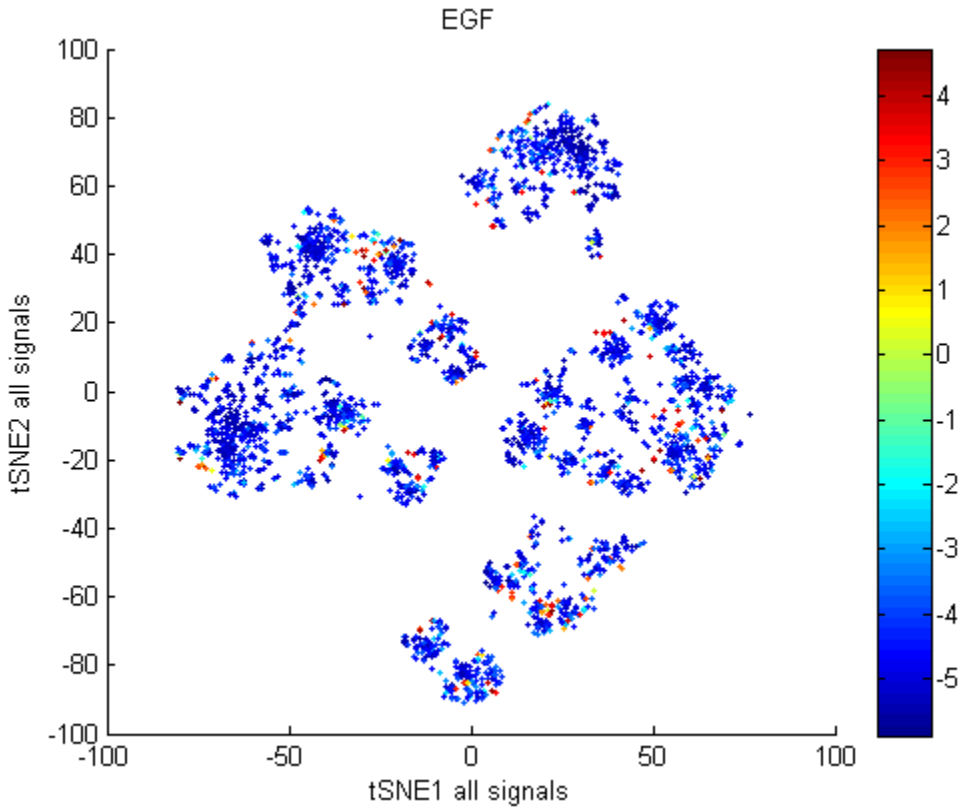
EGF
tSNE2 all signals
tSNE1 all signals

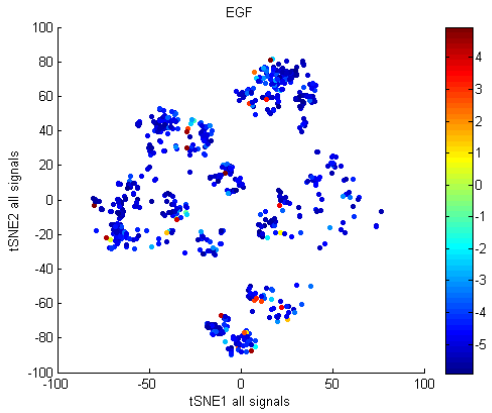
EGF
tSNE2 all signals
tSNE1 all signals

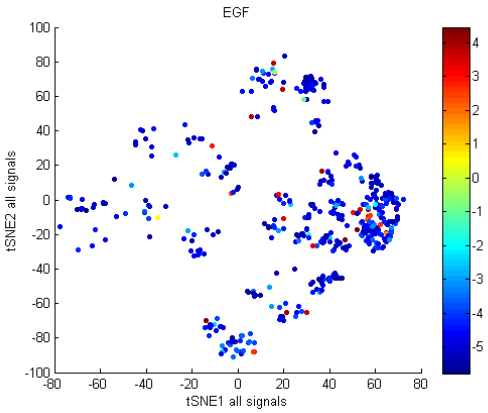
EGF
tSNE2 all signals
tSNE1 all signals

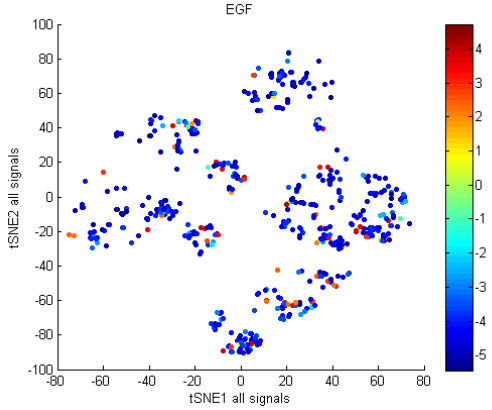
EGF
tSNE2 all signals
tSNE1 all signals

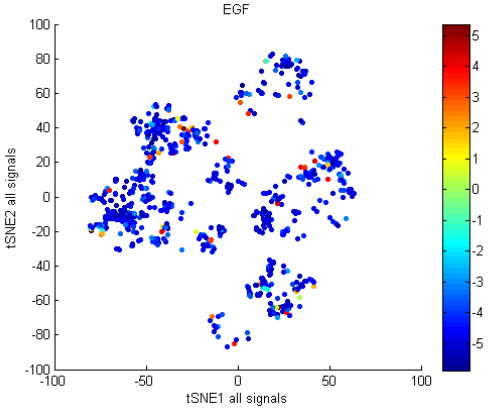
EGF
tSNE2 all signals
tSNE1 all signals

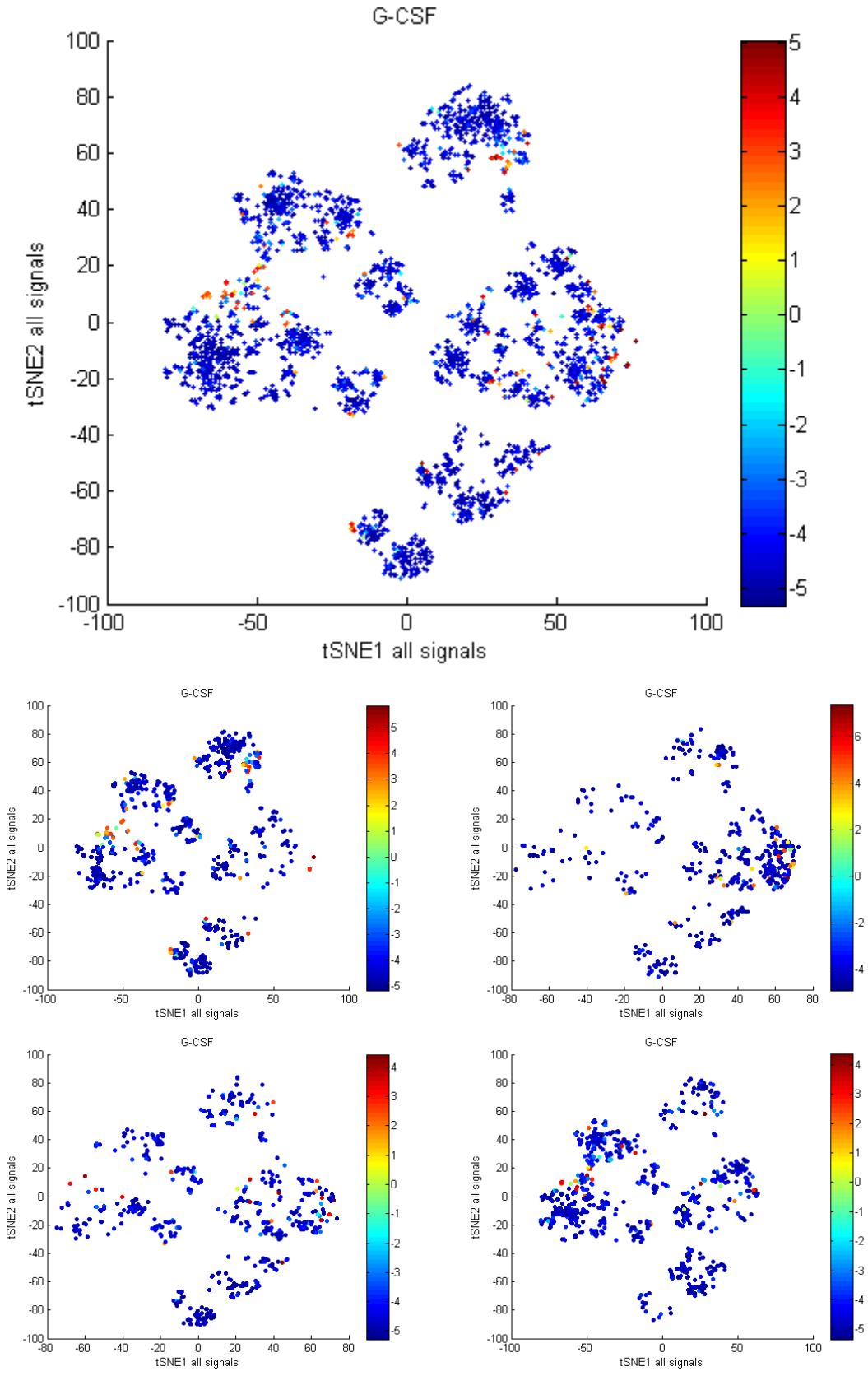
G-CSF
tSNE2 all signals
tSNE1 all signals
G-CSF
tSNE2 all signals
tSNE1 all signals
G-CSF
tSNE2 all signals
tSNE1 all signals
G-CSF
tSNE2 all signals
tSNE1 all signals
G-CSF
tSNE2 all signals
tSNE1 all signals

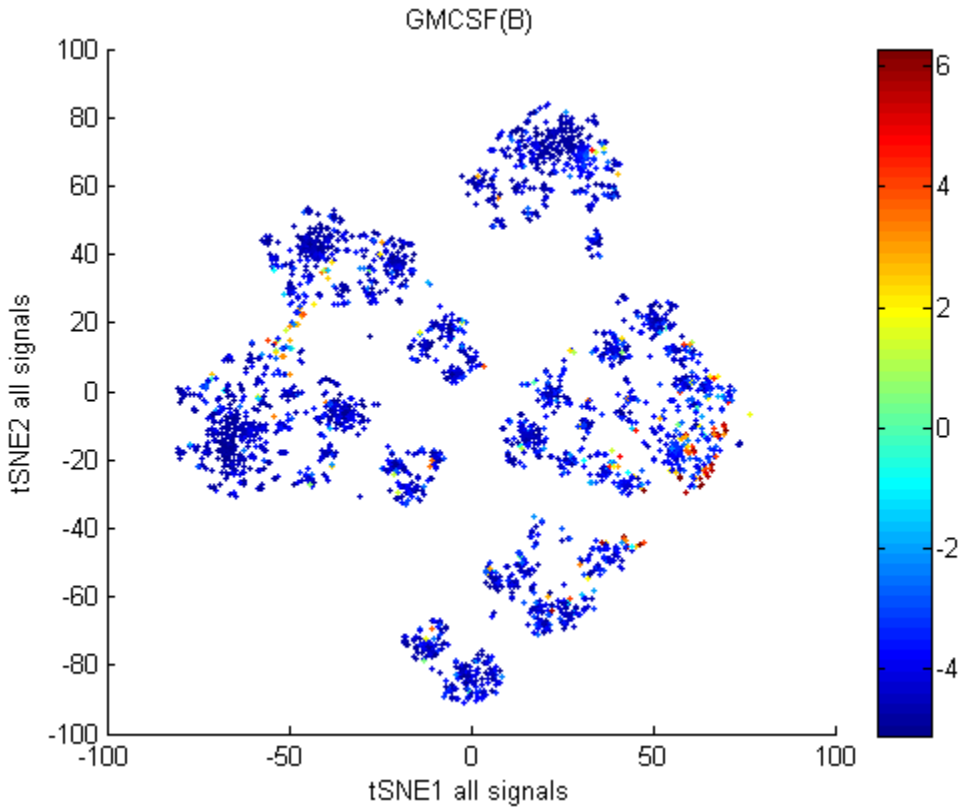
GMCSF(B)
tSNE2 all signals
tSNE1 all signals

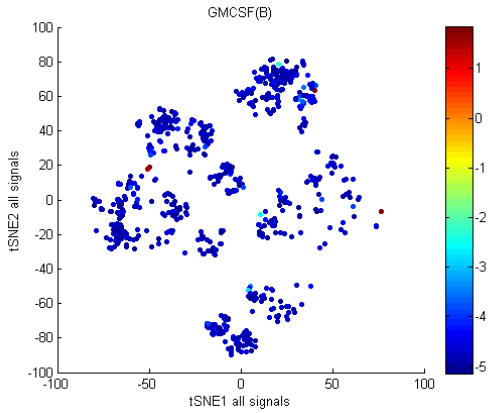
GMCSF(B)
tSNE2 all signals
tSNE1 all signals

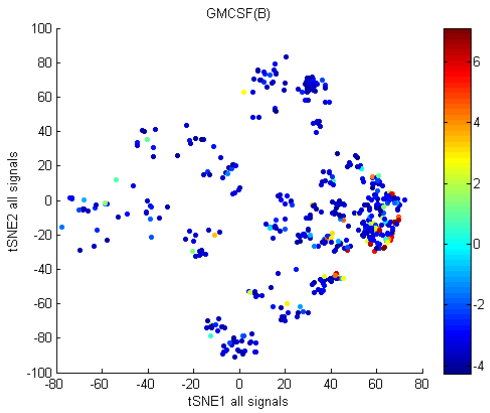
GMCSF(B)
tSNE2 all signals
tSNE1 all signals

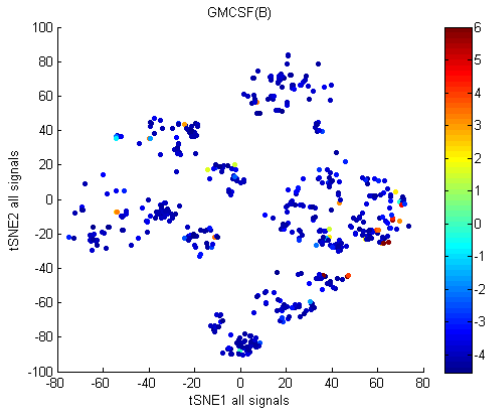
GMCSF(B)
tSNE2 all signals
tSNE1 all signals

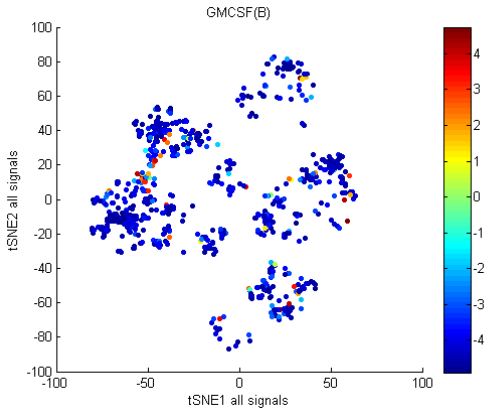
GMCSF(B)
tSNE2 all signals
tSNE1 all signals

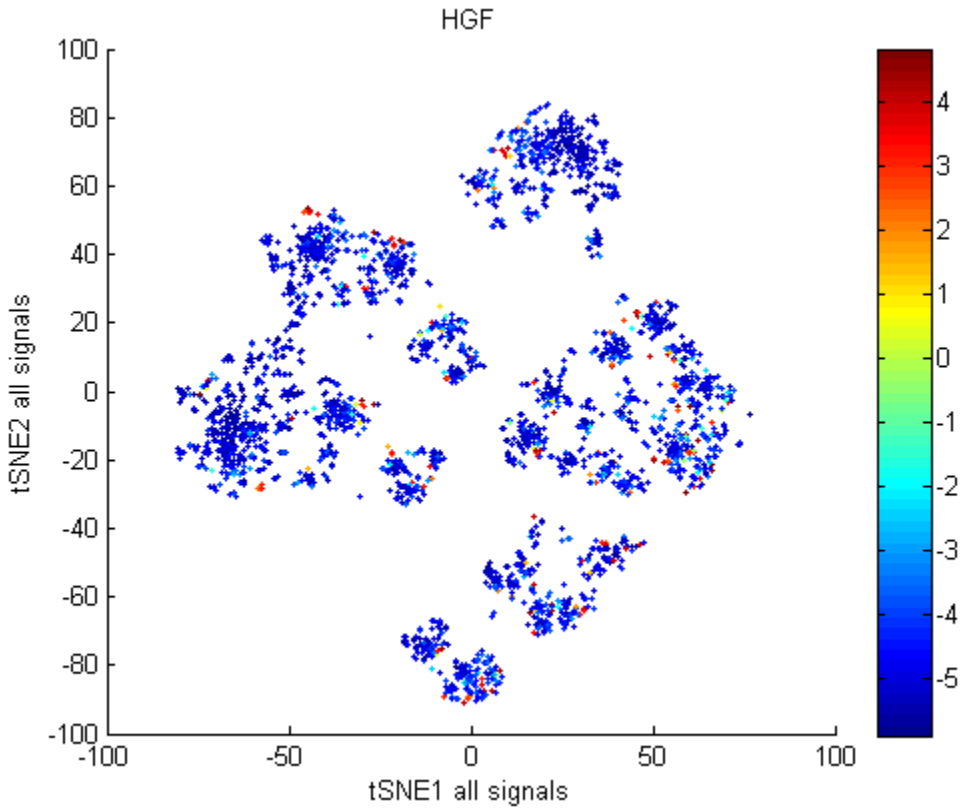
HGF
tSNE2 all signals
tSNE1 all signals

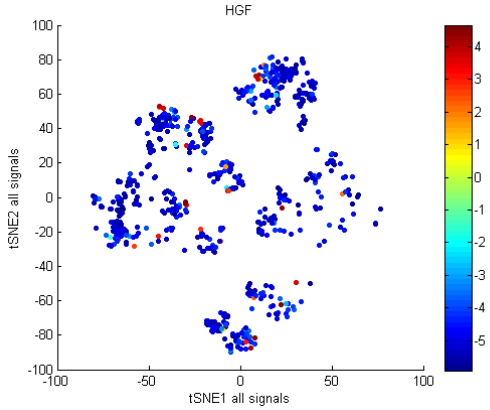
HGF
tSNE2 all signals
tSNE1 all signals

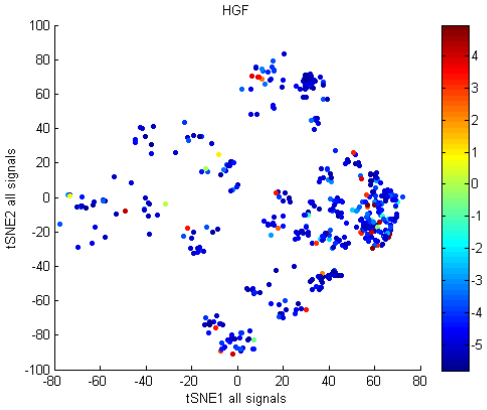
HGF
tSNE2 all signals
tSNE1 all signals

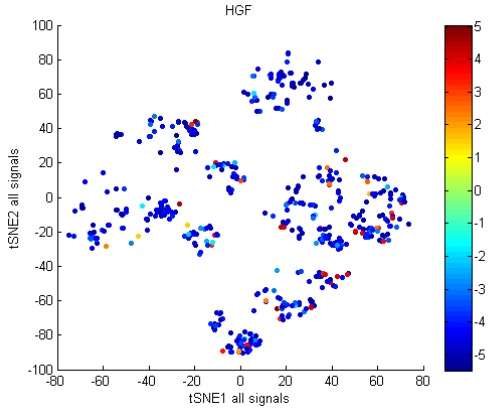
HGF
tSNE2 all signals
tSNE1 all signals

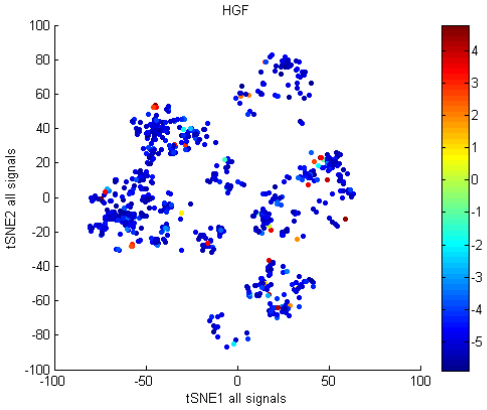
HGF
tSNE2 all signals
tSNE1 all signals

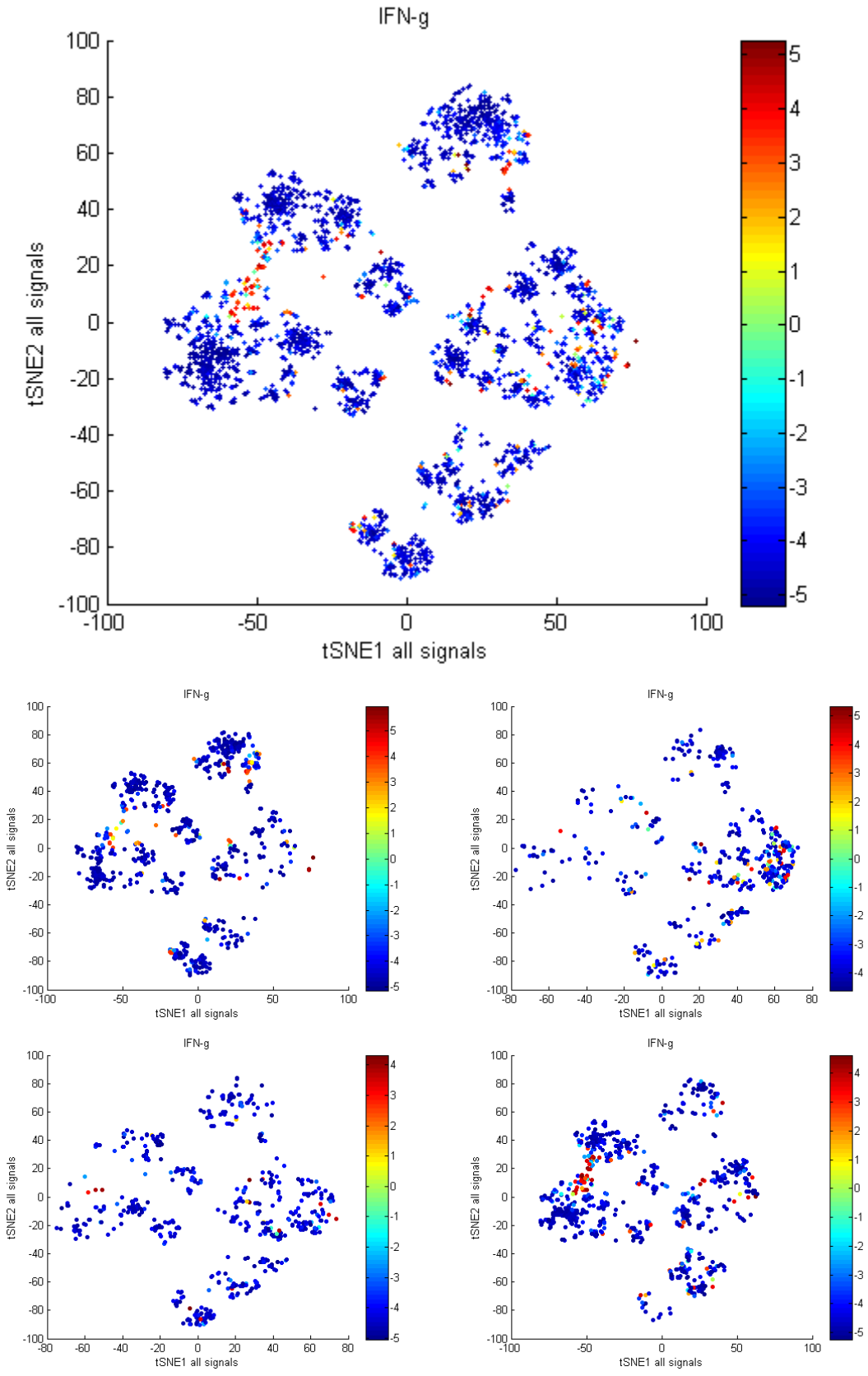
IFN-g
tSNE2 all signals
tSNE1 all signals
IFN-g
tSNE2 all signals
tSNE1 all signals
IFN-g
tSNE2 all signals
tSNE1 all signals
IFN-g
tSNE2 all signals
tSNE1 all signals
IFN-g
tSNE2 all signals
tSNE1 all signals

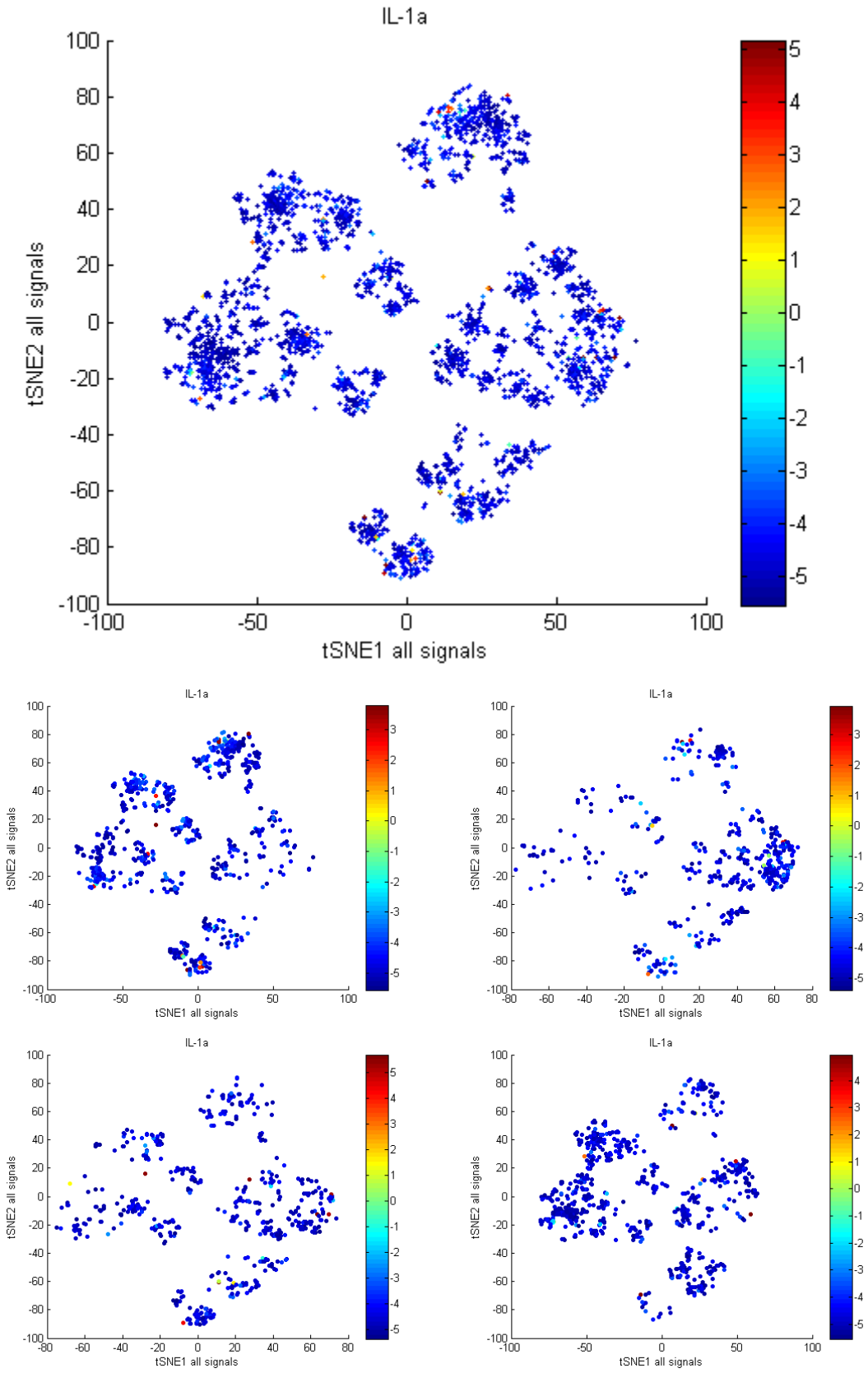
IL-1a
tSNE2 all signals
tSNE1 all signals
IL-1a
tSNE2 all signals
tSNE1 all signals
IL-1a
tSNE2 all signals
tSNE1 all signals
IL-1a
tSNE2 all signals
tSNE1 all signals
IL-1a
tSNE2 all signals
tSNE1 all signals

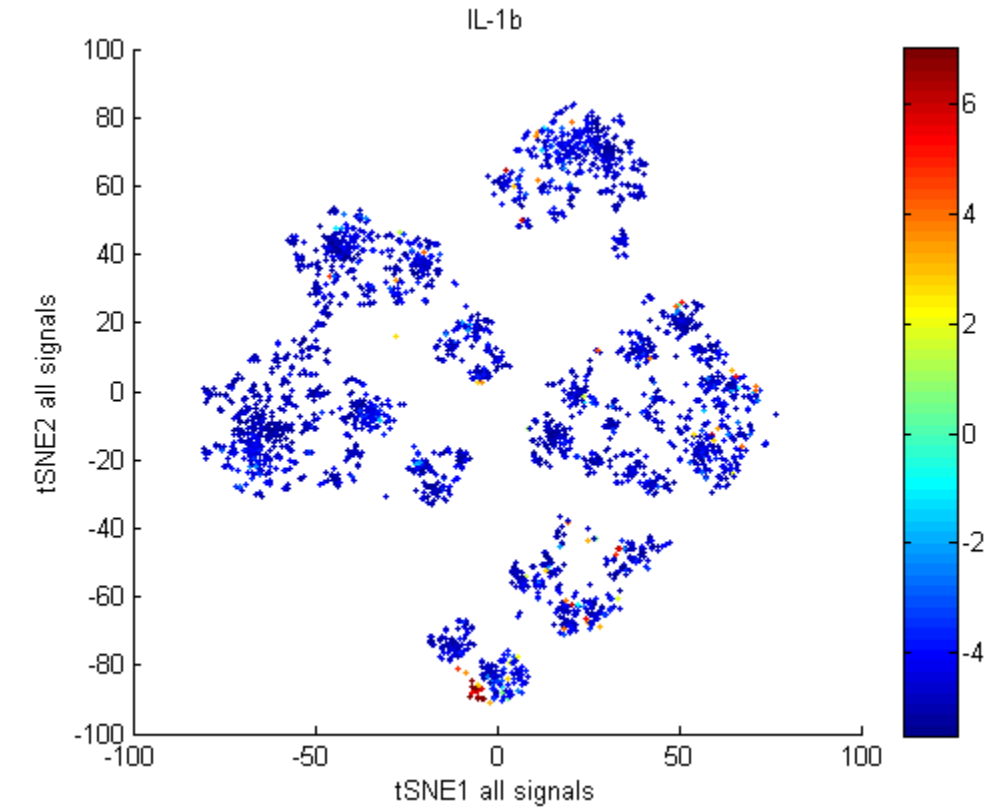
IL-1b
tSNE2 all signals
tSNE1 all signals

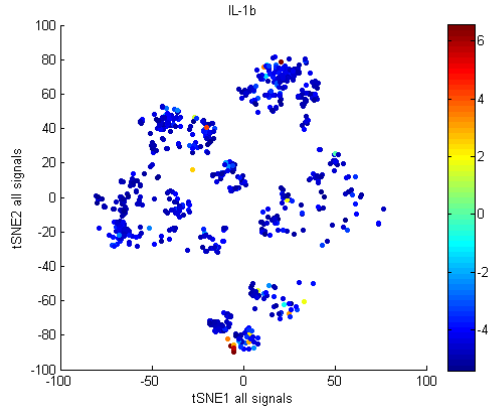
IL-1b
tSNE2 all signals
tSNE1 all signals

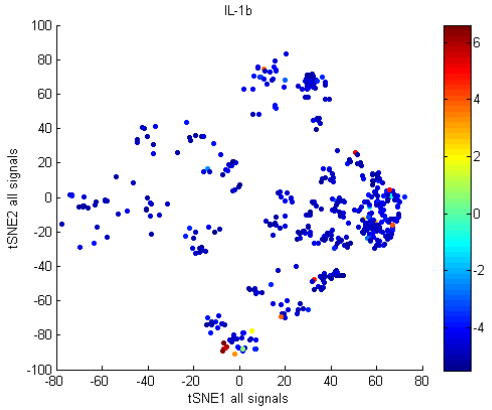
IL-1b
tSNE2 all signals
tSNE1 all signals

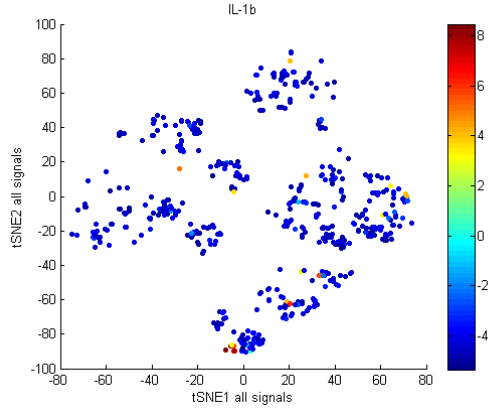
IL-1b
tSNE2 all signals
tSNE1 all signals

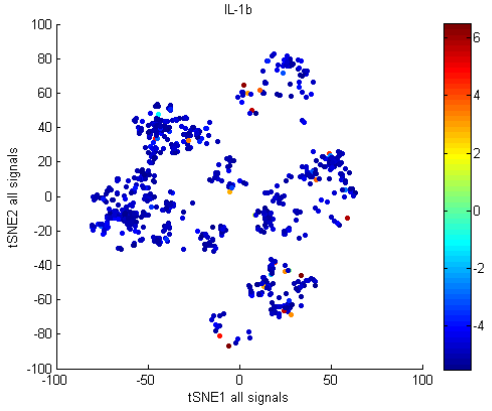
IL-1b
tSNE2 all signals
tSNE1 all signals

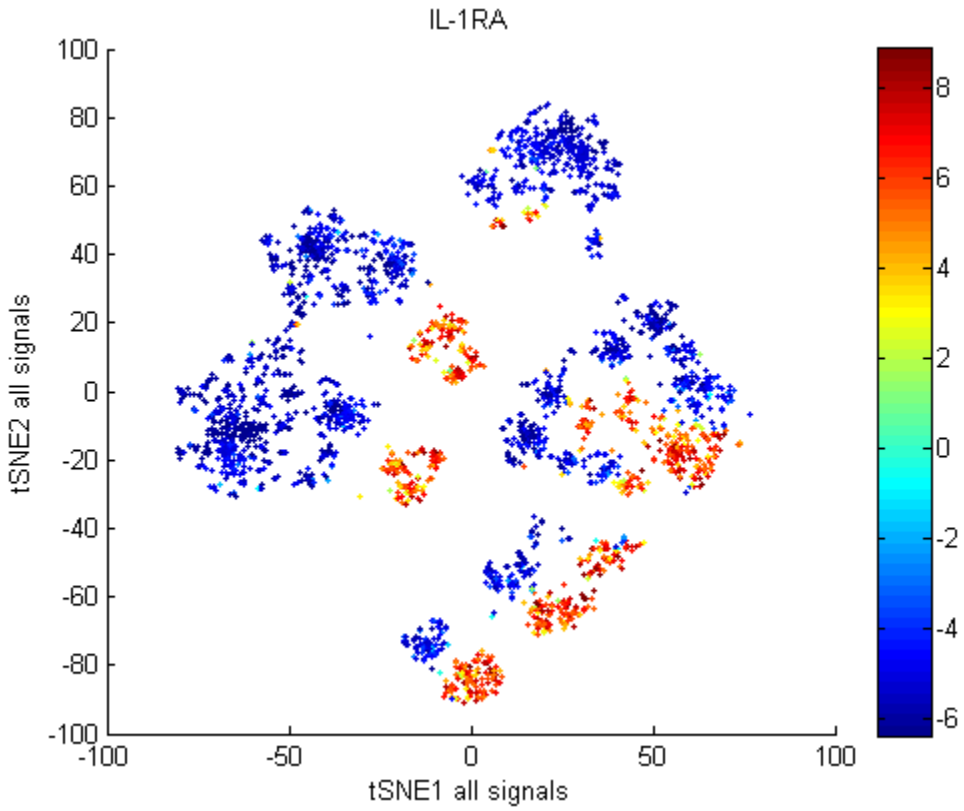
IL-1RA
tSNE2 all signals
tSNE1 all signals

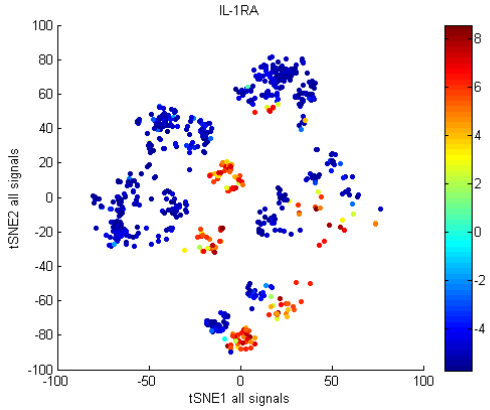
IL-1RA
tSNE2 all signals
tSNE1 all signals

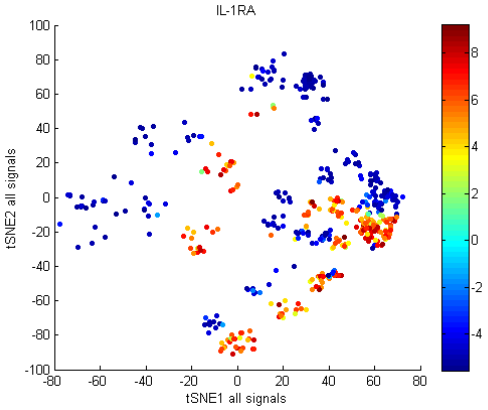
IL-1RA
tSNE2 all signals
tSNE1 all signals

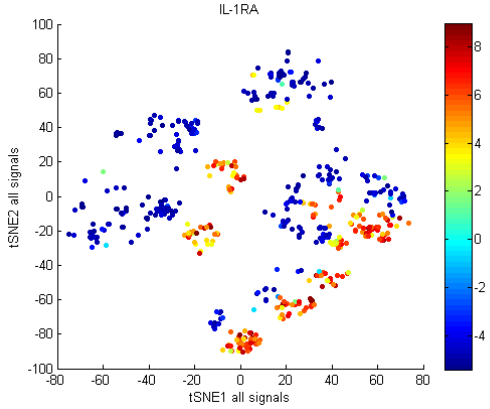
IL-1RA
tSNE2 all signals
tSNE1 all signals

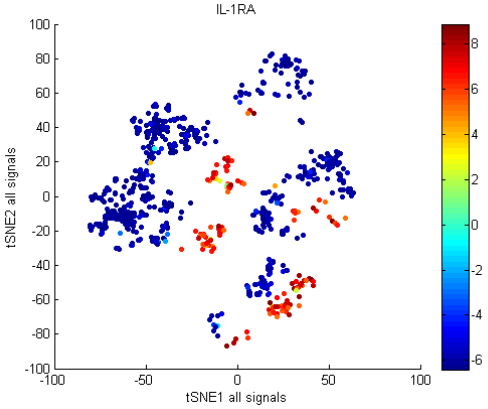
IL-1RA
tSNE2 all signals
tSNE1 all signals

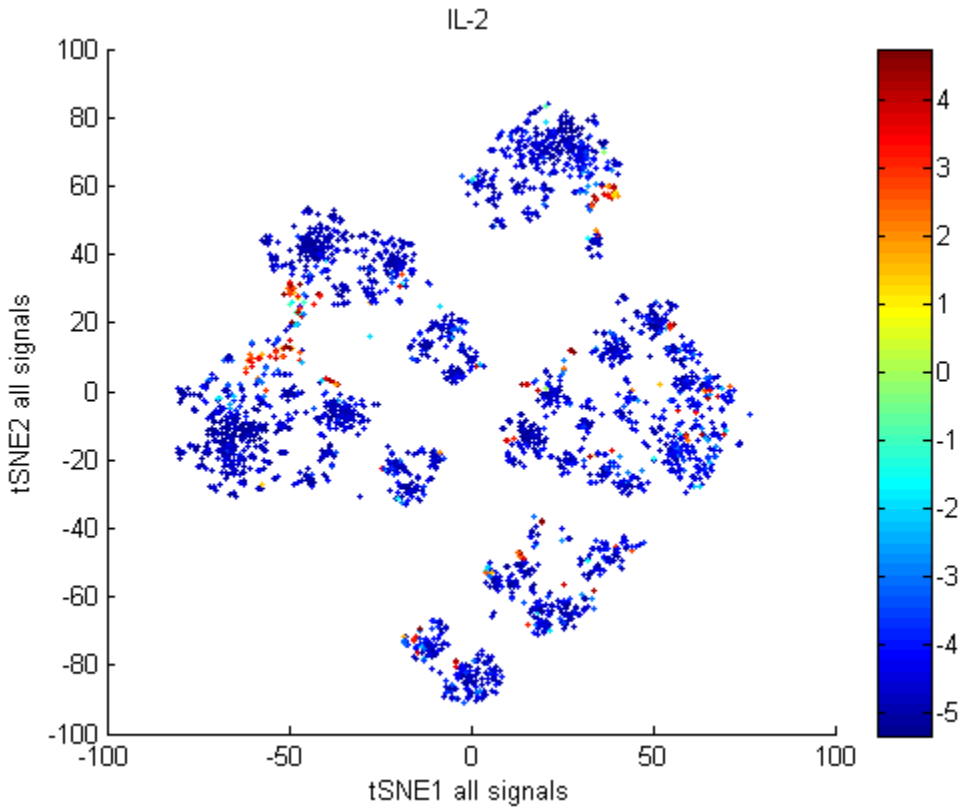
IL-2
tSNE2 all signals
tSNE1 all signals

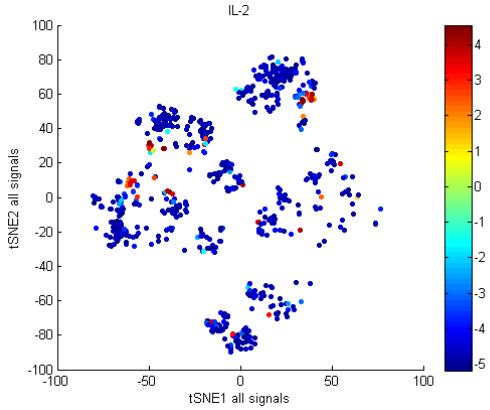
IL-2
tSNE2 all signals
tSNE1 all signals

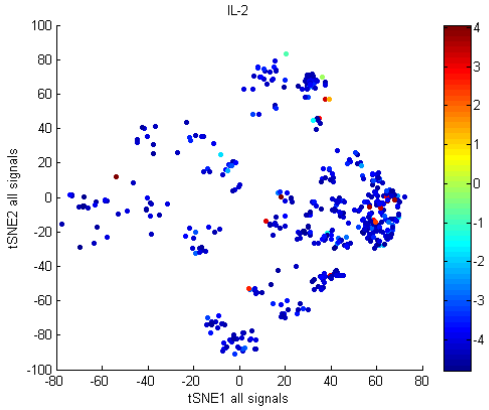
IL-2
tSNE2 all signals
tSNE1 all signals

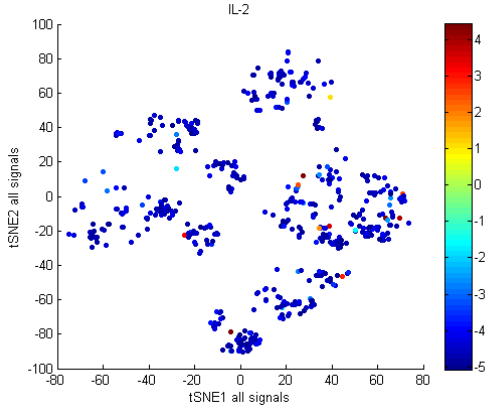
IL-2
tSNE2 all signals
tSNE1 all signals

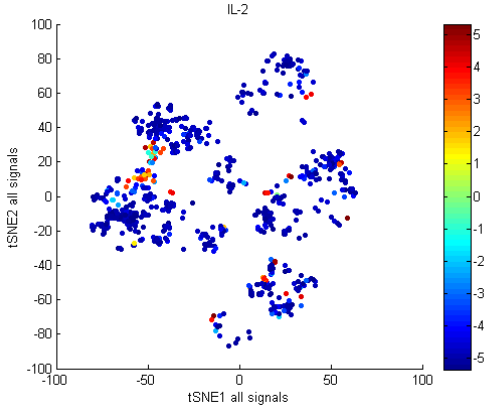
IL-2
tSNE2 all signals
tSNE1 all signals

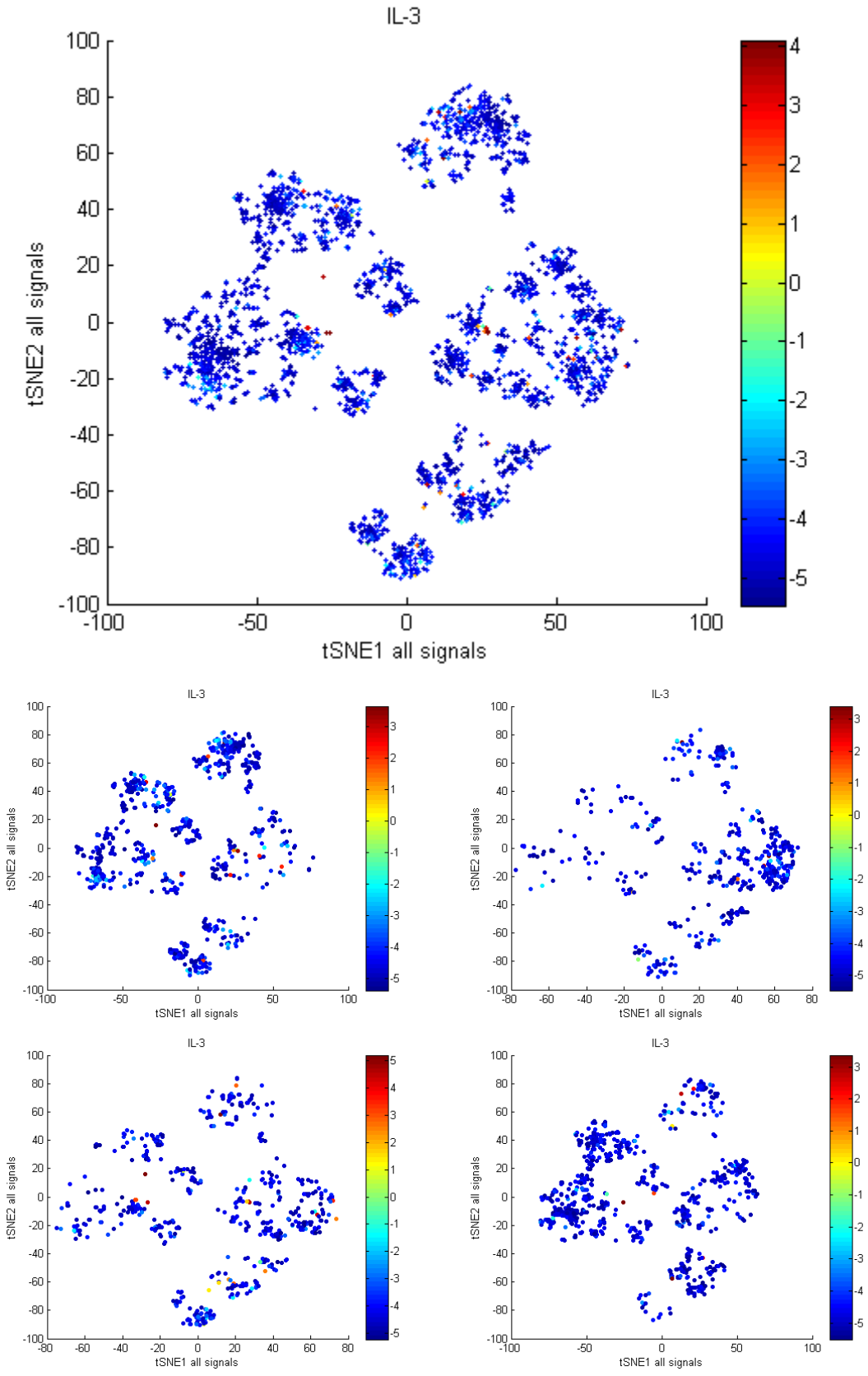
IL-3
tSNE2 all signals
tSNE1 all signals
IL-3
tSNE2 all signals
tSNE1 all signals
IL-3
tSNE2 all signals
tSNE1 all signals
IL-3
tSNE2 all signals
tSNE1 all signals
IL-3
tSNE2 all signals
tSNE1 all signals

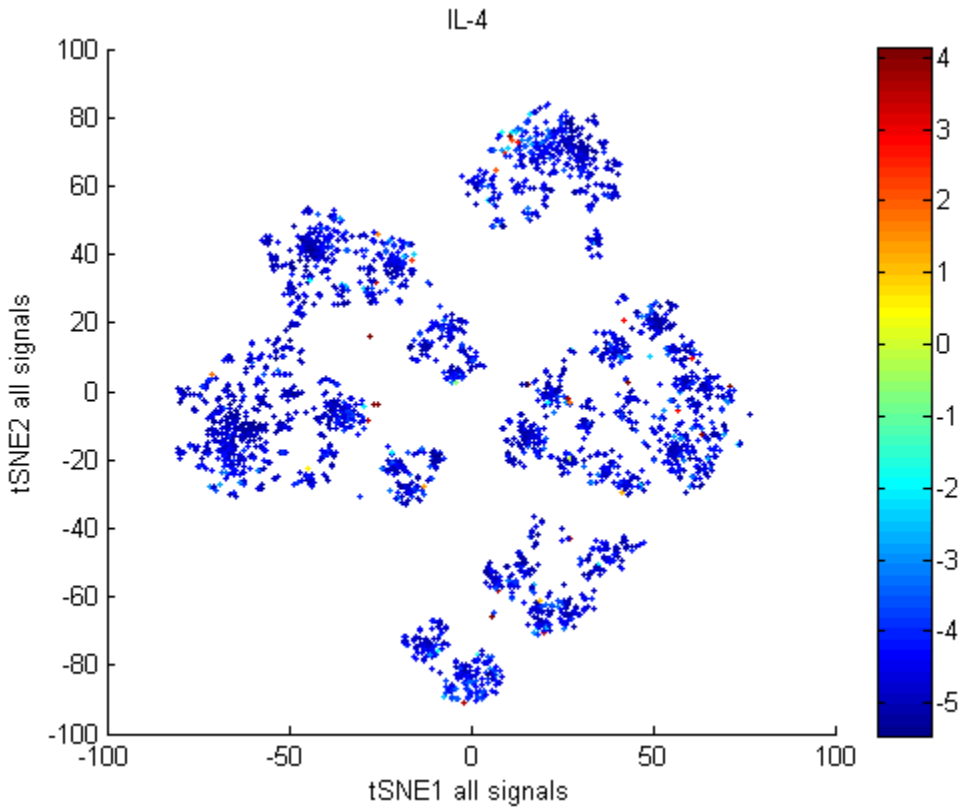
IL-4
tSNE2 all signals
tSNE1 all signals

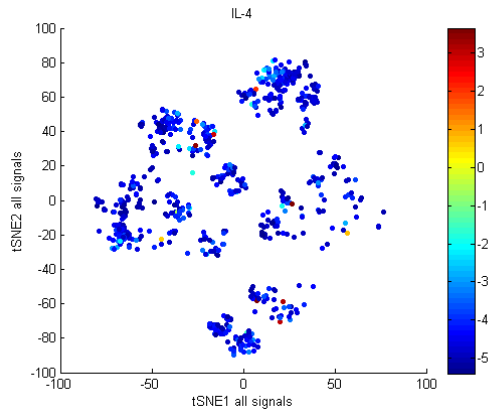
IL-4
tSNE2 all signals
tSNE1 all signals

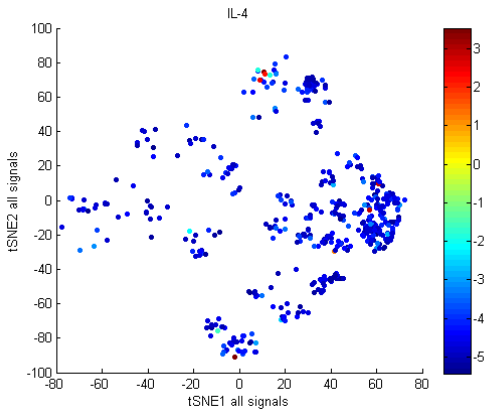
IL-4
tSNE2 all signals
tSNE1 all signals

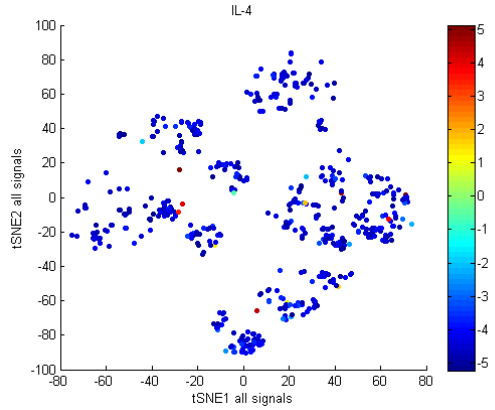
IL-4
tSNE2 all signals
tSNE1 all signals

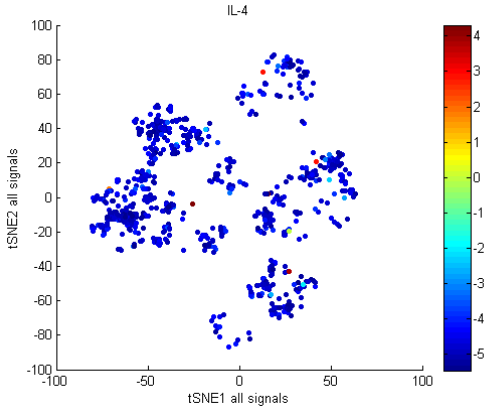
IL-4
tSNE2 all signals
tSNE1 all signals

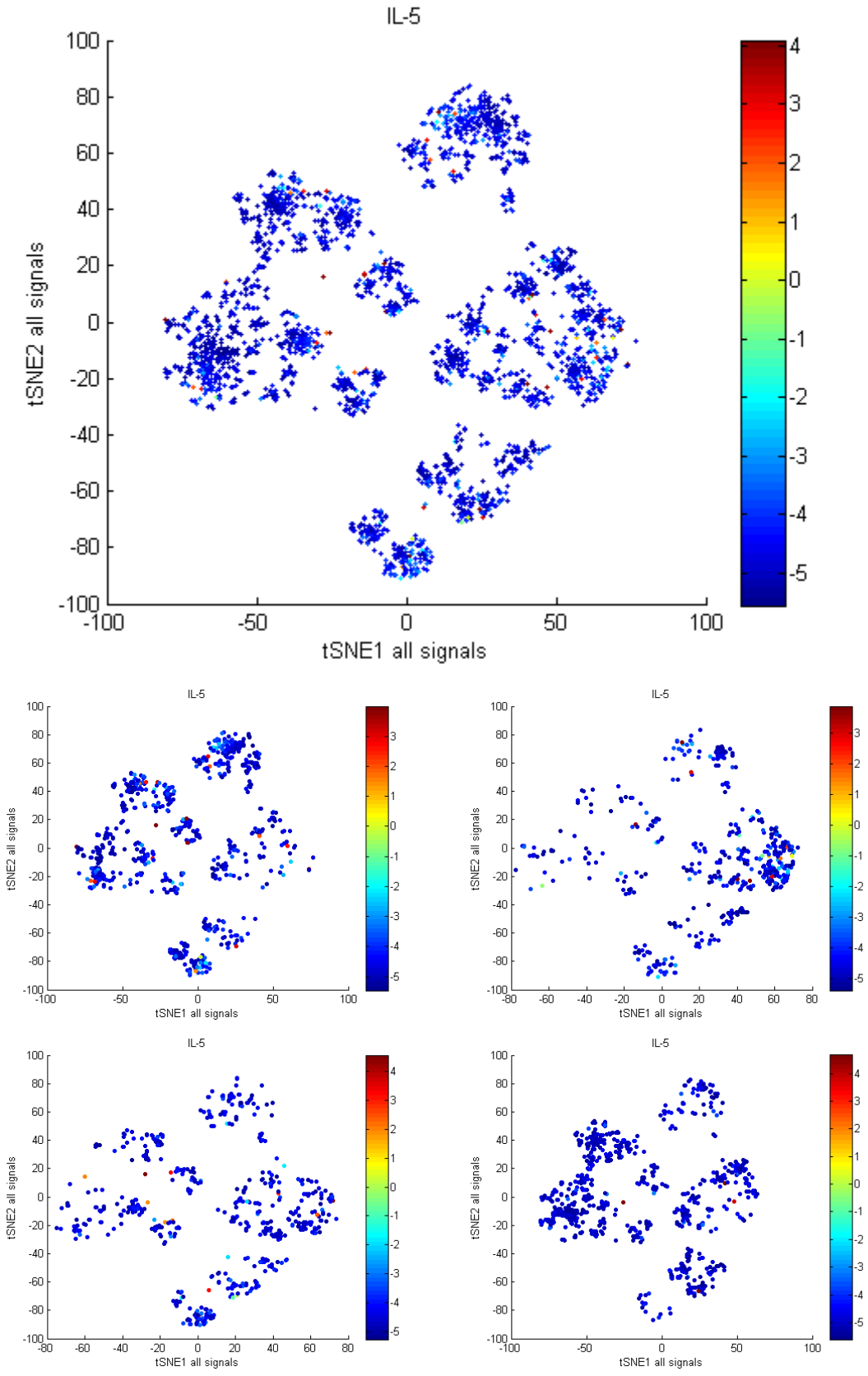
IL-5
tSNE2 all signals
tSNE1 all signals
IL-5
tSNE2 all signals
tSNE1 all signals
IL-5
tSNE2 all signals
tSNE1 all signals
IL-5
tSNE2 all signals
tSNE1 all signals
IL-5
tSNE2 all signals
tSNE1 all signals

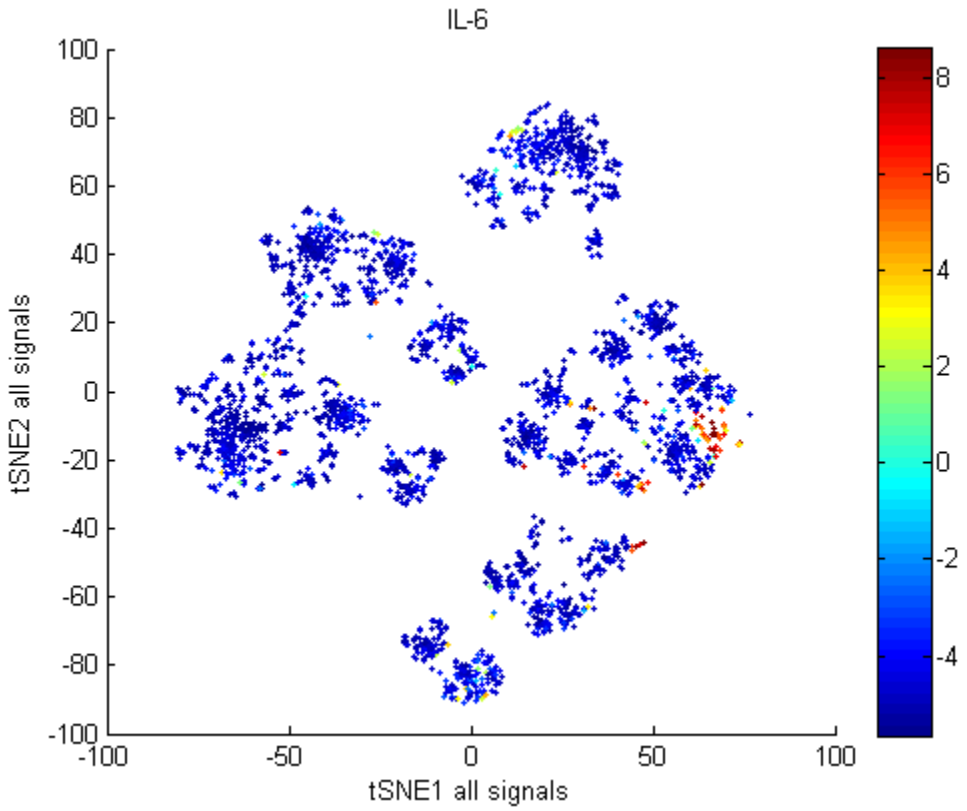
IL-6
tSNE2 all signals
tSNE1 all signals

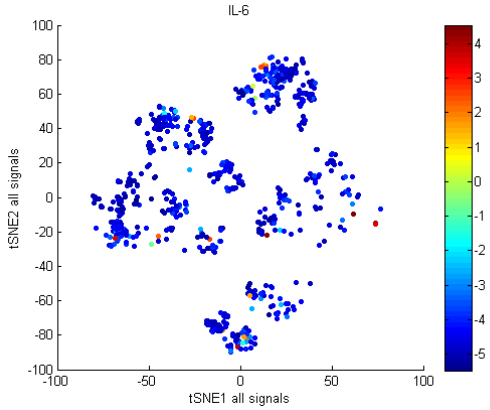
IL-6
tSNE2 all signals
tSNE1 all signals

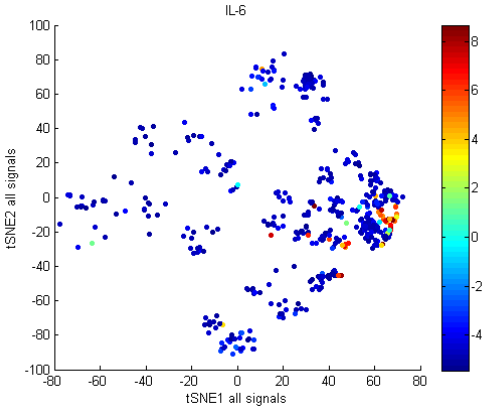
IL-6
tSNE2 all signals
tSNE1 all signals

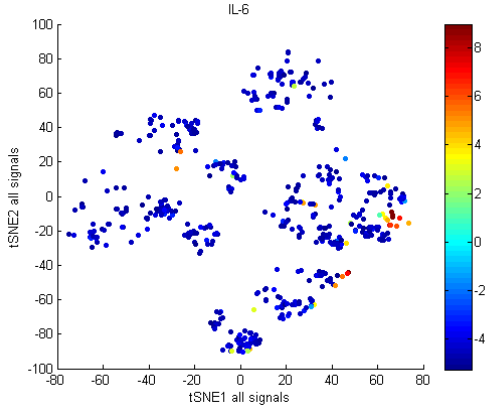
IL-6
tSNE2 all signals
tSNE1 all signals

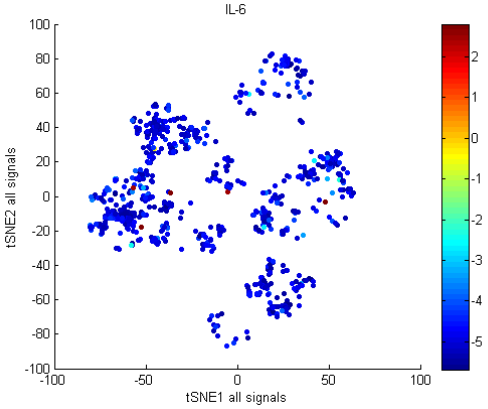
IL-6
tSNE2 all signals
tSNE1 all signals

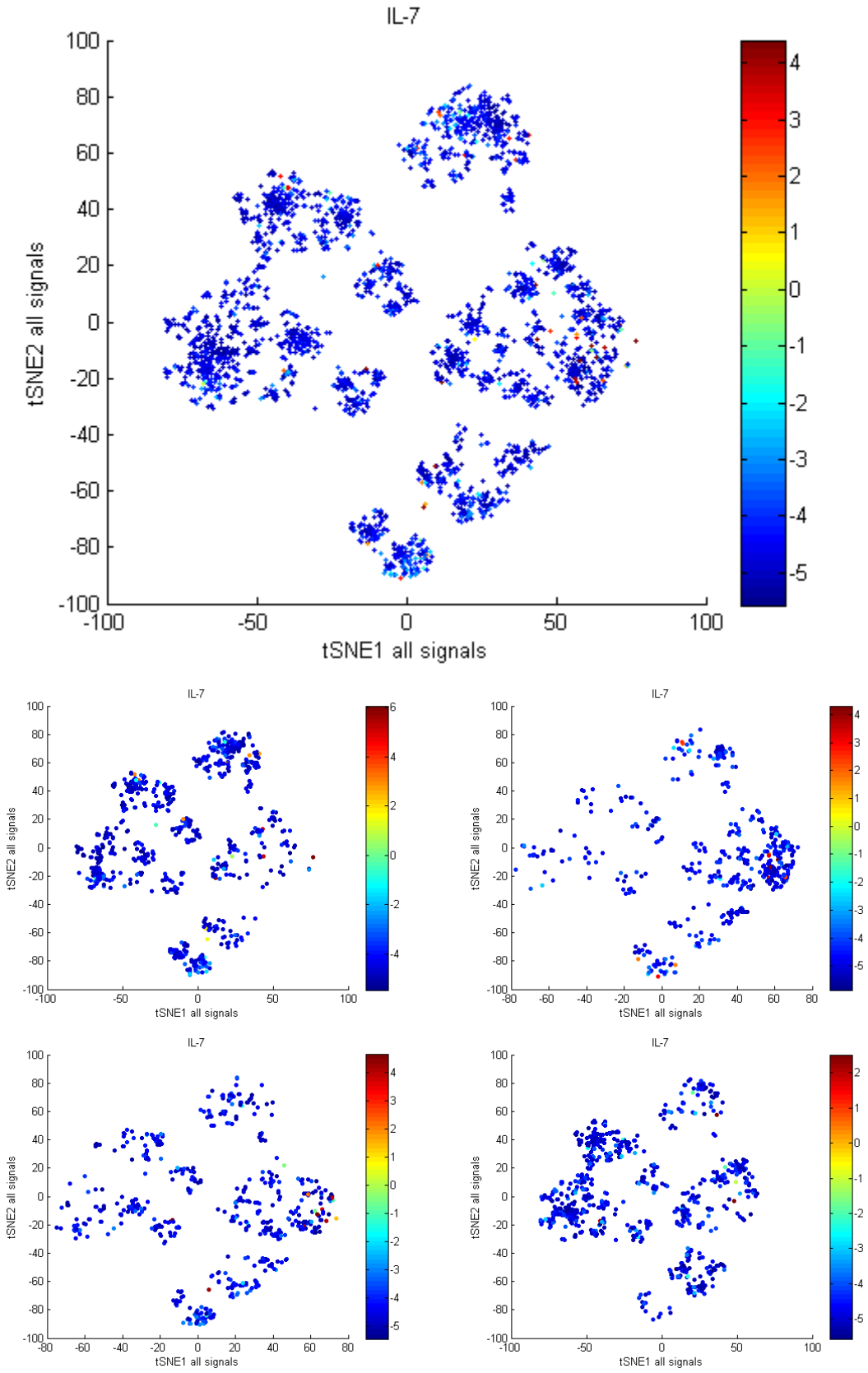
IL-7
tSNE2 all signals
tSNE1 all signals
IL-7
tSNE2 all signals
tSNE1 all signals
IL-7
tSNE2 all signals
tSNE1 all signals
IL-7
tSNE2 all signals
tSNE1 all signals
IL-7
tSNE2 all signals
tSNE1 all signals

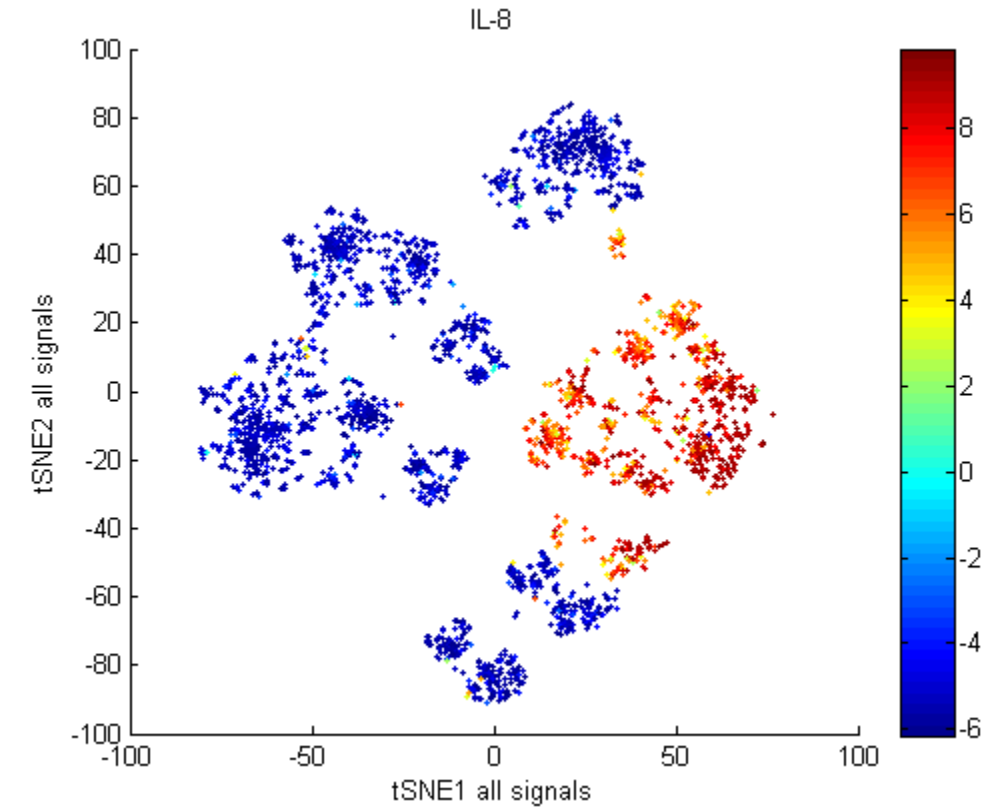
IL-8
tSNE2 all signals
tSNE1 all signals

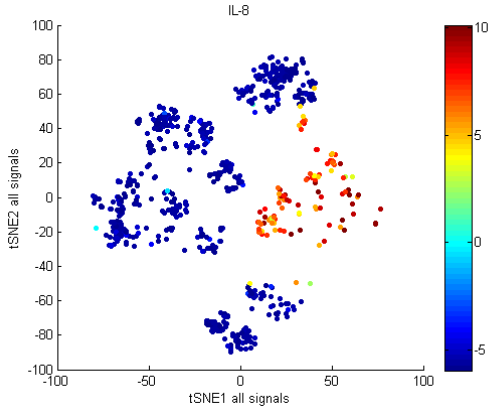
IL-8
tSNE2 all signals
tSNE1 all signals

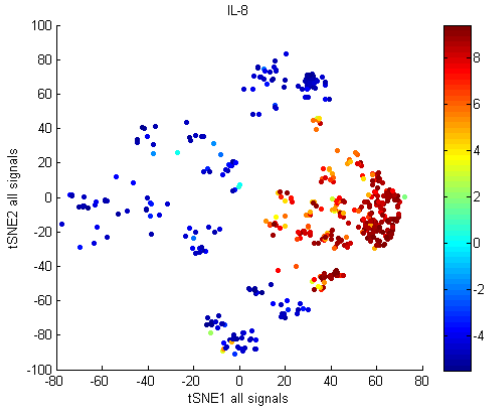
IL-8
tSNE2 all signals
tSNE1 all signals

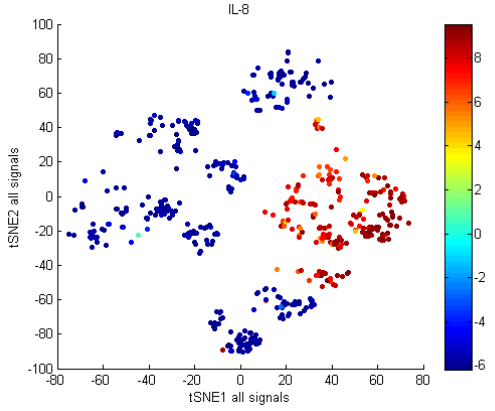
IL-8
tSNE2 all signals
tSNE1 all signals

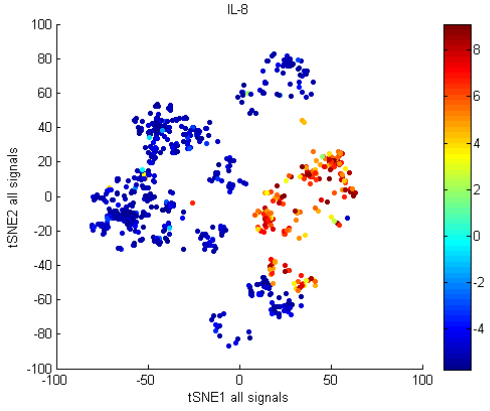
IL-8
tSNE2 all signals
tSNE1 all signals

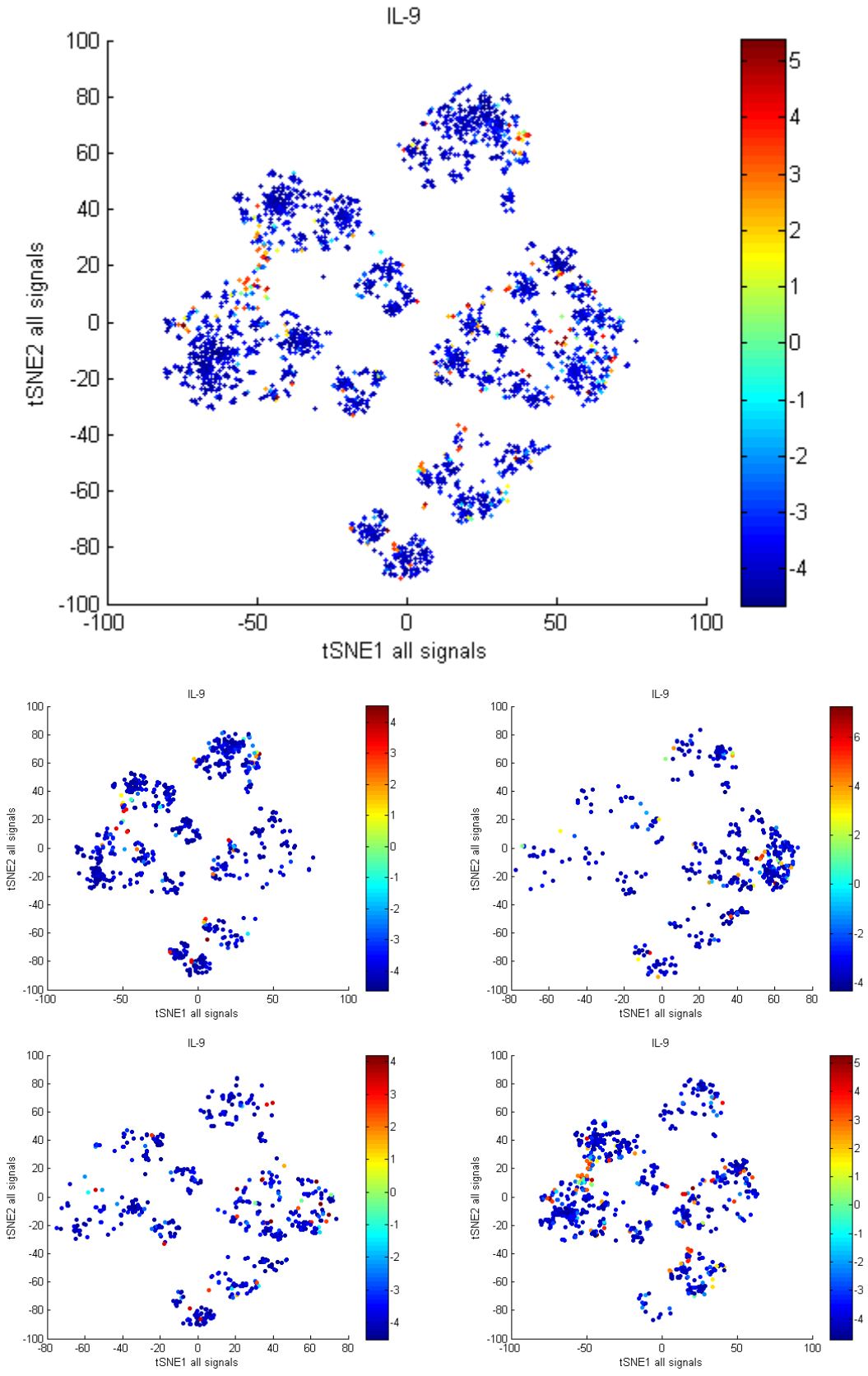
IL-9
tSNE2 all signals
tSNE1 all signals
IL-9
tSNE2 all signals
tSNE1 all signals
IL-9
tSNE2 all signals
tSNE1 all signals
IL-9
tSNE2 all signals
tSNE1 all signals
IL-9
tSNE2 all signals
tSNE1 all signals

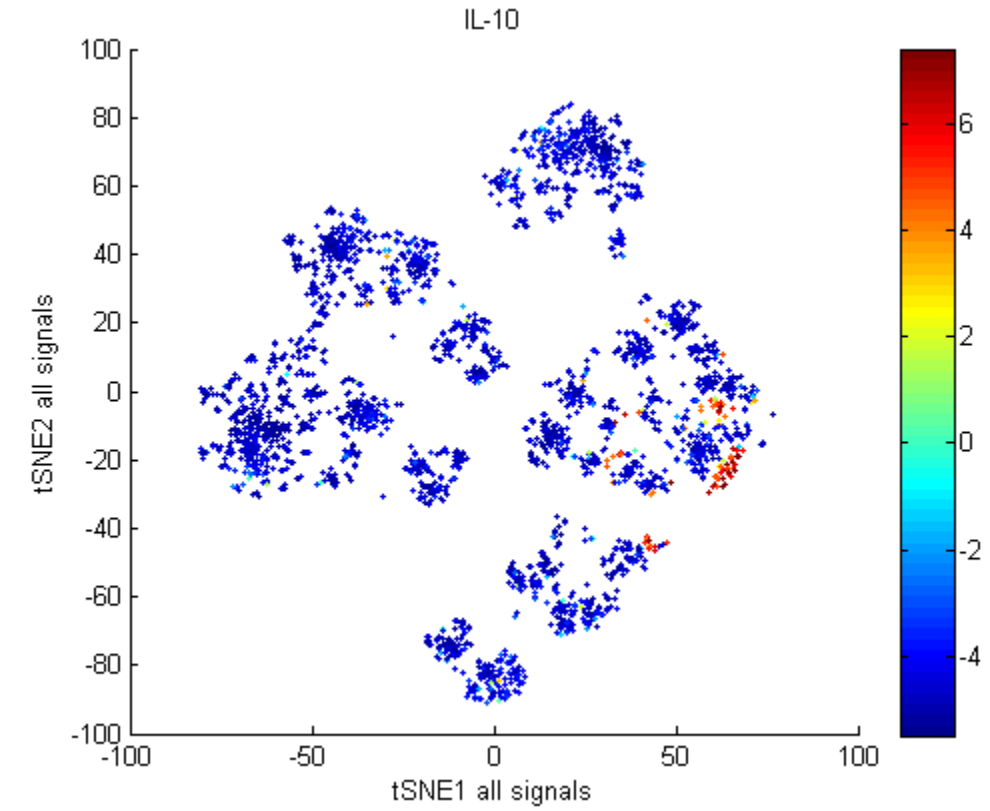
IL-10
tSNE2 all signals
tSNE1 all signals

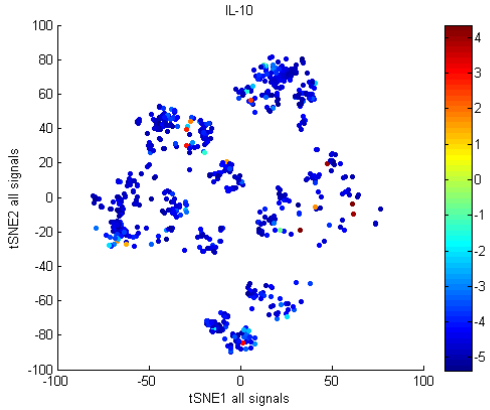
IL-10
tSNE2 all signals
tSNE1 all signals

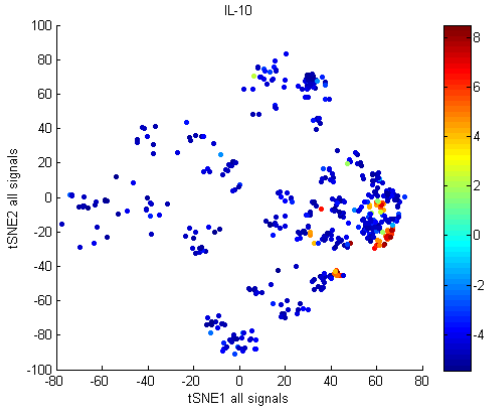
IL-10
tSNE2 all signals
tSNE1 all signals

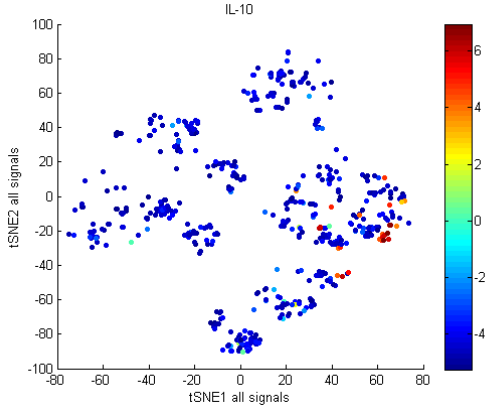
IL-10
tSNE2 all signals
tSNE1 all signals

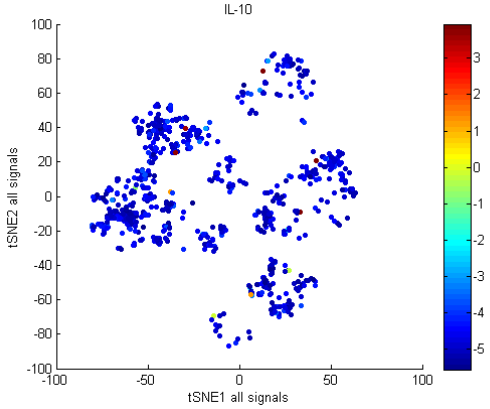
IL-10
tSNE2 all signals
tSNE1 all signals

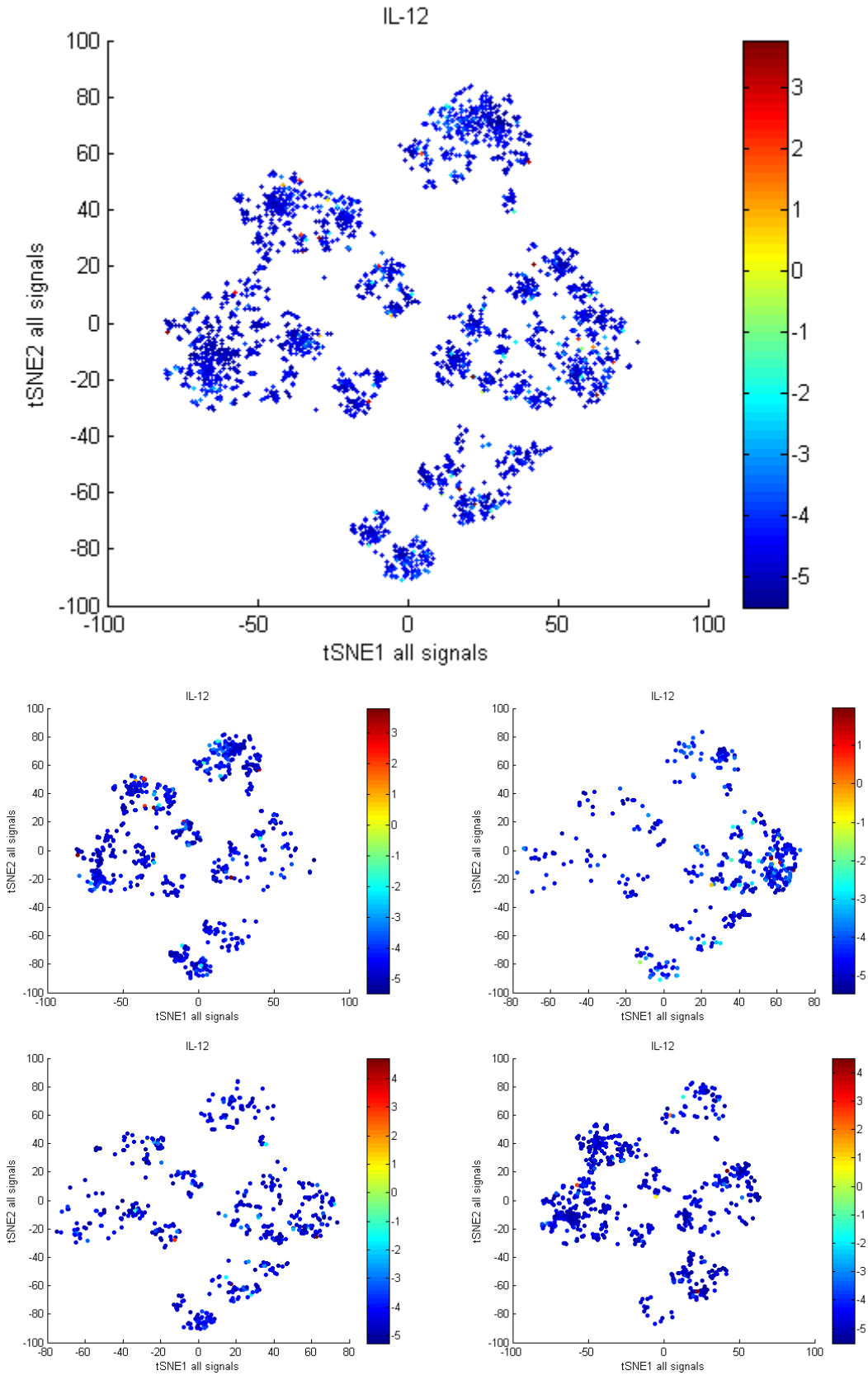
IL-12
tSNE2 all signals
tSNE1 all signals
IL-12
tSNE2 all signals
tSNE1 all signals
IL-12
tSNE2 all signals
tSNE1 all signals
IL-12
tSNE2 all signals
tSNE1 all signals
IL-12
tSNE2 all signals
tSNE1 all signals

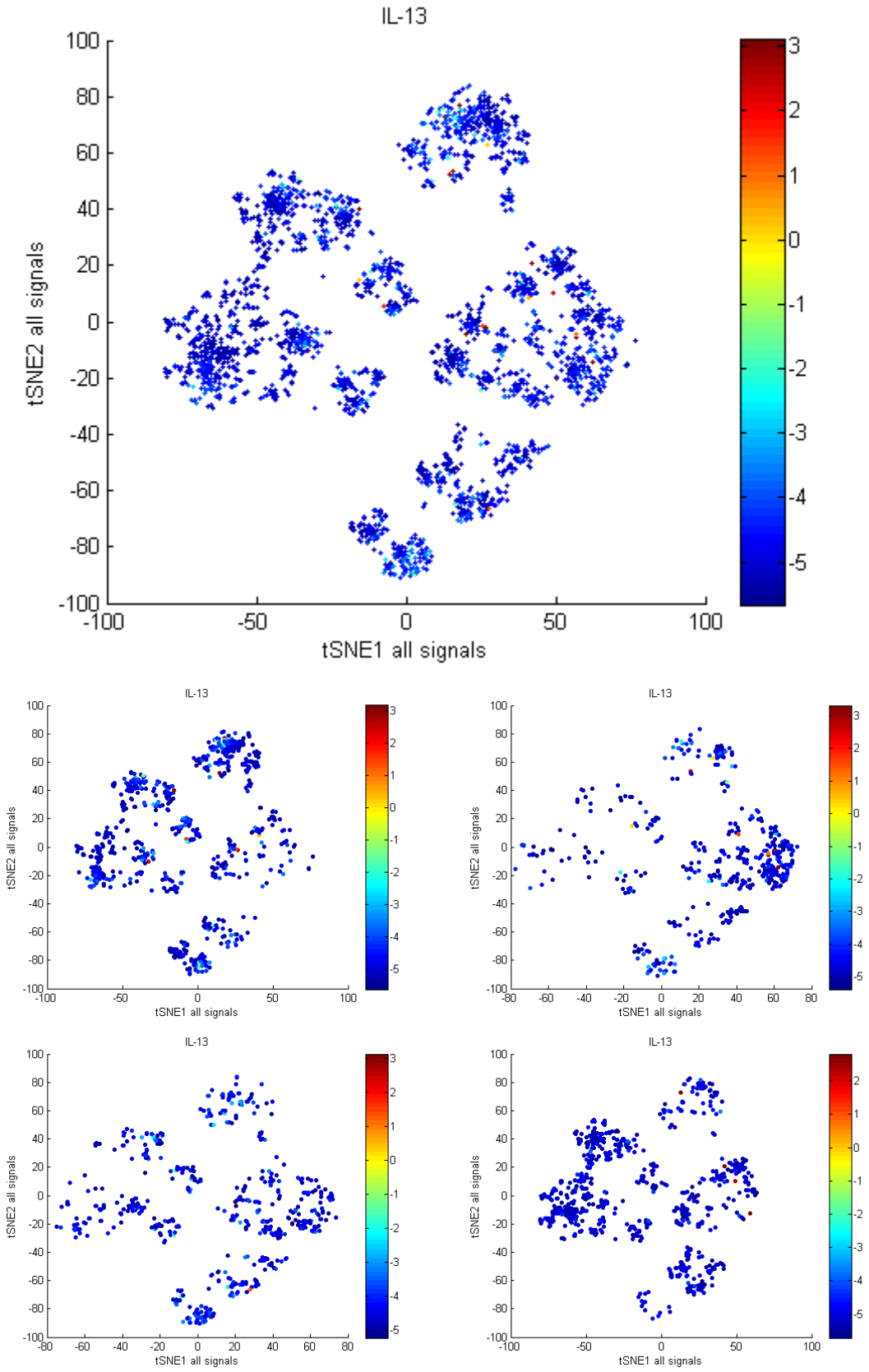
IL-13
tSNE2 all signals
tSNE1 all signals
IL-13
tSNE2 all signals
tSNE1 all signals
IL-13
tSNE2 all signals
tSNE1 all signals
IL-13
tSNE2 all signals
tSNE1 all signals
IL-13
tSNE2 all signals
tSNE1 all signals

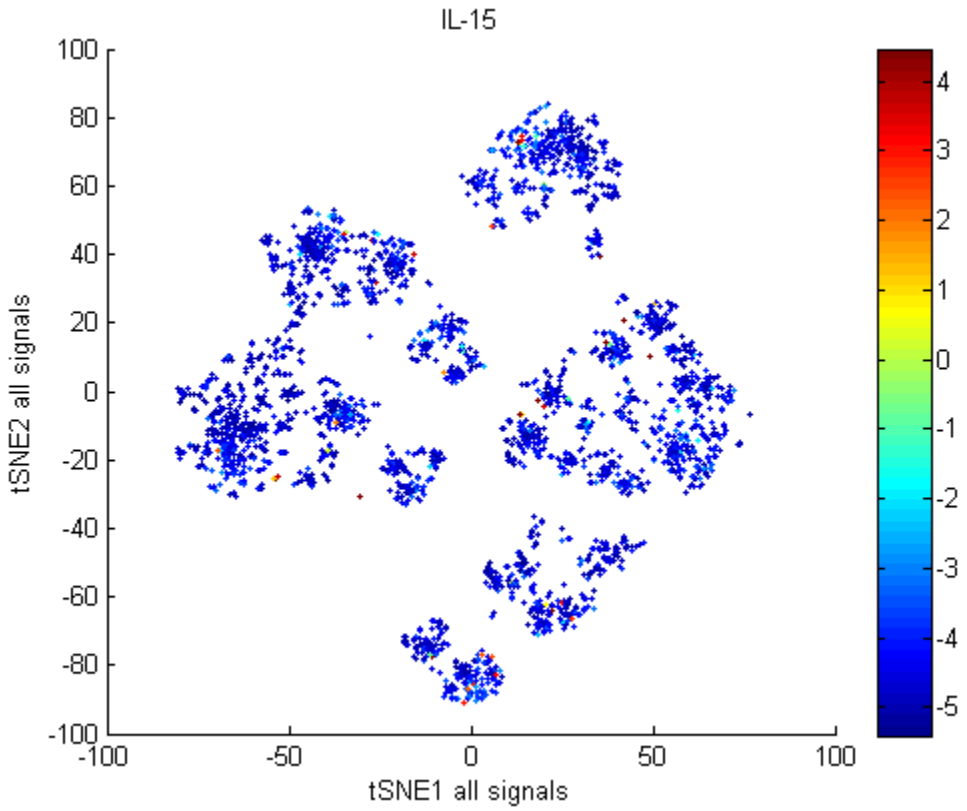
IL-15
tSNE2 all signals
tSNE1 all signals

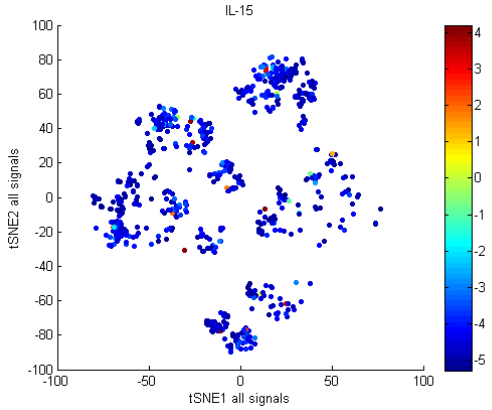
IL-15
tSNE2 all signals
tSNE1 all signals

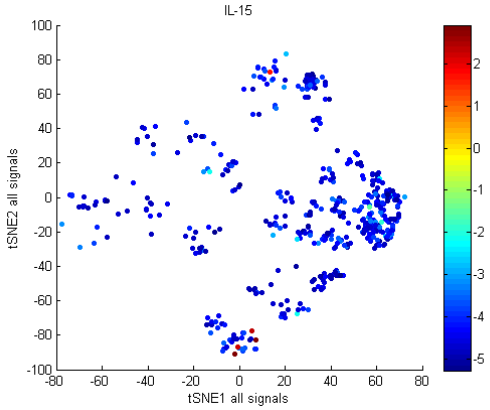
IL-15
tSNE2 all signals
tSNE1 all signals

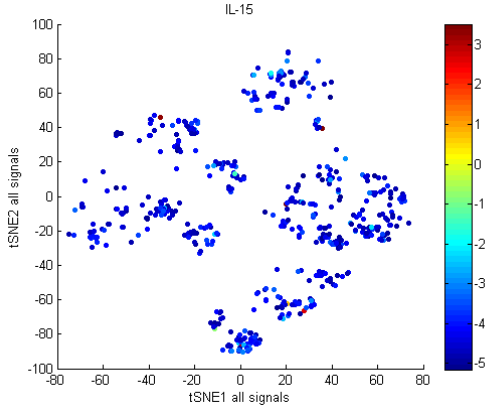
IL-15
tSNE2 all signals
tSNE1 all signals

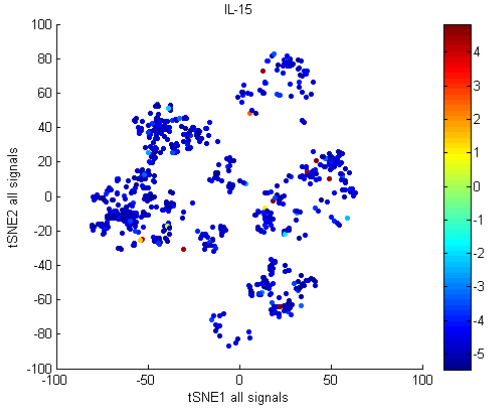
IL-15
tSNE2 all signals
tSNE1 all signals

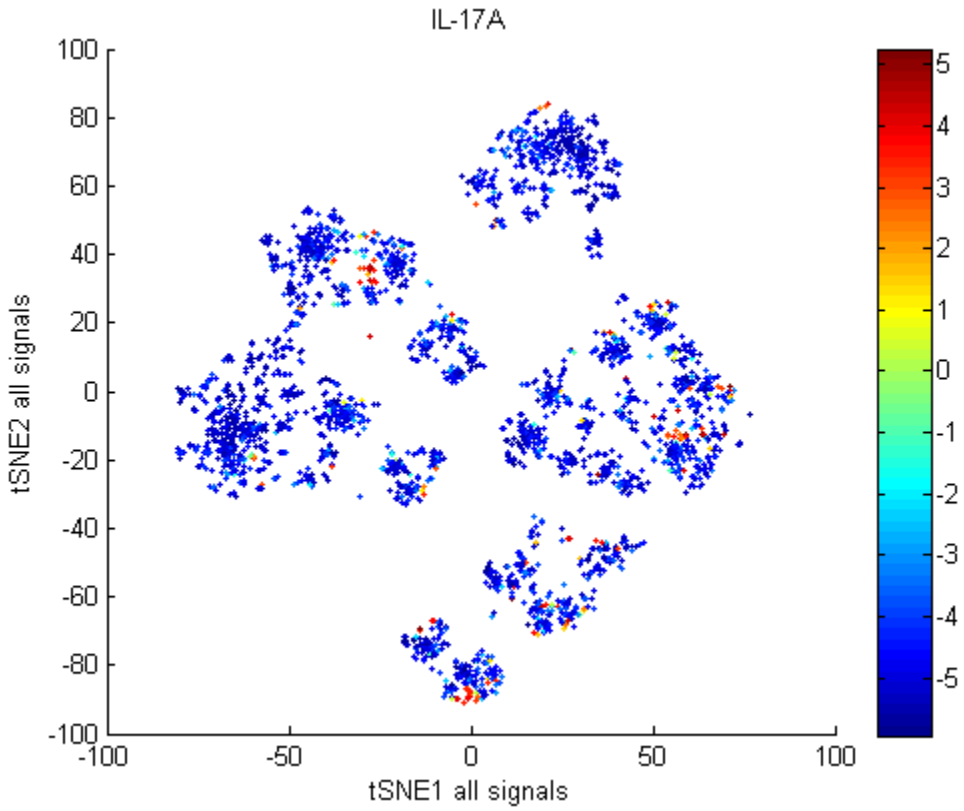
IL-17A
tSNE2 all signals
tSNE1 all signals

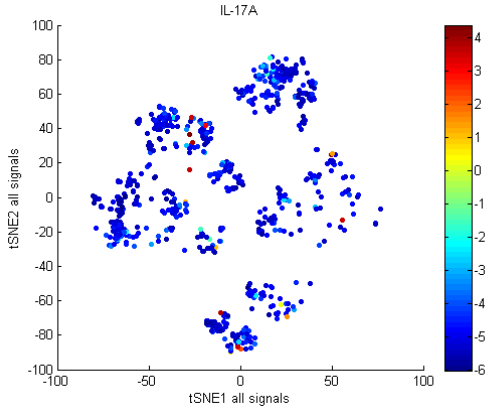
IL-17A
tSNE2 all signals
tSNE1 all signals

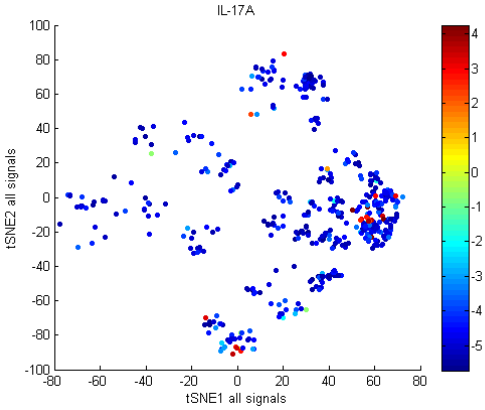
IL-17A
tSNE2 all signals
tSNE1 all signals

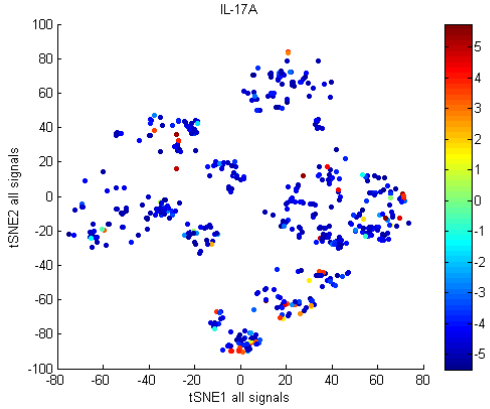
IL-17A
tSNE2 all signals
tSNE1 all signals

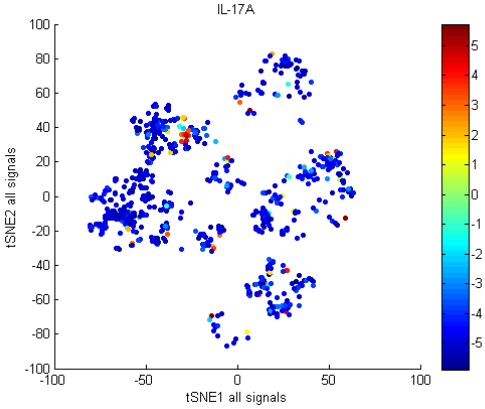
IL-17A
tSNE2 all signals
tSNE1 all signals

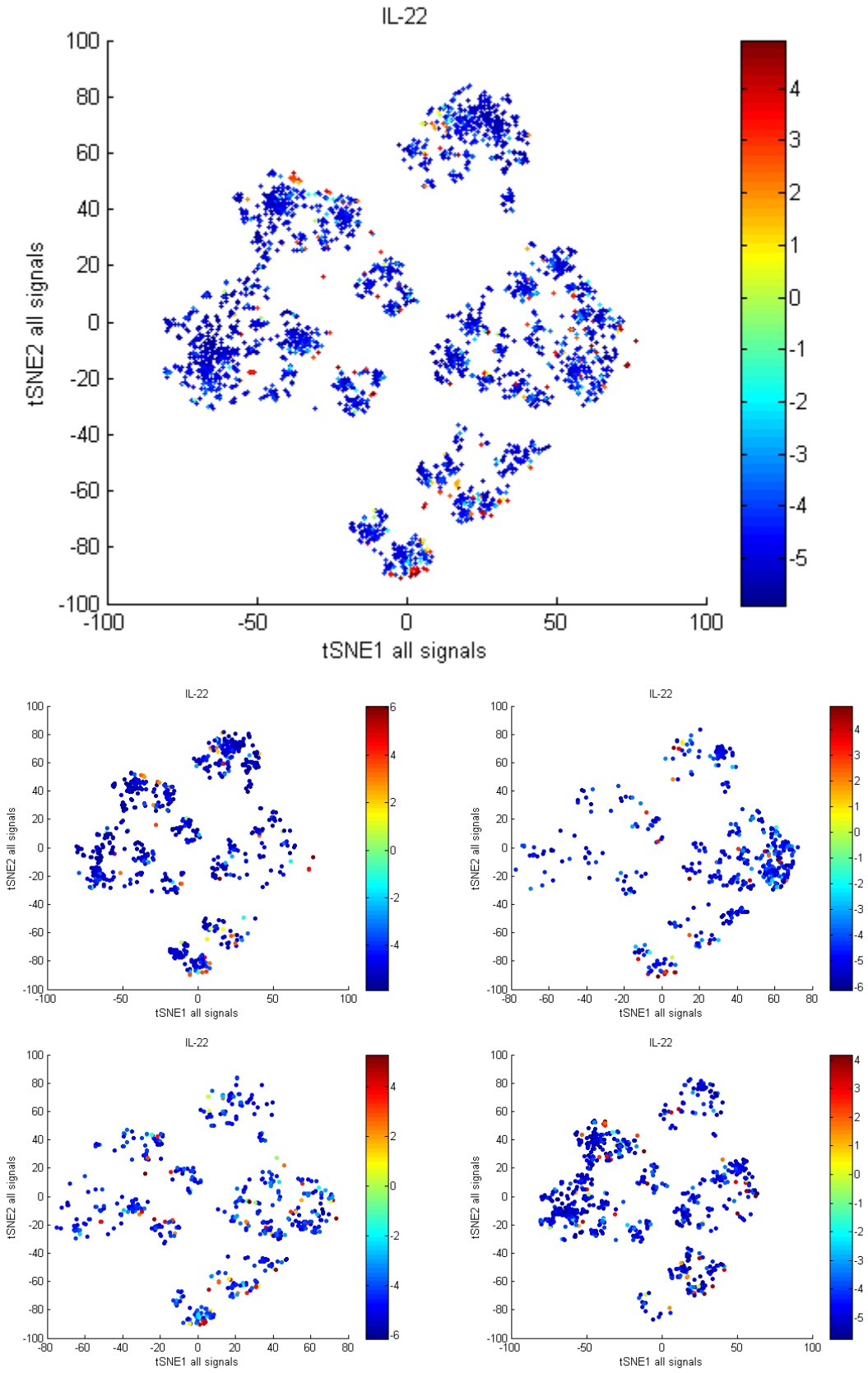
IL-22
tSNE2 all signals
tSNE1 all signals
IL-22
tSNE2 all signals
tSNE1 all signals
IL-22
tSNE2 all signals
tSNE1 all signals
IL-22
tSNE2 all signals
tSNE1 all signals
IL-22
tSNE2 all signals
tSNE1 all signals

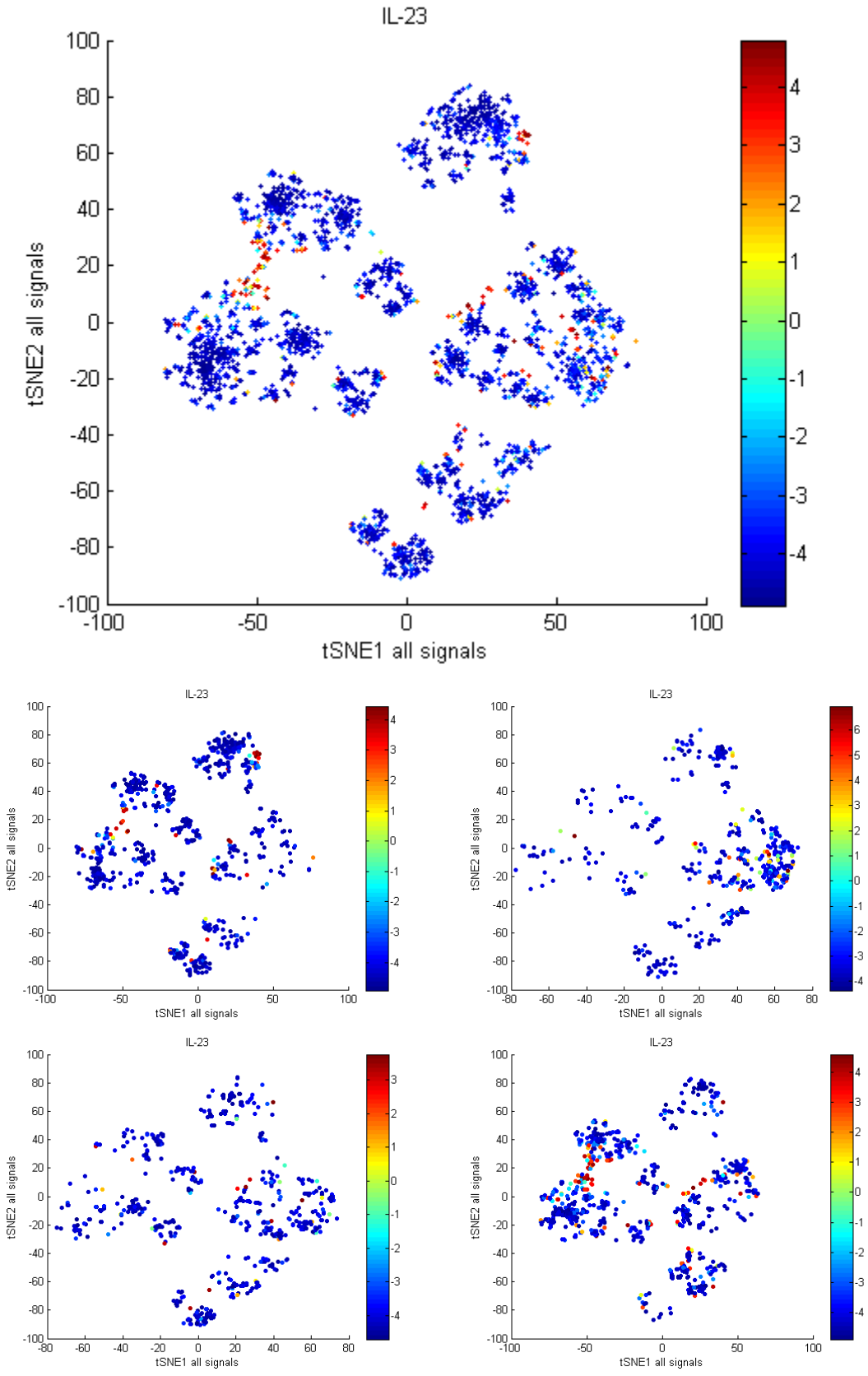
IL-23
tSNE2 all signals
tSNE1 all signals
IL-23
tSNE2 all signals
tSNE1 all signals
IL-23
tSNE2 all signals
tSNE1 all signals
IL-23
tSNE2 all signals
tSNE1 all signals
IL-23
tSNE2 all signals
tSNE1 all signals

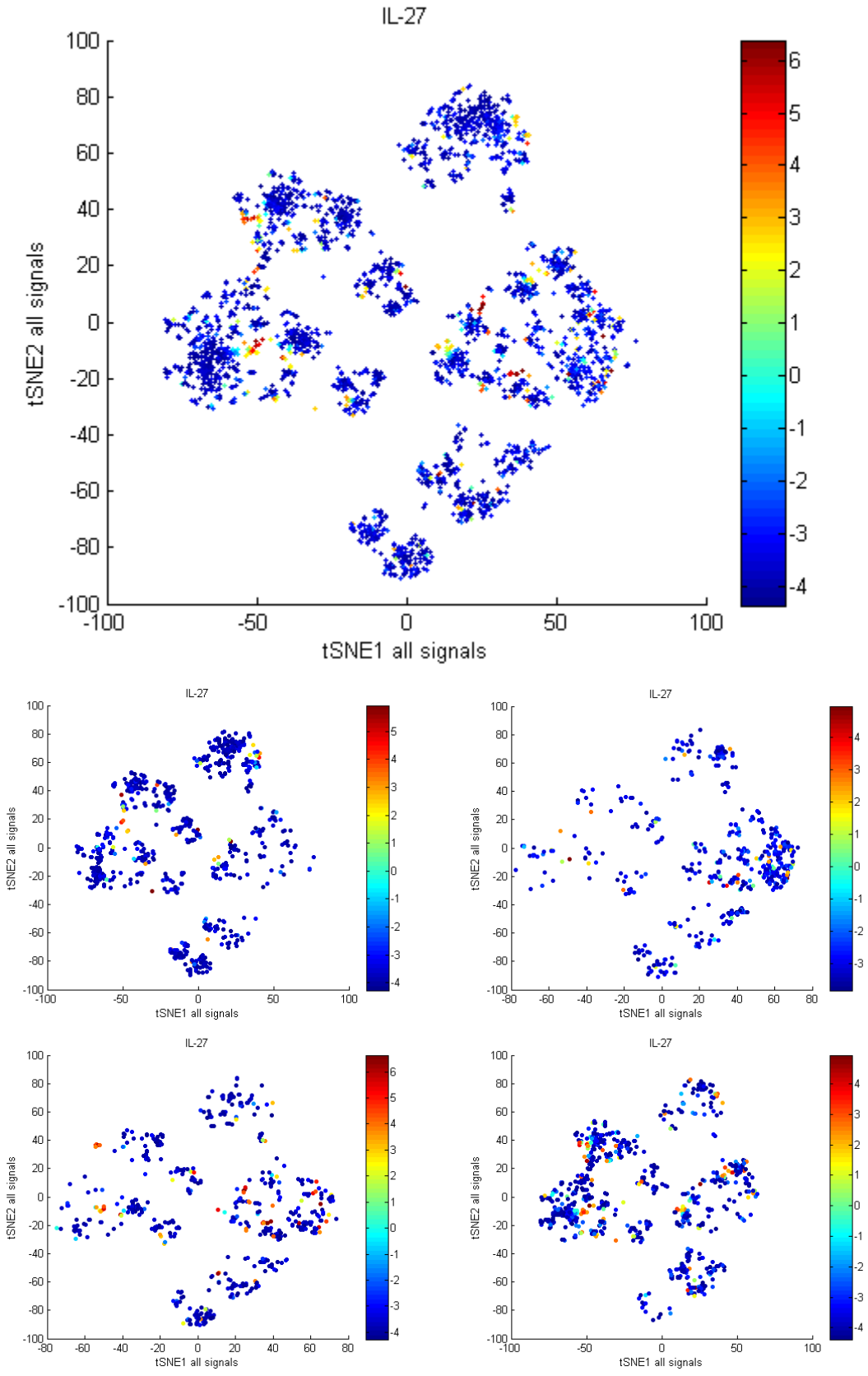
IL-27
tSNE2 all signals
tSNE1 all signals
IL-27
tSNE2 all signals
tSNE1 all signals
IL-27
tSNE2 all signals
tSNE1 all signals
IL-27
tSNE2 all signals
tSNE1 all signals
IL-27
tSNE2 all signals
tSNE1 all signals

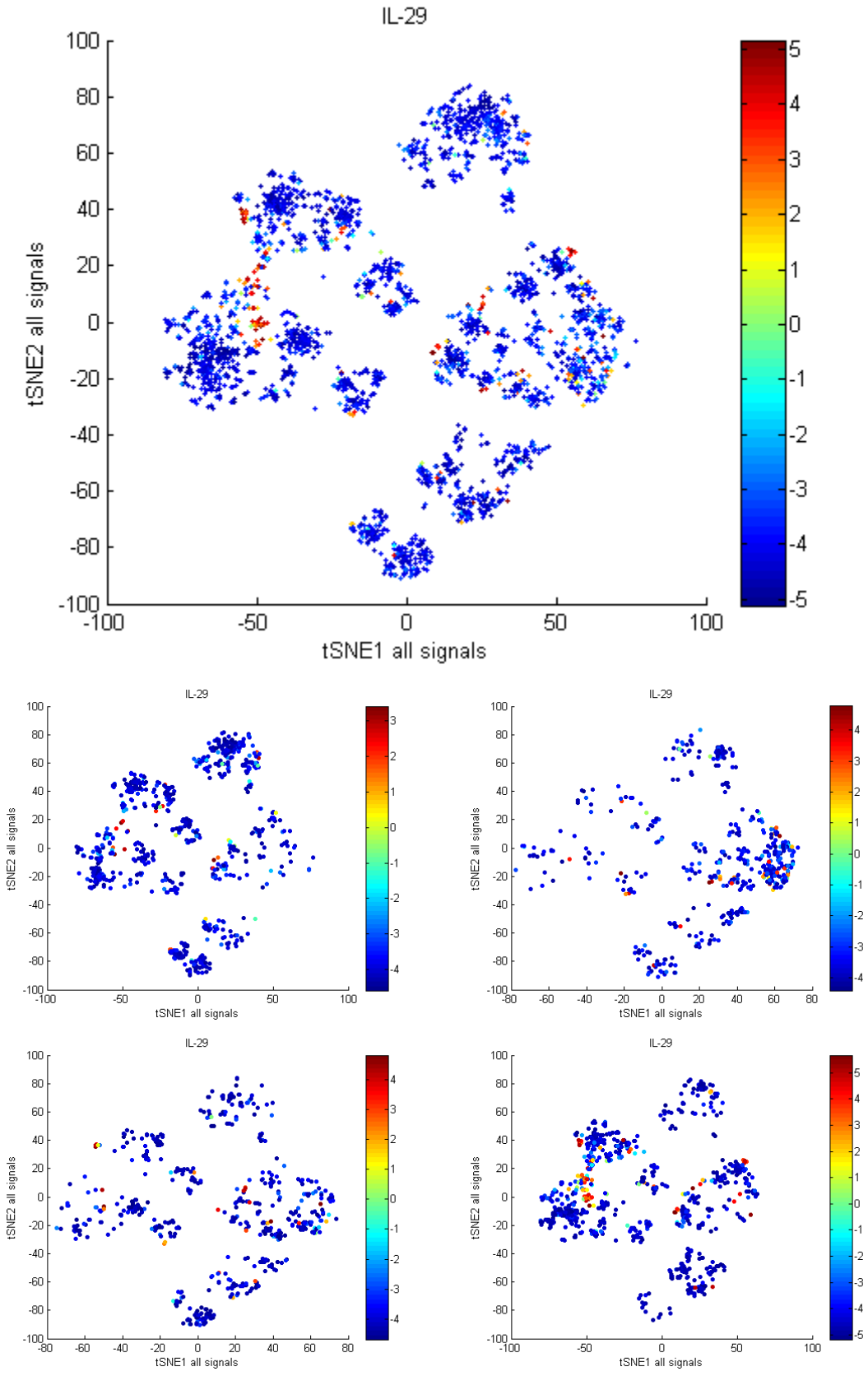
IL-29
tSNE2 all signals
tSNE1 all signals
IL-29
tSNE2 all signals
tSNE1 all signals
IL-29
tSNE2 all signals
tSNE1 all signals
IL-29
tSNE2 all signals
tSNE1 all signals
IL-29
tSNE2 all signals
tSNE1 all signals

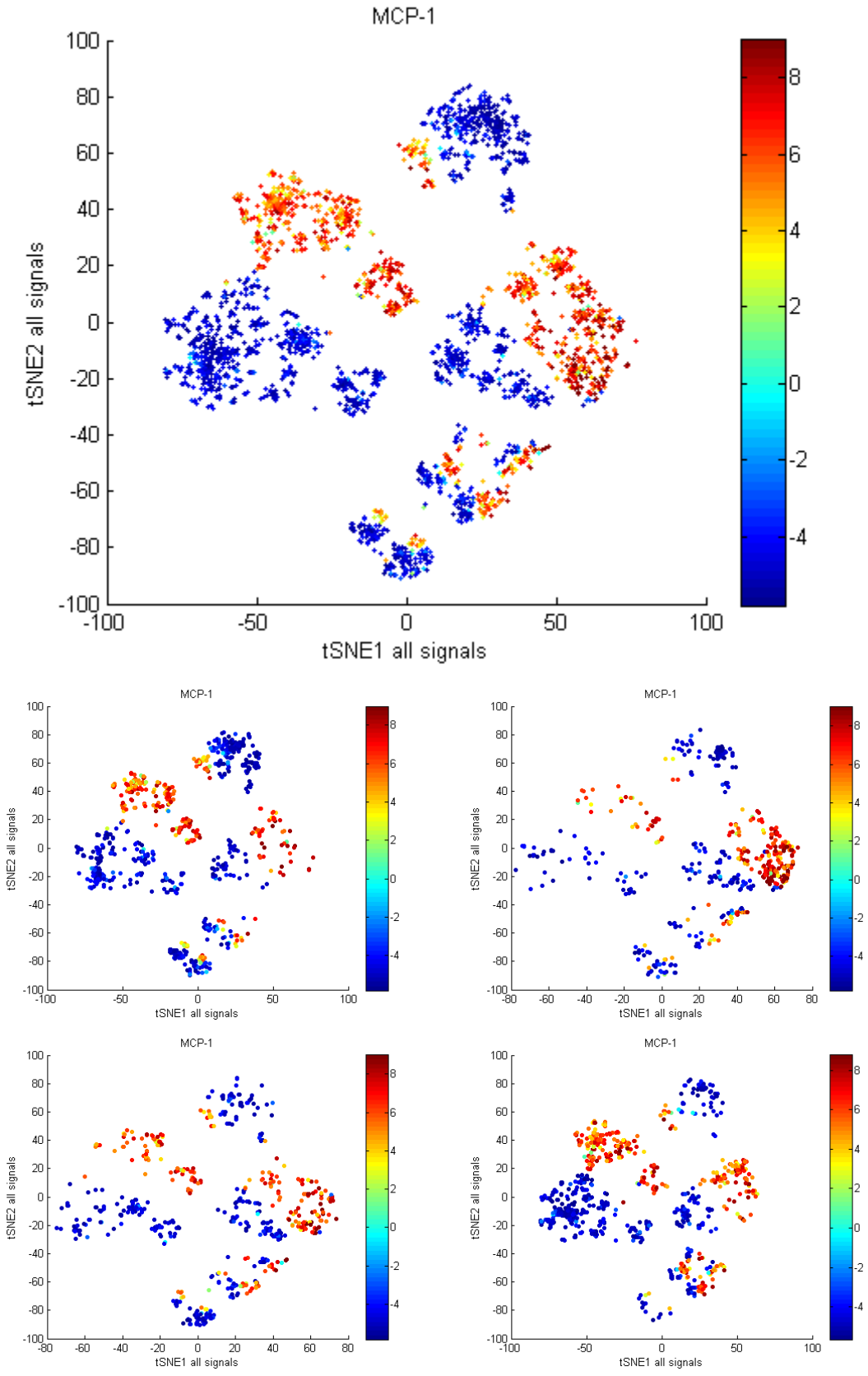
MCP-1
tSNE2 all signals
tSNE1 all signals
MCP-1
tSNE2 all signals
tSNE1 all signals
MCP-1
tSNE2 all signals
tSNE1 all signals
MCP-1
tSNE2 all signals
tSNE1 all signals
MCP-1
tSNE2 all signals
tSNE1 all signals

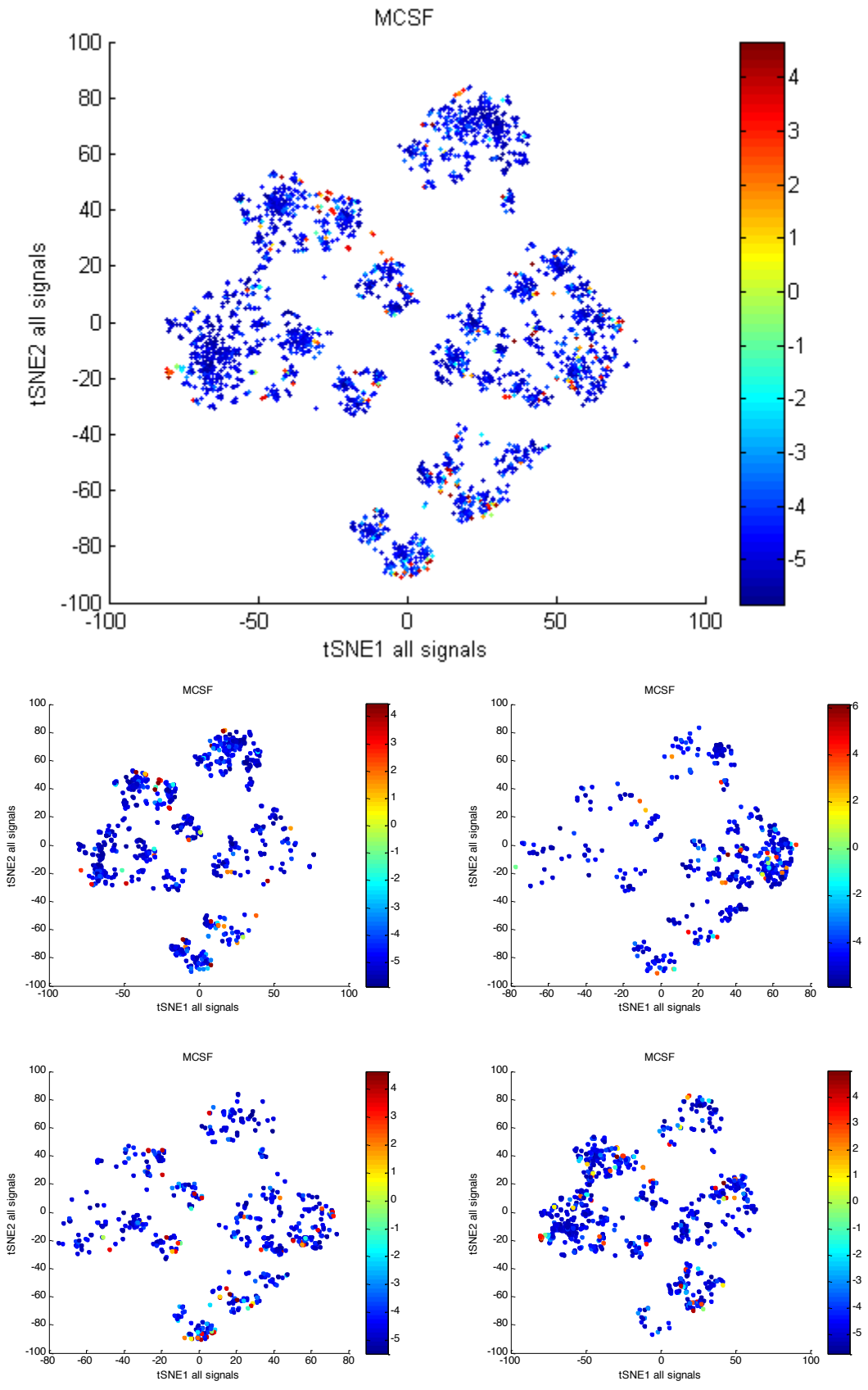
MCSF
tSNE2 all signals
tSNE1 all signals
MCSF
tSNE2 all signals
tSNE1 all signals
MCSF
tSNE2 all signals
tSNE1 all signals
MCSF
tSNE2 all signals
tSNE1 all signals
MCSF
tSNE2 all signals
tSNE1 all signals

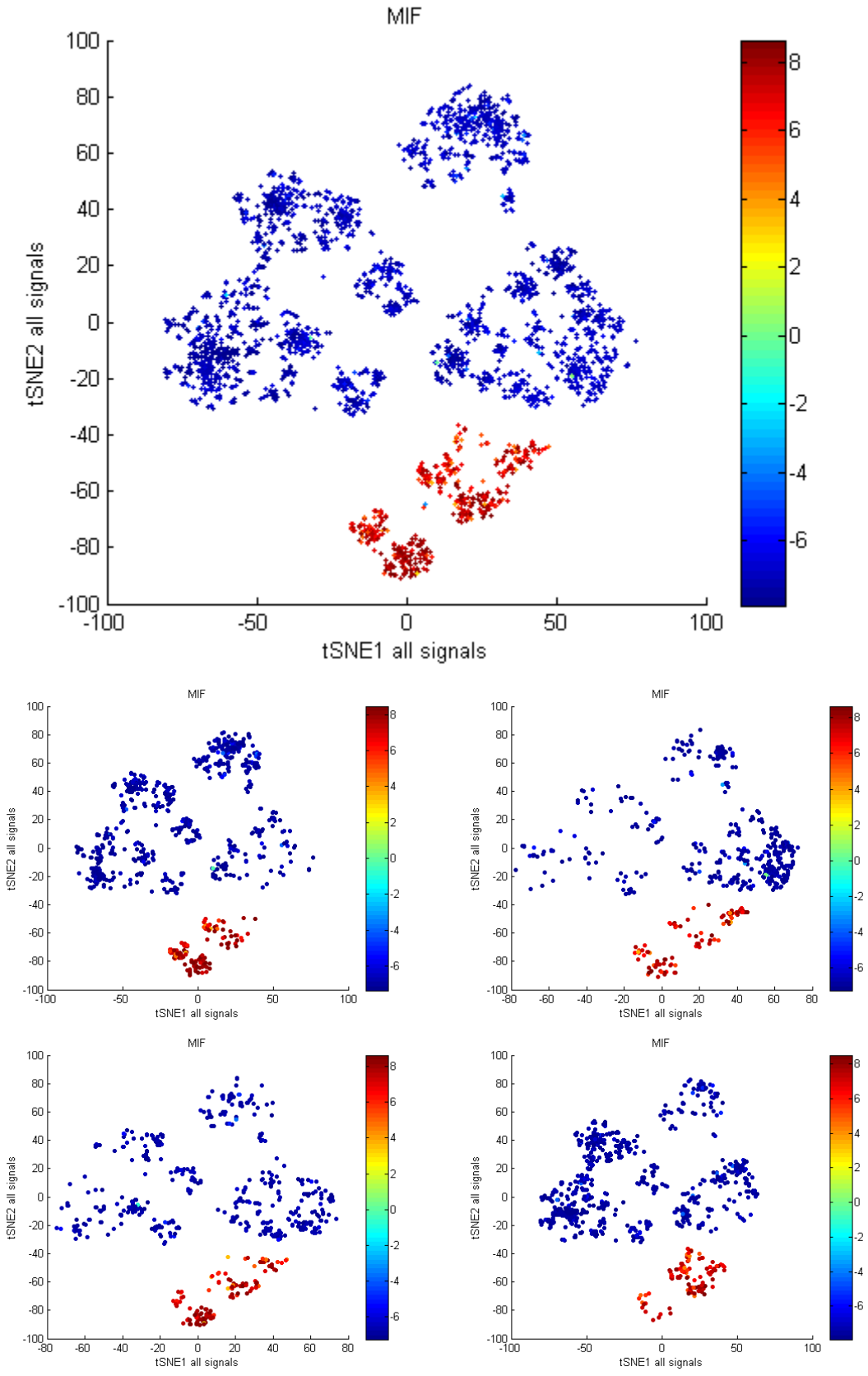
MIF
tSNE2 all signals
tSNE1 all signals
MIF
tSNE2 all signals
tSNE1 all signals
MIF
tSNE2 all signals
tSNE1 all signals
MIF
tSNE2 all signals
tSNE1 all signals
MIF
tSNE2 all signals
tSNE1 all signals

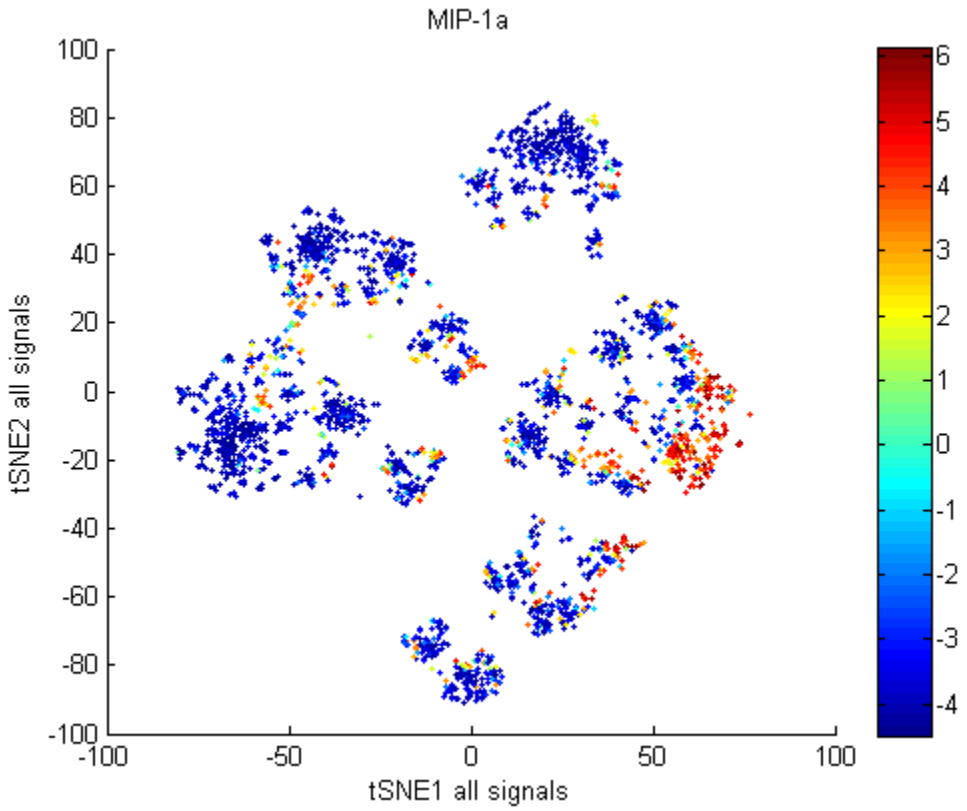
MIP-1a
tSNE2 all signals
tSNE1 all signals

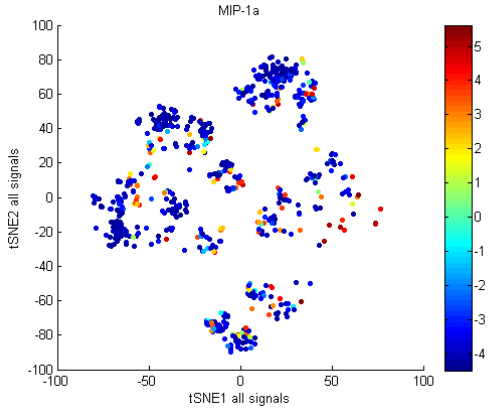
MIP-1a
tSNE2 all signals
tSNE1 all signals

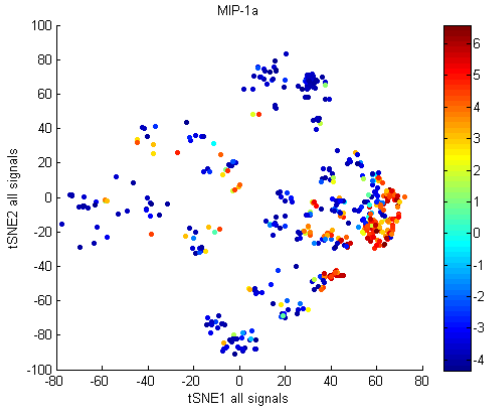
MIP-1a
tSNE2 all signals
tSNE1 all signals

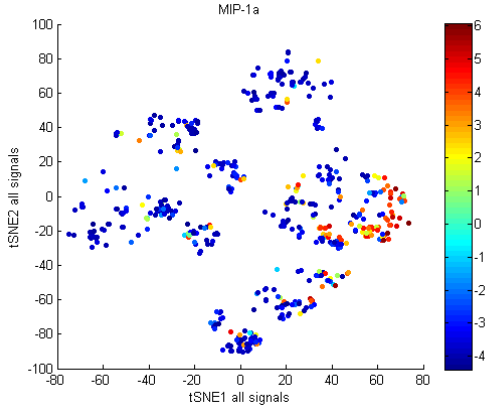
MIP-1a
tSNE2 all signals
tSNE1 all signals

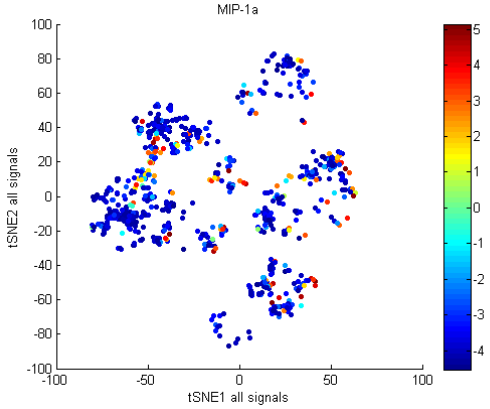
MIP-1a
tSNE2 all signals
tSNE1 all signals

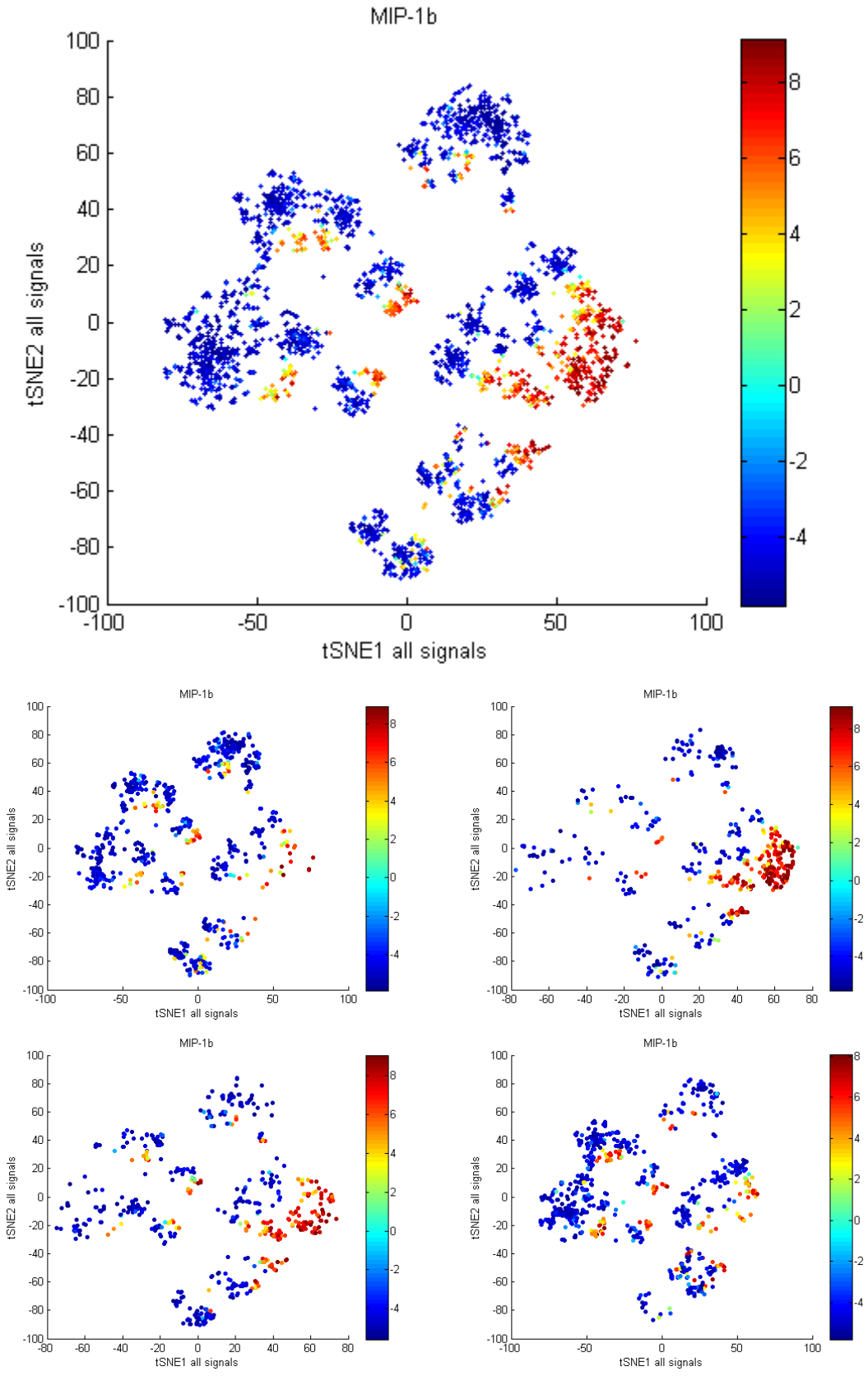
MIP-1b
tSNE2 all signals
tSNE1 all signals
MIP-1b
tSNE2 all signals
tSNE1 all signals
MIP-1b
tSNE2 all signals
tSNE1 all signals
MIP-1b
tSNE2 all signals
tSNE1 all signals
MIP-1b
tSNE2 all signals
tSNE1 all signals

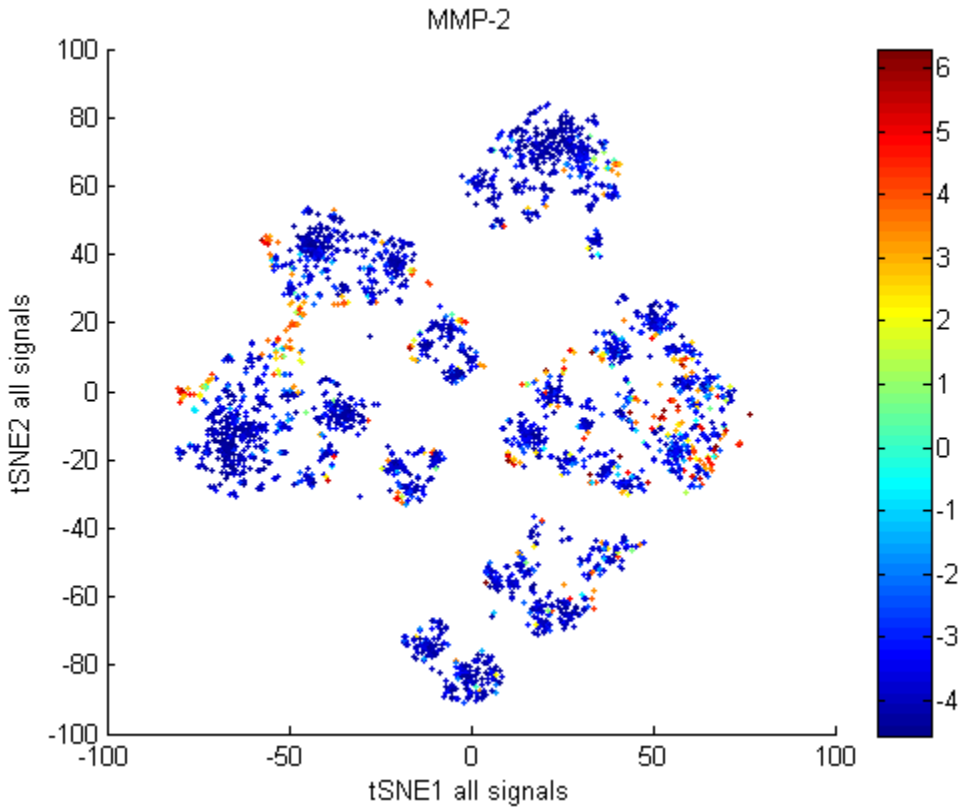
MMP-2
tSNE2 all signals
tSNE1 all signals

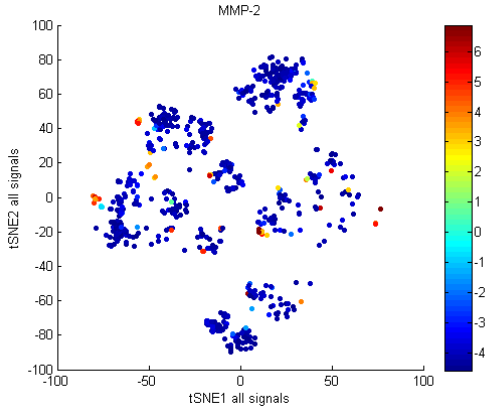
MMP-2
tSNE2 all signals
tSNE1 all signals

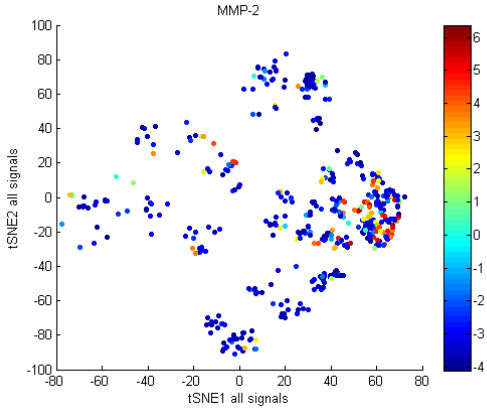
MMP-2
tSNE2 all signals
tSNE1 all signals

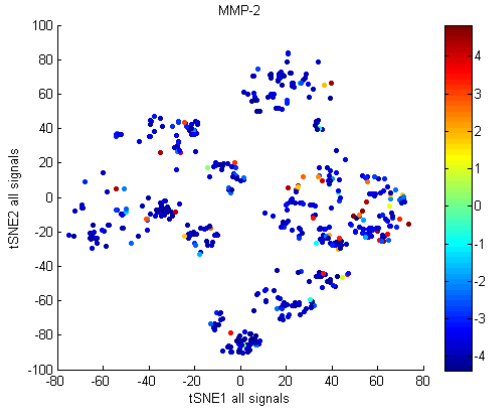
MMP-2
tSNE2 all signals
tSNE1 all signals

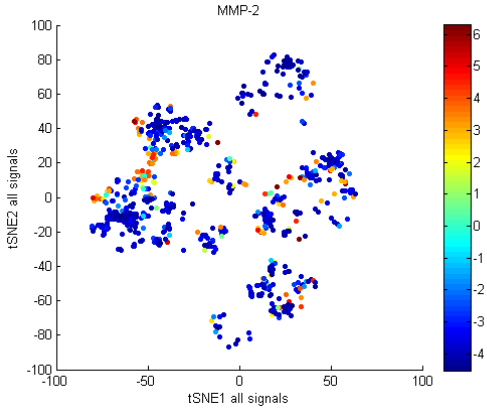
MMP-2
tSNE2 all signals
tSNE1 all signals

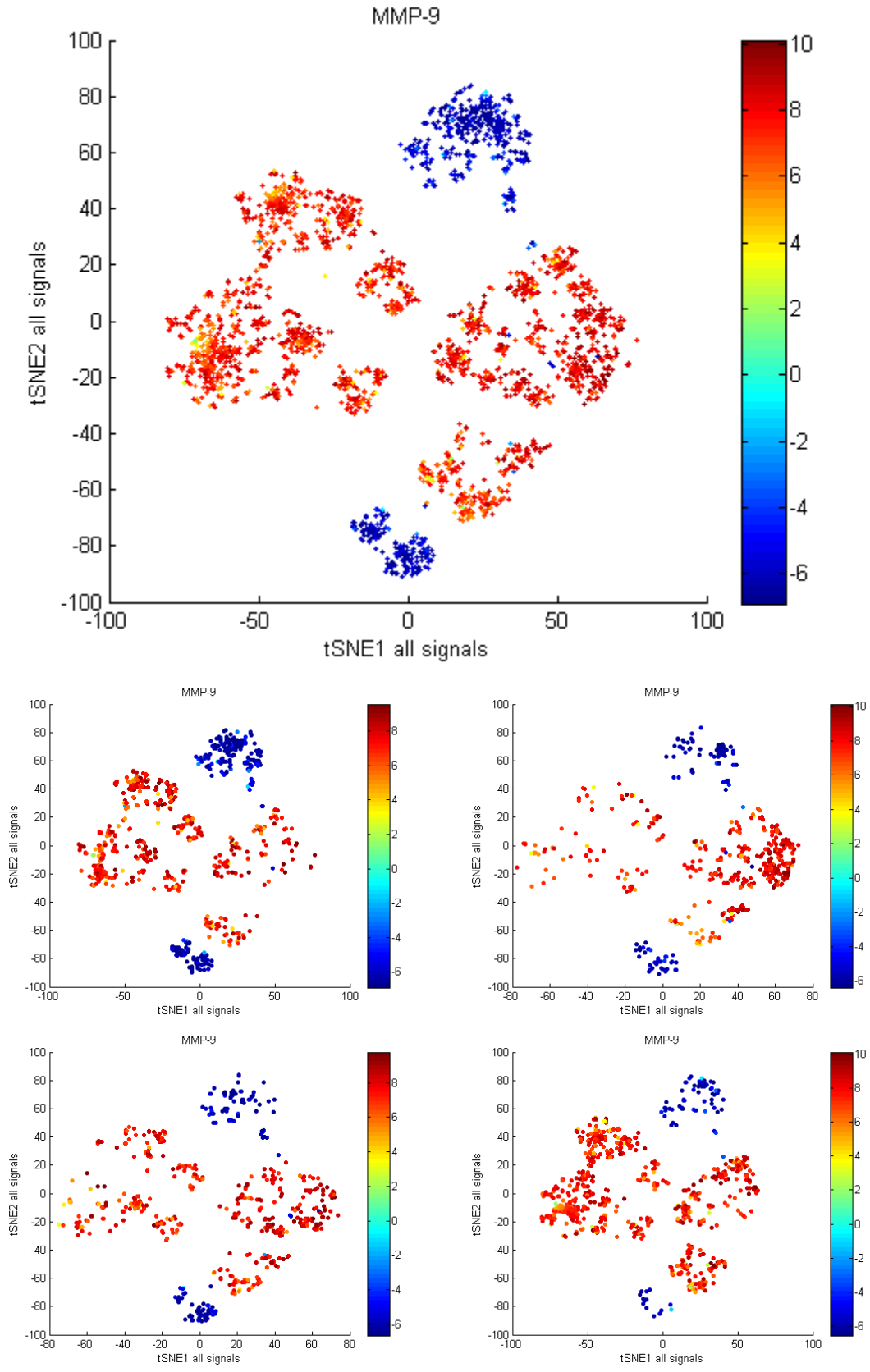
MMP-9
tSNE2 all signals
tSNE1 all signals
MMP-9
tSNE2 all signals
tSNE1 all signals
MMP-9
tSNE2 all signals
tSNE1 all signals
MMP-9
tSNE2 all signals
tSNE1 all signals
MMP-9
tSNE2 all signals
tSNE1 all signals

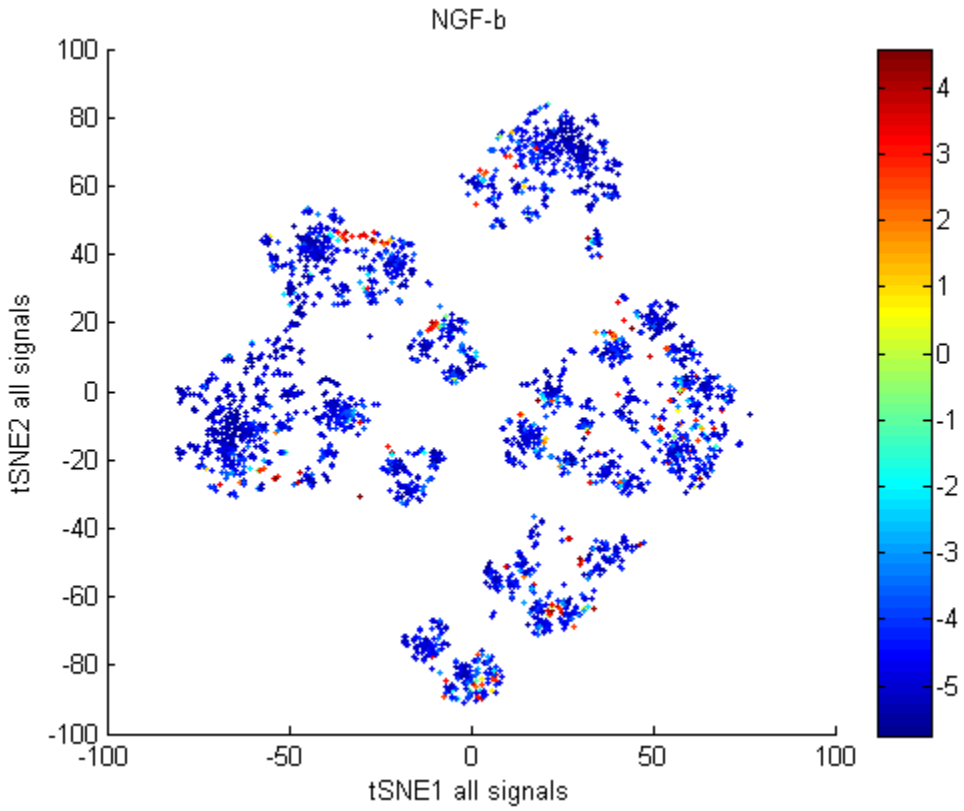
NGF-b
tSNE2 all signals
tSNE1 all signals

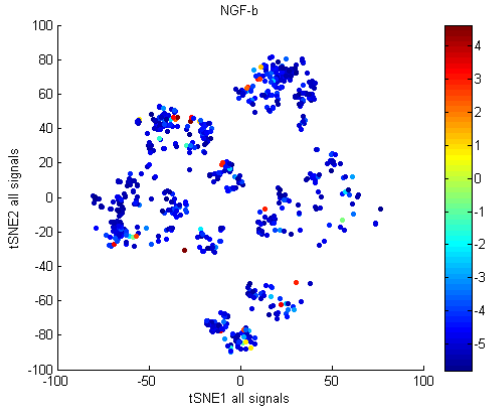
NGF-b
tSNE2 all signals
tSNE1 all signals

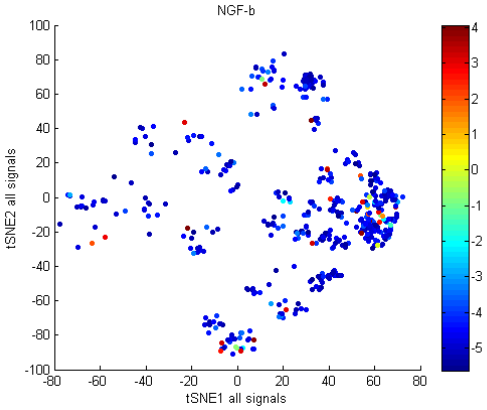
NGF-b
tSNE2 all signals
tSNE1 all signals

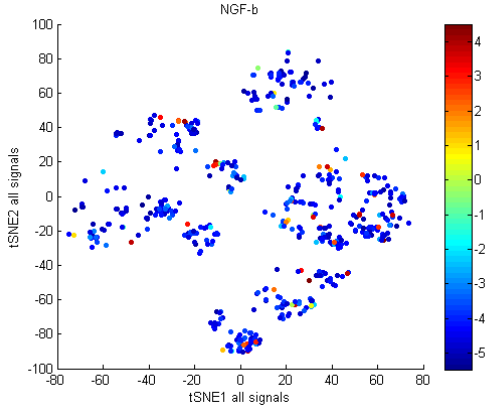
NGF-b
tSNE2 all signals
tSNE1 all signals

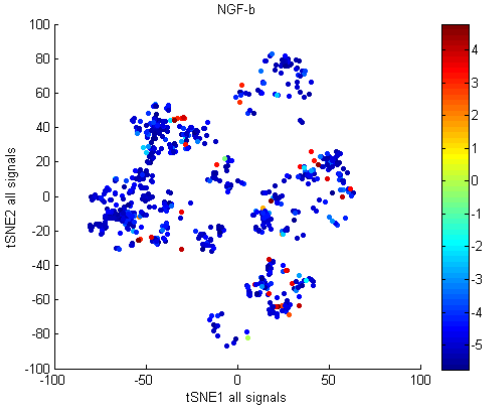
NGF-b
tSNE2 all signals
tSNE1 all signals

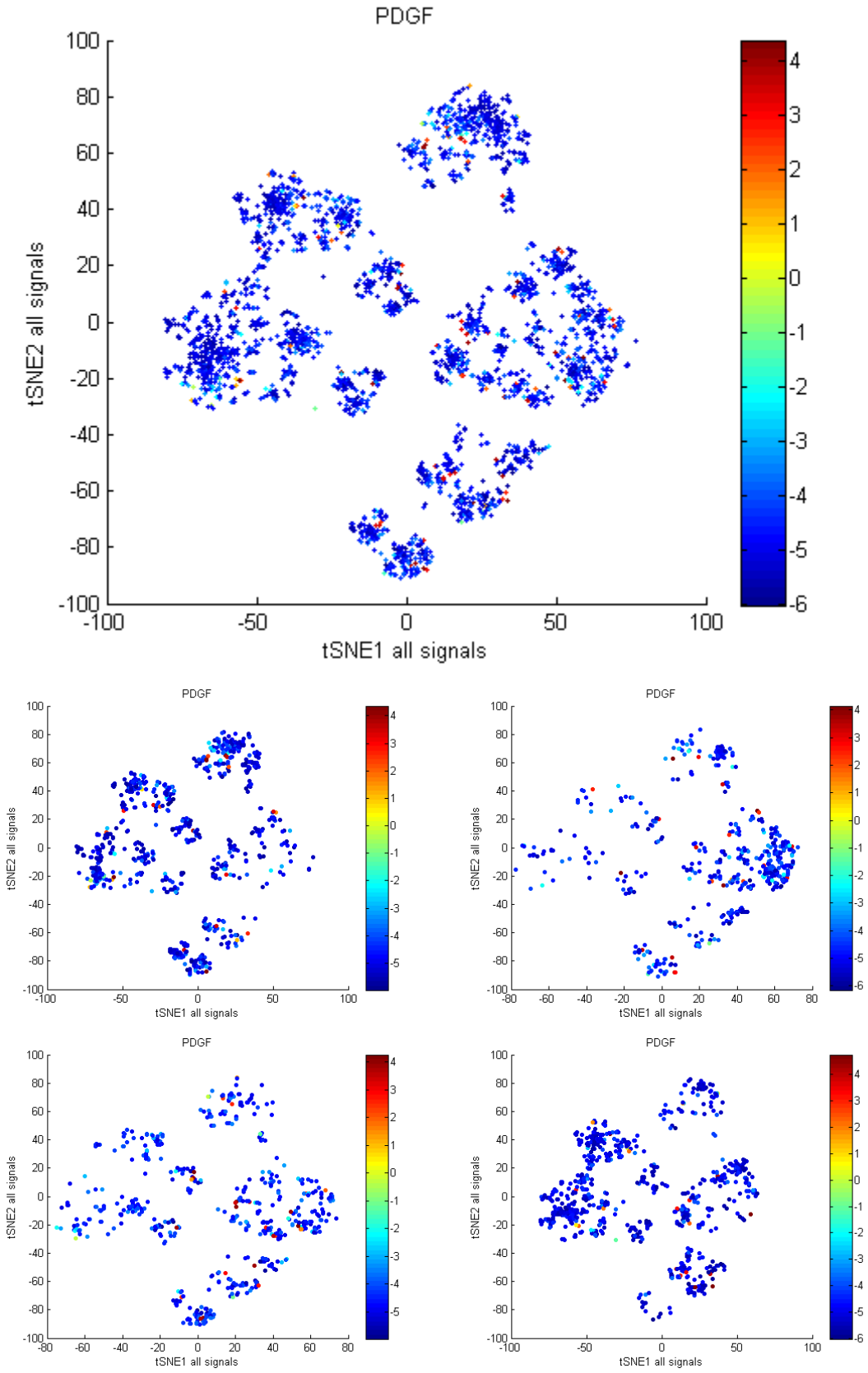
PDGF
tSNE2 all signals
tSNE1 all signals
PDGF
tSNE2 all signals
tSNE1 all signals
PDGF
tSNE2 all signals
tSNE1 all signals
PDGF
tSNE2 all signals
tSNE1 all signals
PDGF
tSNE2 all signals
tSNE1 all signals

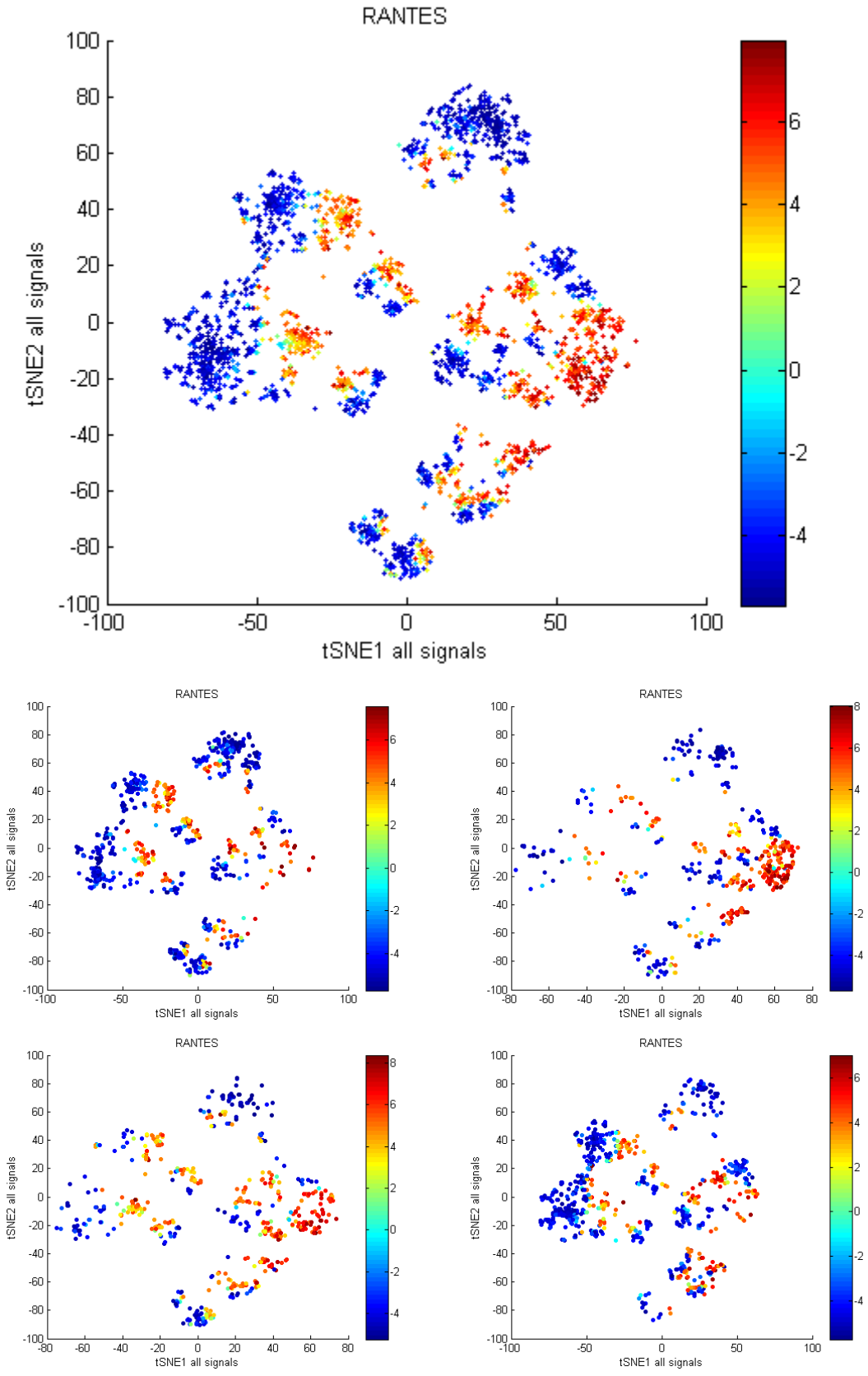
RANTES
tSNE2 all signals
tSNE1 all signals
RANTES
tSNE2 all signals
tSNE1 all signals
RANTES
tSNE2 all signals
tSNE1 all signals
RANTES
tSNE2 all signals
tSNE1 all signals
RANTES
tSNE2 all signals
tSNE1 all signals

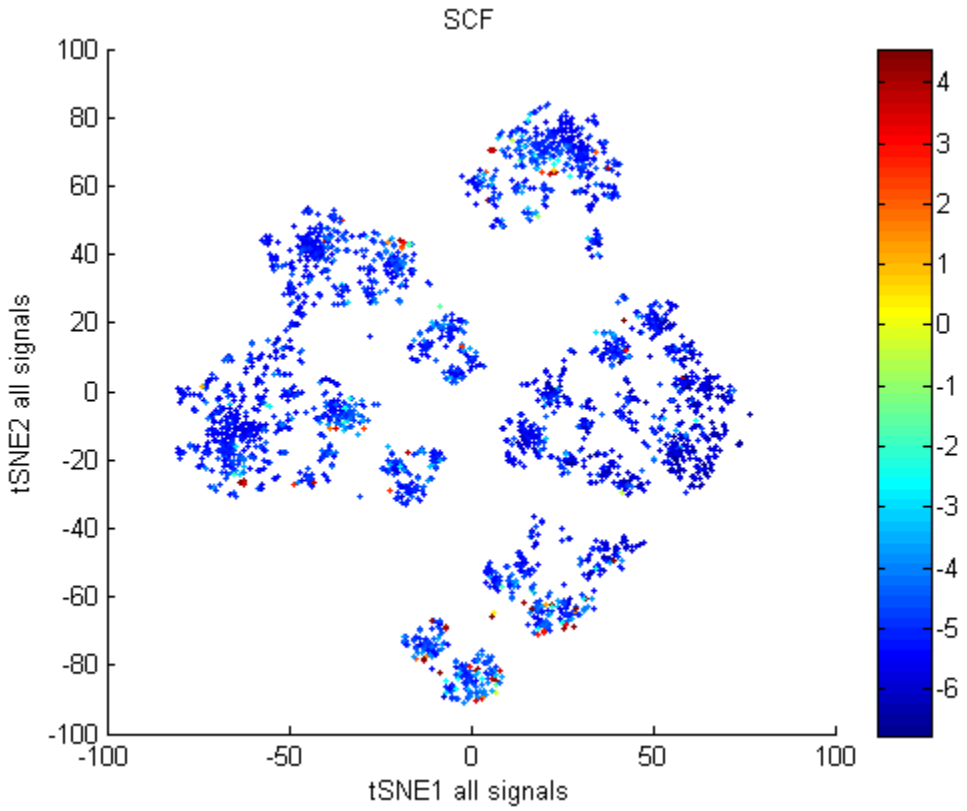
SCF
tSNE2 all signals
tSNE1 all signals

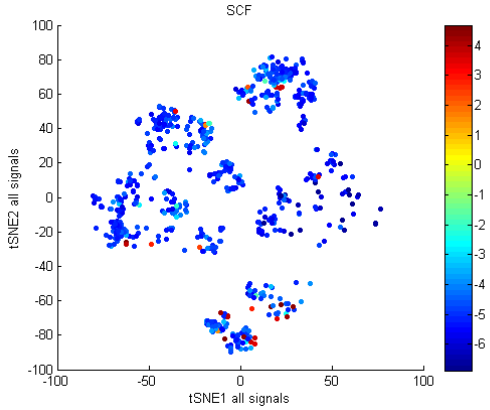
SCF
tSNE2 all signals
tSNE1 all signals

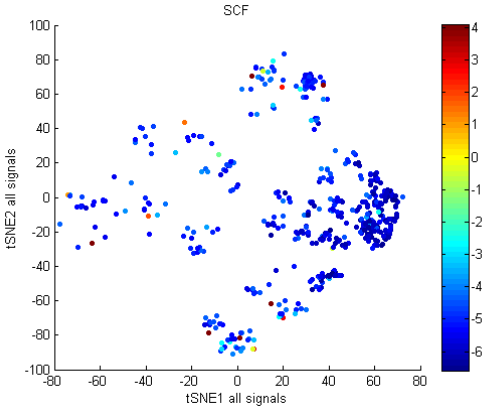
SCF
tSNE2 all signals
tSNE1 all signals

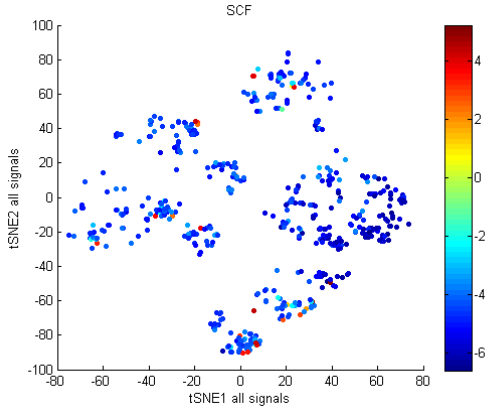
SCF
tSNE2 all signals
tSNE1 all signals

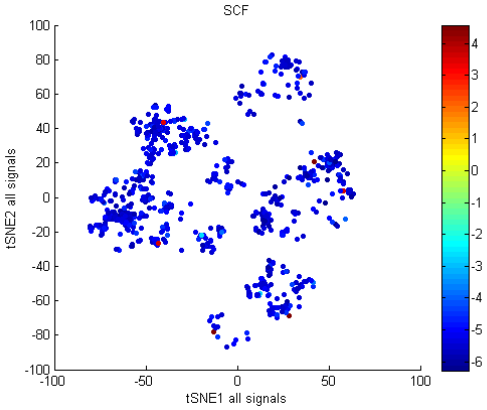
SCF
tSNE2 all signals
tSNE1 all signals

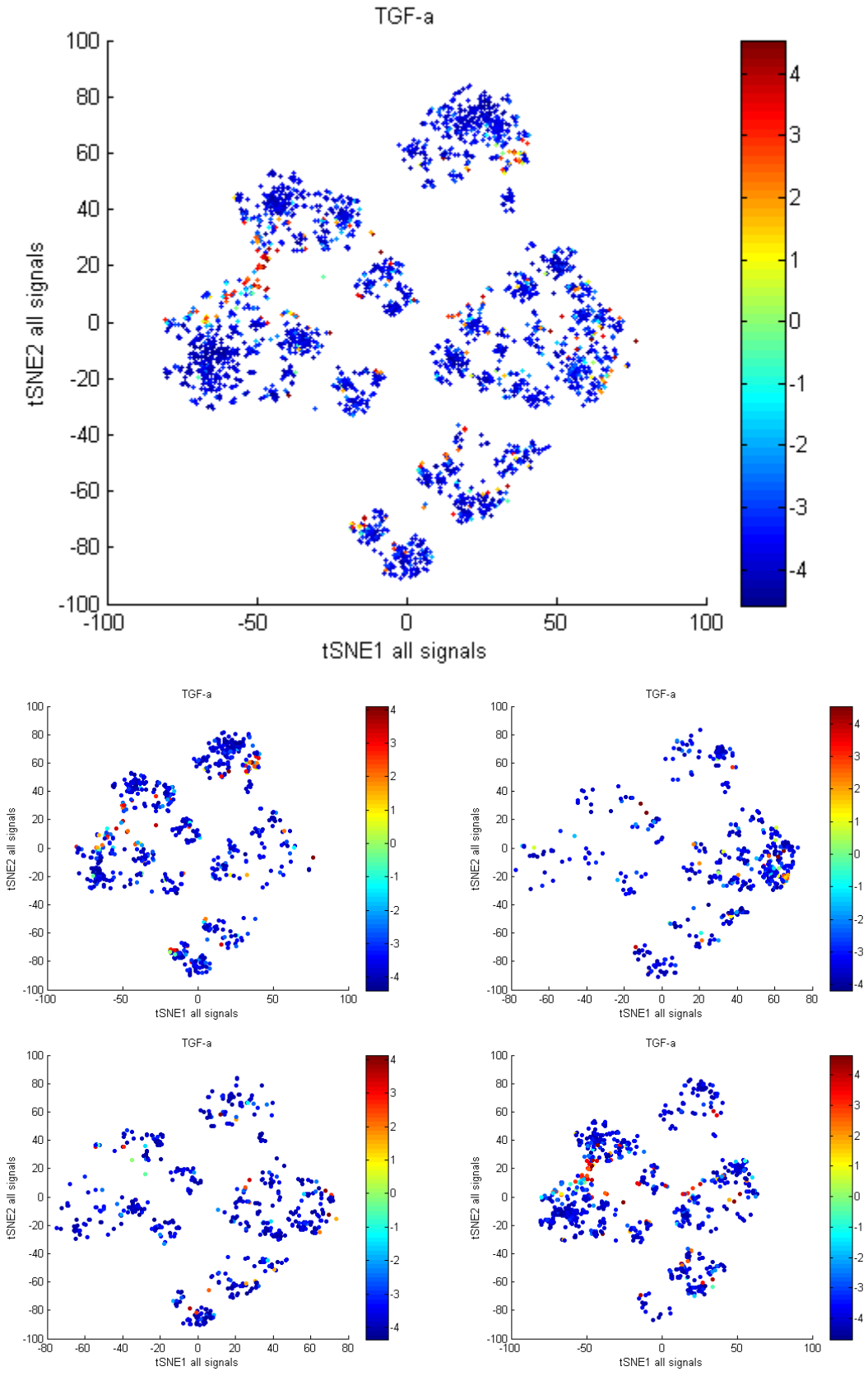
TGF-a
tSNE2 all signals
tSNE1 all signals
TGF-a
tSNE2 all signals
tSNE1 all signals
TGF-a
tSNE2 all signals
tSNE1 all signals
TGF-a
tSNE2 all signals
tSNE1 all signals
TGF-a
tSNE2 all signals
tSNE1 all signals

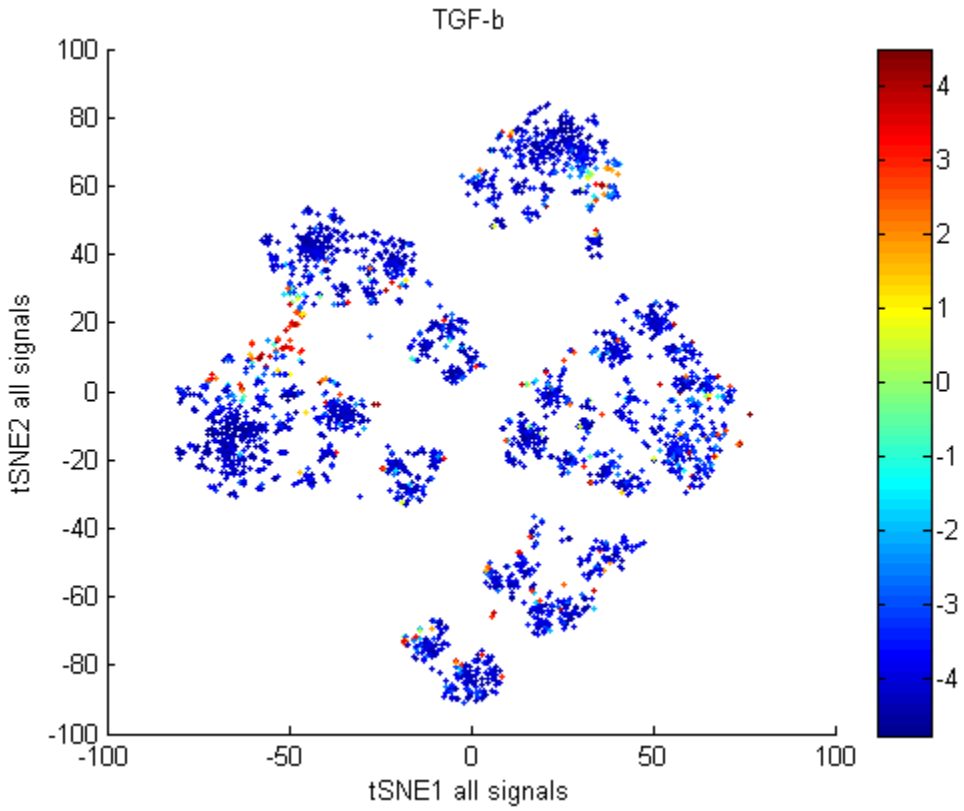
TGF-b
tSNE2 all signals
tSNE1 all signals

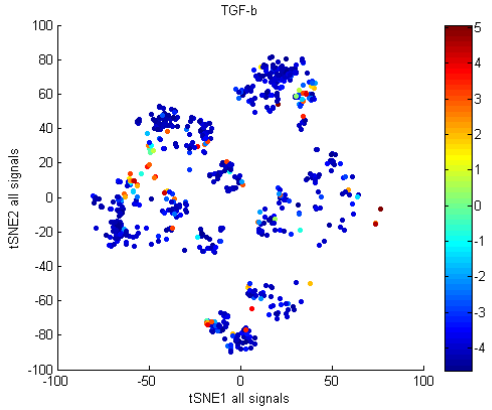
TGF-b
tSNE2 all signals
tSNE1 all signals

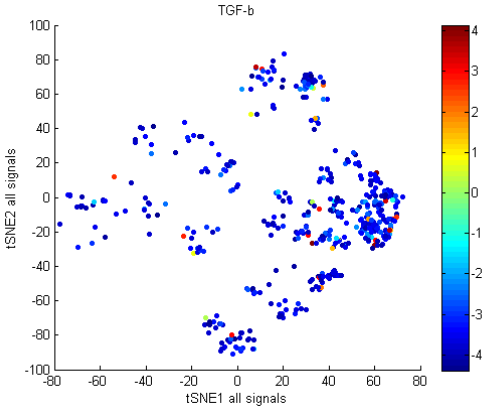
TGF-b
tSNE2 all signals
tSNE1 all signals

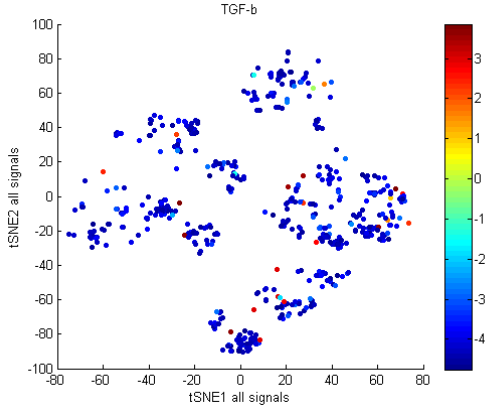
TGF-b
tSNE2 all signals
tSNE1 all signals

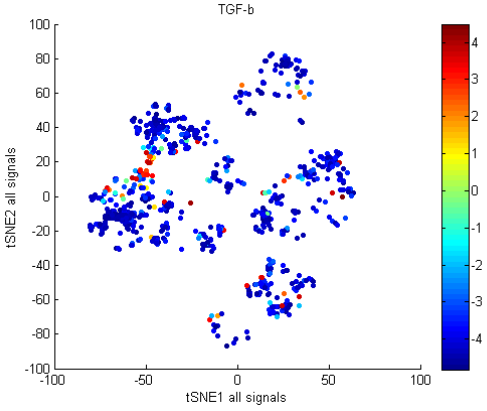
TGF-b
tSNE2 all signals
tSNE1 all signals

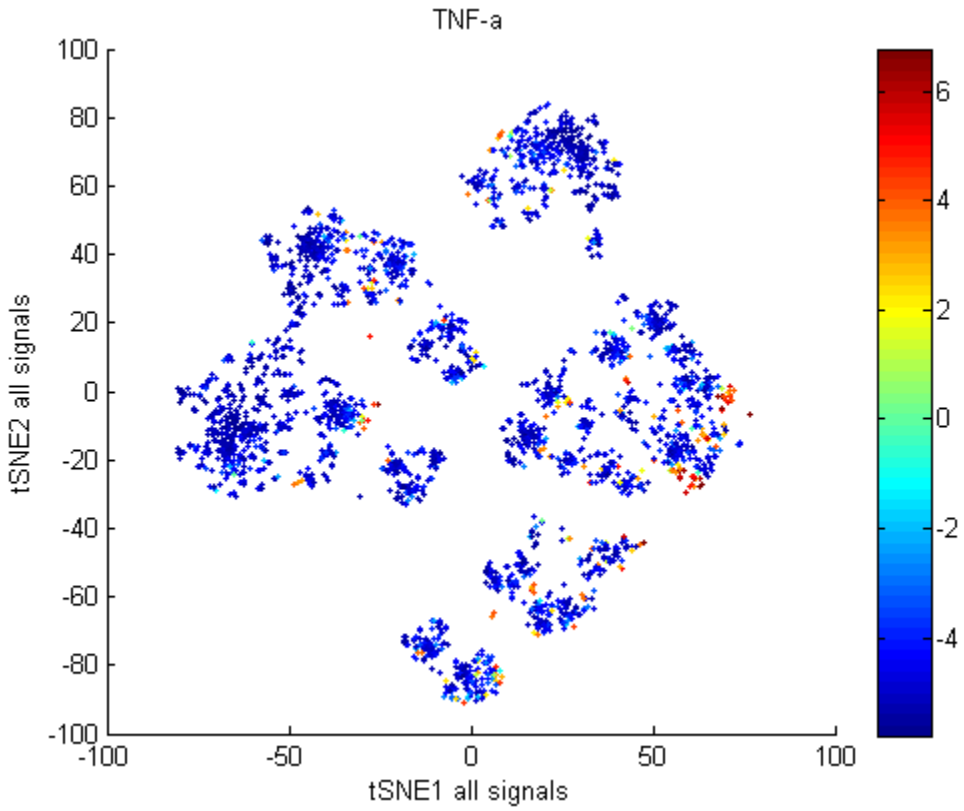
TNF-a
tSNE2 all signals
tSNE1 all signals

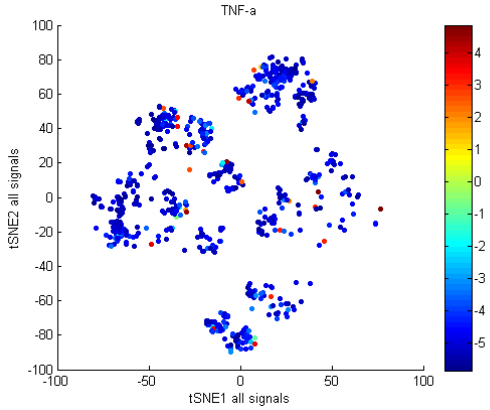
TNF-a
tSNE2 all signals
tSNE1 all signals

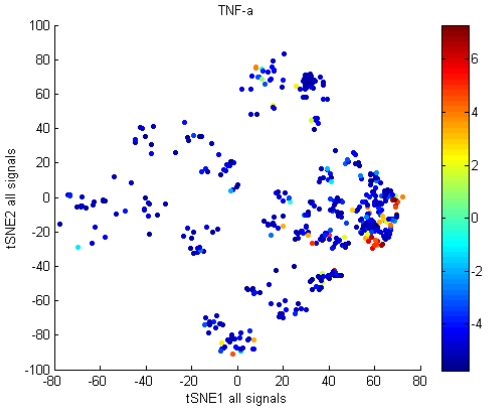
TNF-a
tSNE2 all signals
tSNE1 all signals

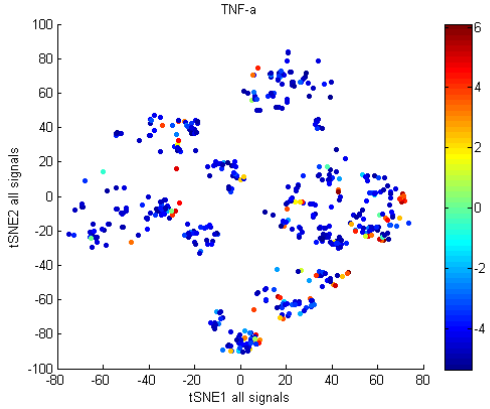
TNF-a
tSNE2 all signals
tSNE1 all signals

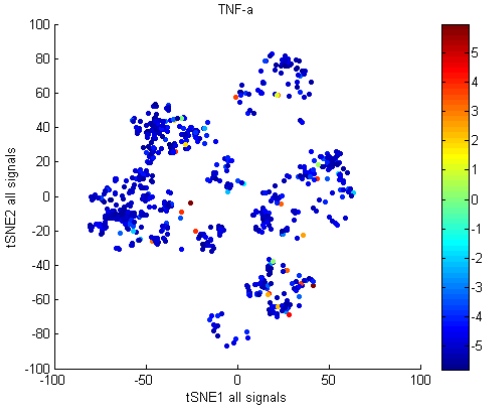
TNF-a
tSNE2 all signals
tSNE1 all signals

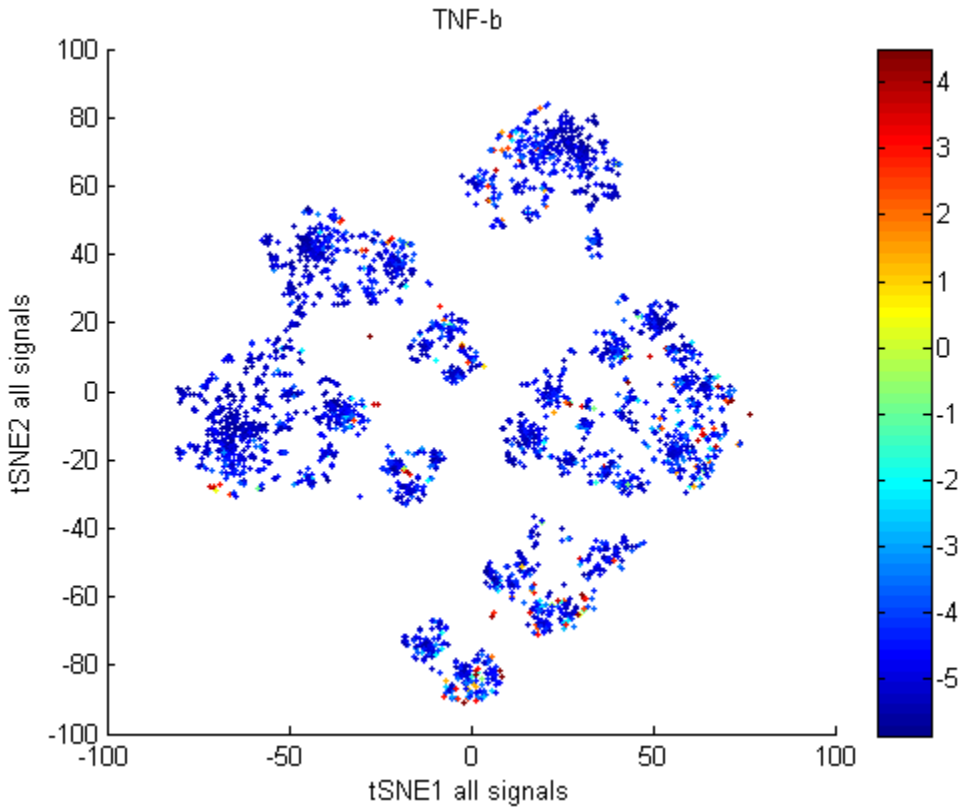
TNF-b
tSNE2 all signals
tSNE1 all signals

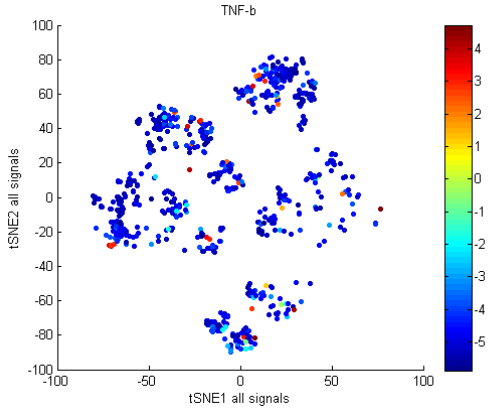
TNF-b
tSNE2 all signals
tSNE1 all signals

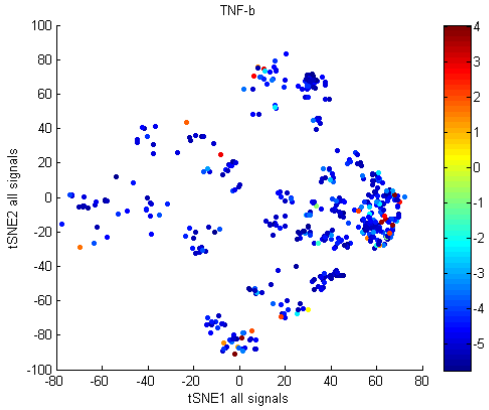
TNF-b
tSNE2 all signals
tSNE1 all signals

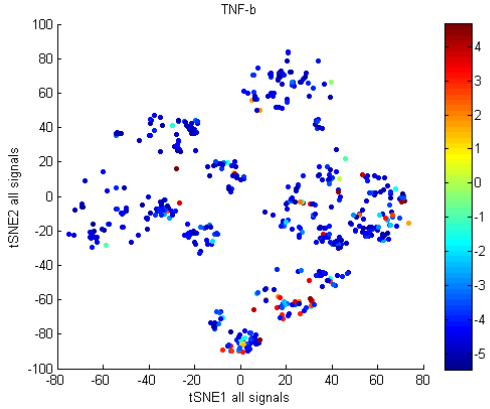
TNF-b
tSNE2 all signals
tSNE1 all signals

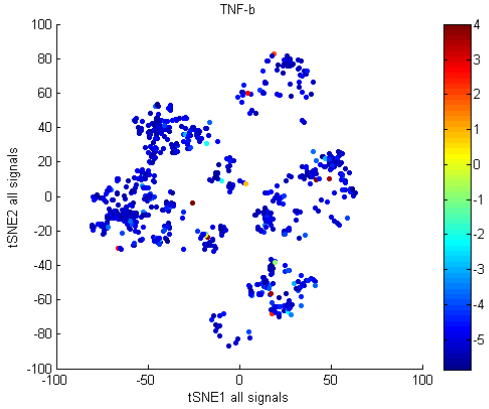
TNF-b
tSNE2 all signals
tSNE1 all signals

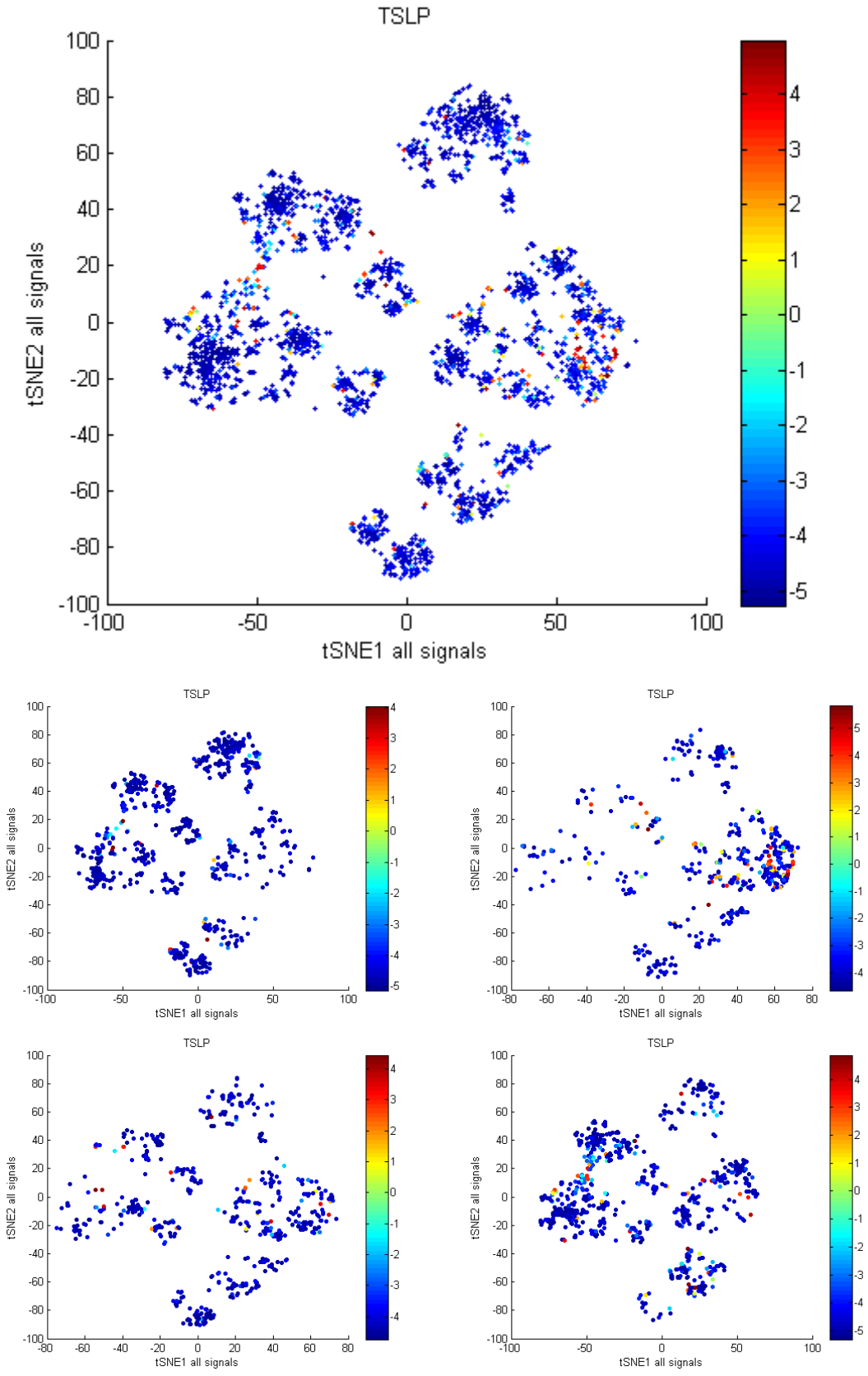
TSLP
tSNE2 all signals
tSNE1 all signals
TSLP
tSNE2 all signals
tSNE1 all signals
TSLP
tSNE2 all signals
tSNE1 all signals
TSLP
tSNE2 all signals
tSNE1 all signals
TSLP
tSNE2 all signals
tSNE1 all signals

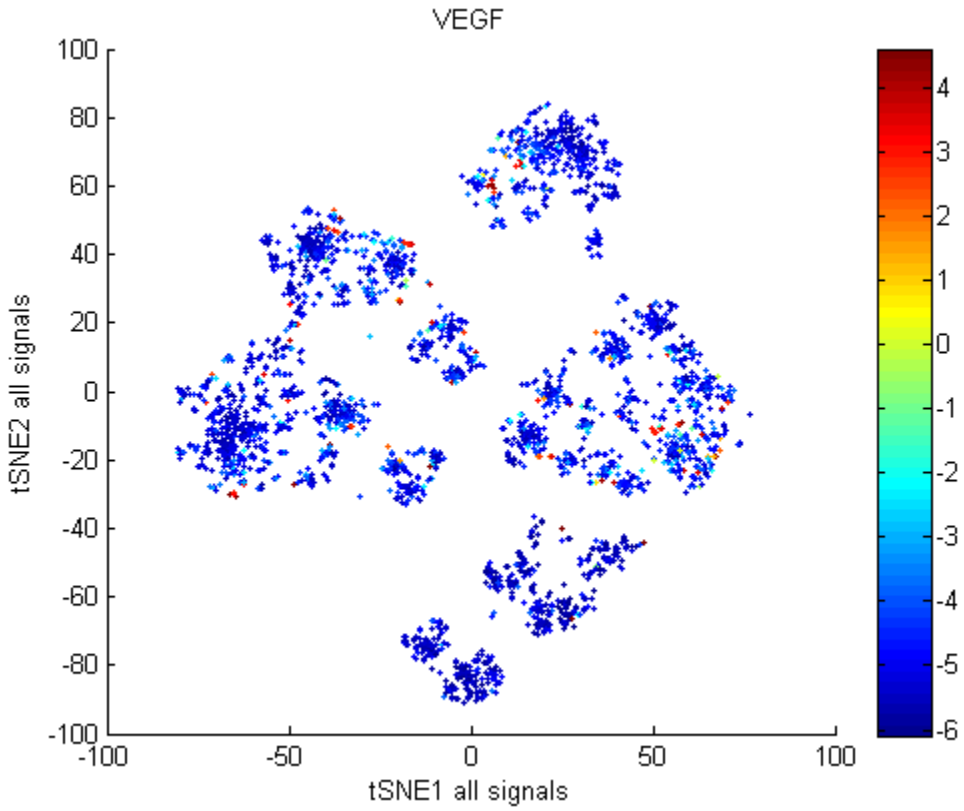
VEGF
tSNE2 all signals
tSNE1 all signals

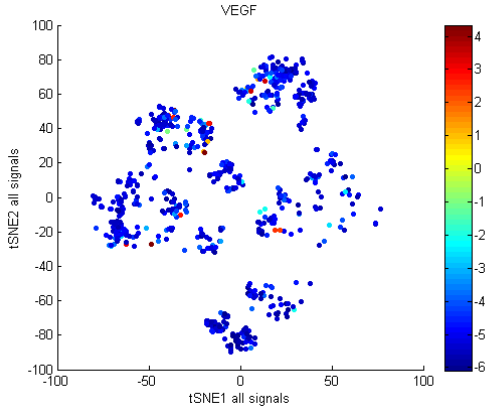
VEGF
tSNE2 all signals
tSNE1 all signals

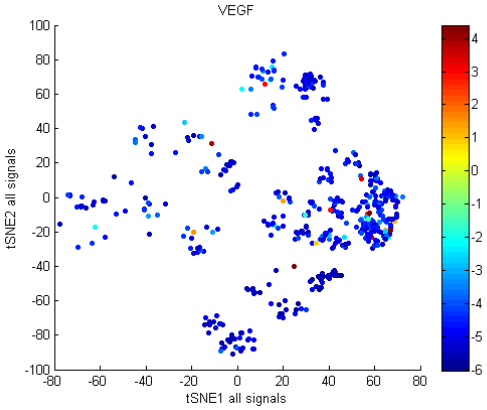
VEGF
tSNE2 all signals
tSNE1 all signals

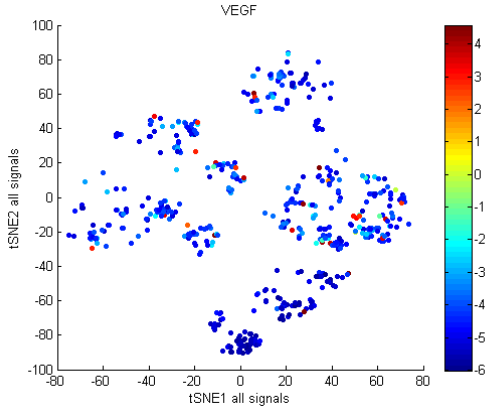
VEGF
tSNE2 all signals
tSNE1 all signals

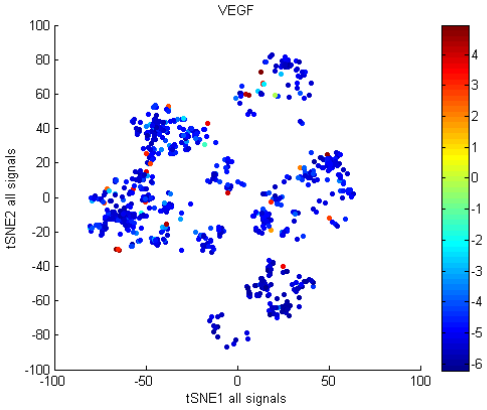
VEGF
tSNE2 all signals
tSNE1 all signals

Fig. S16. Protein distribution in the viSNE maps of U937-derived macrophages at the basal level and stimulated with different TLR ligands. Cytokine functions in all subpopulations identified by the viSNE analysis for U937 derived macrophage cells under the stimulation of different TLR ligands (basal, TLR4 by LPS, TLR1/2 by PAM3, TLR3 by poly IC). The figures are arranged in the following sequence: combined (top) vs basal (middle left) vs LPS stimulated (middle right) vs PAM3 stimulated (bottom left) vs poly IC stimulated (bottom right).

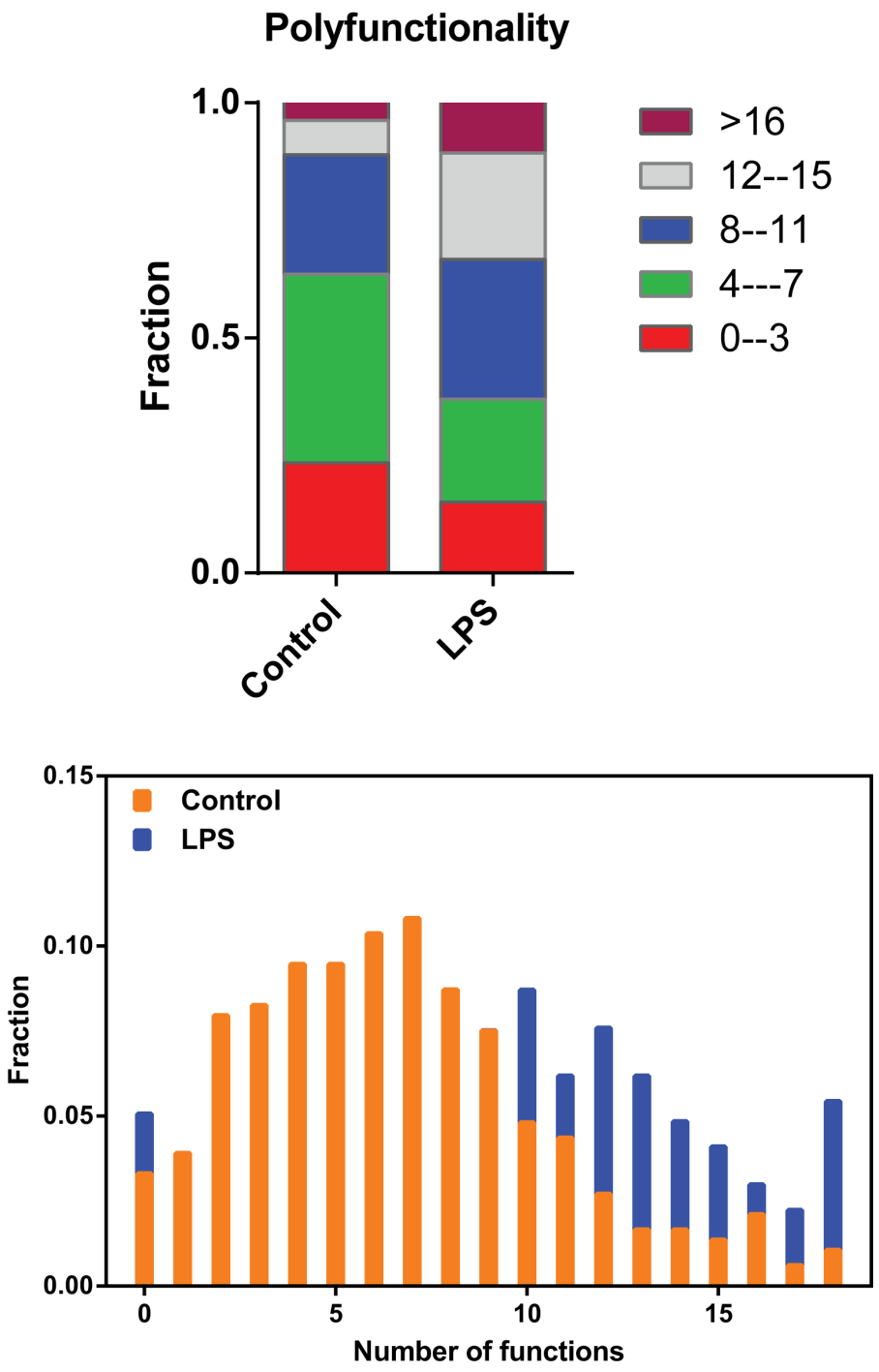

Fig. S17 Single-cell polyfunctionality in response to LPS stimulation. It shows poly-functionality analysis of U937 macrophage (control and LPS stimulated), in which a wide variety of single cell poly-functionality was observed and U937 derived macrophage cells showed more poly-functionality upon LPS stimulation.

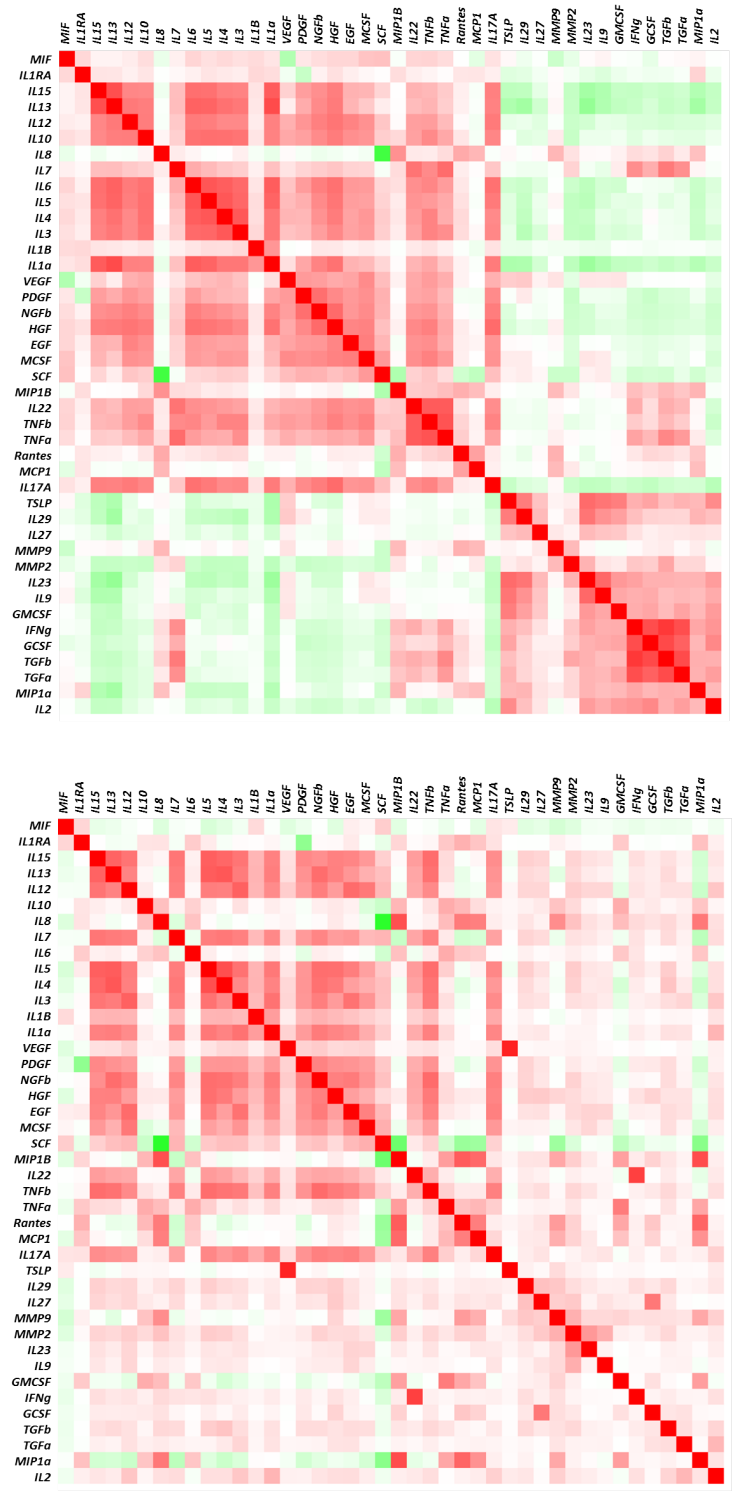

Figure S18. Correlation analysis indicates increased co-secretion of multiple cytokines in U937-derived macrophages in response to LPS stimulation. Upper panel: basal cells. Lower panel: LPS stimulated cells.

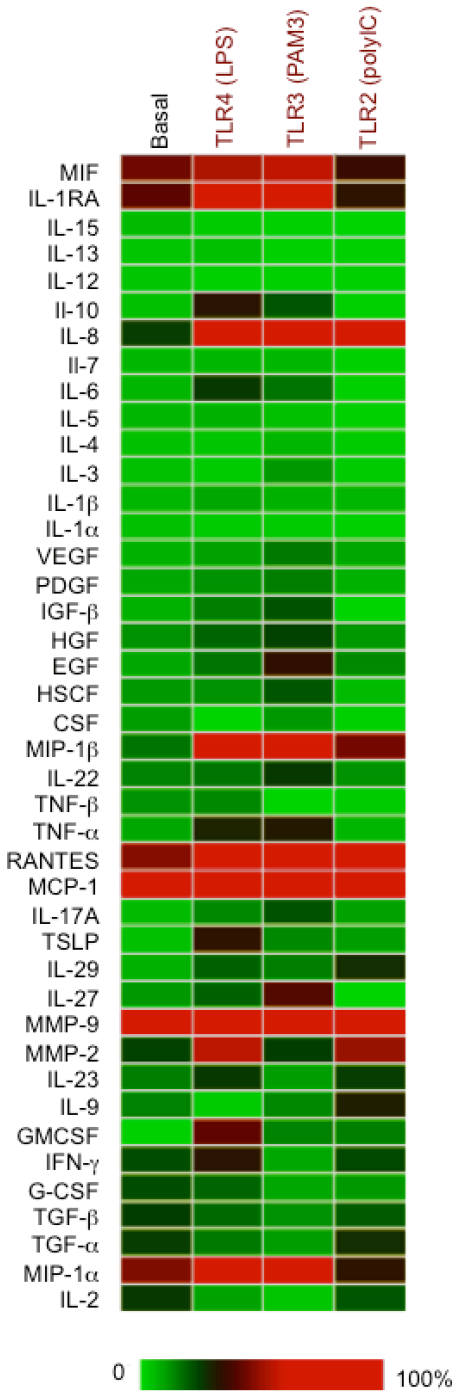

Fig. S19 Heatmap summarizing the frequency (%) of proteins-secreting cells in the whole population. U937-derived macrophage cells at the basal level and the cells stimulated by LPS, PAM3 or polyIC were measured for all 42 cytokines. The frequency of cells secreting a given cytokine is shown as the color intensity.

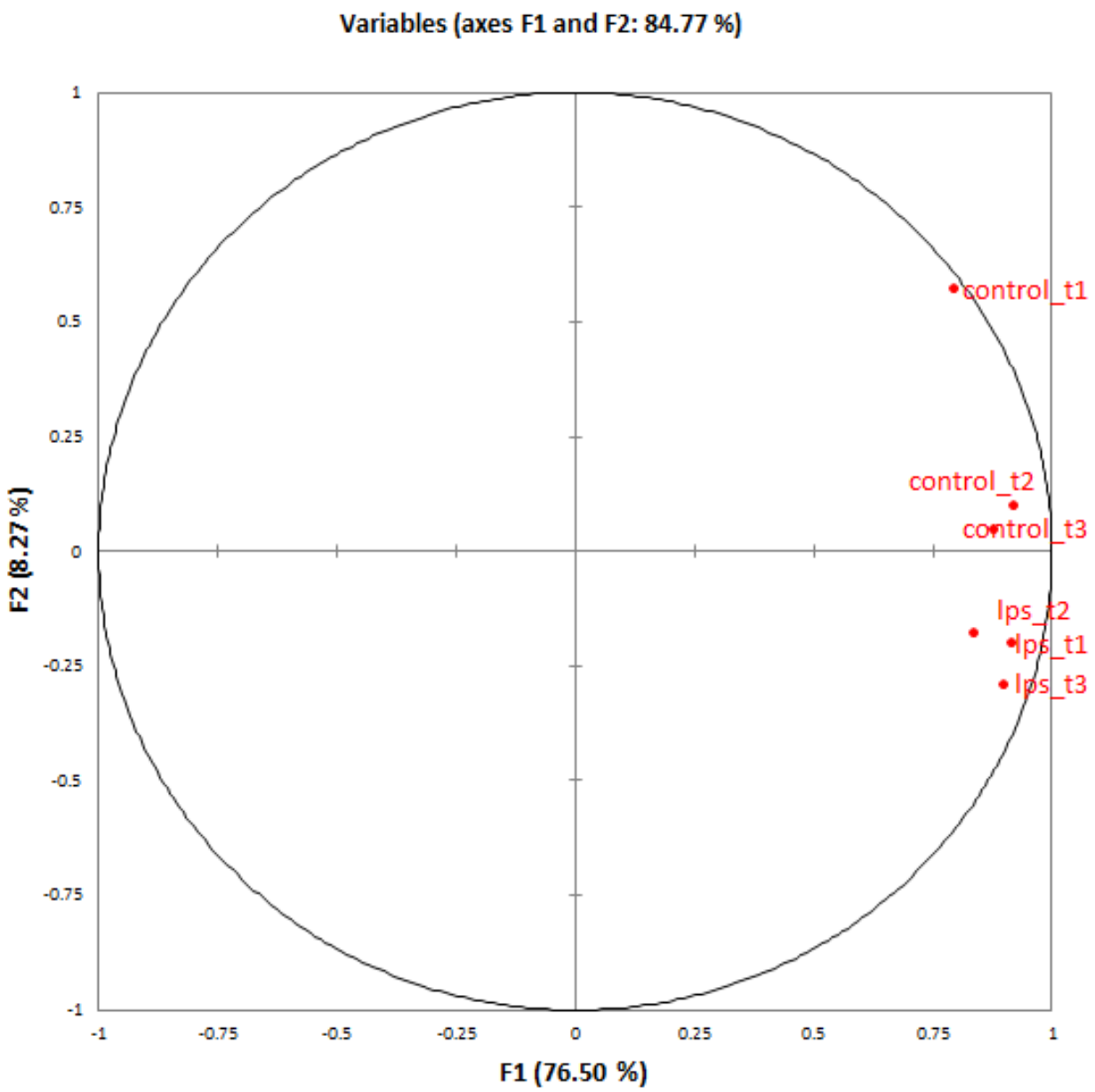

Fig. S20 Principal Component Analysis of the samples in a triplicate basal vs. LPS treatment experiment. Six independent single-cell protein secretion experiments were conducted on U937-derived macrophages. Three were measured in the basal condition (control_t1, 2, and 3) and three were measured on the macrophage cells treated by LPS for 20 hr.

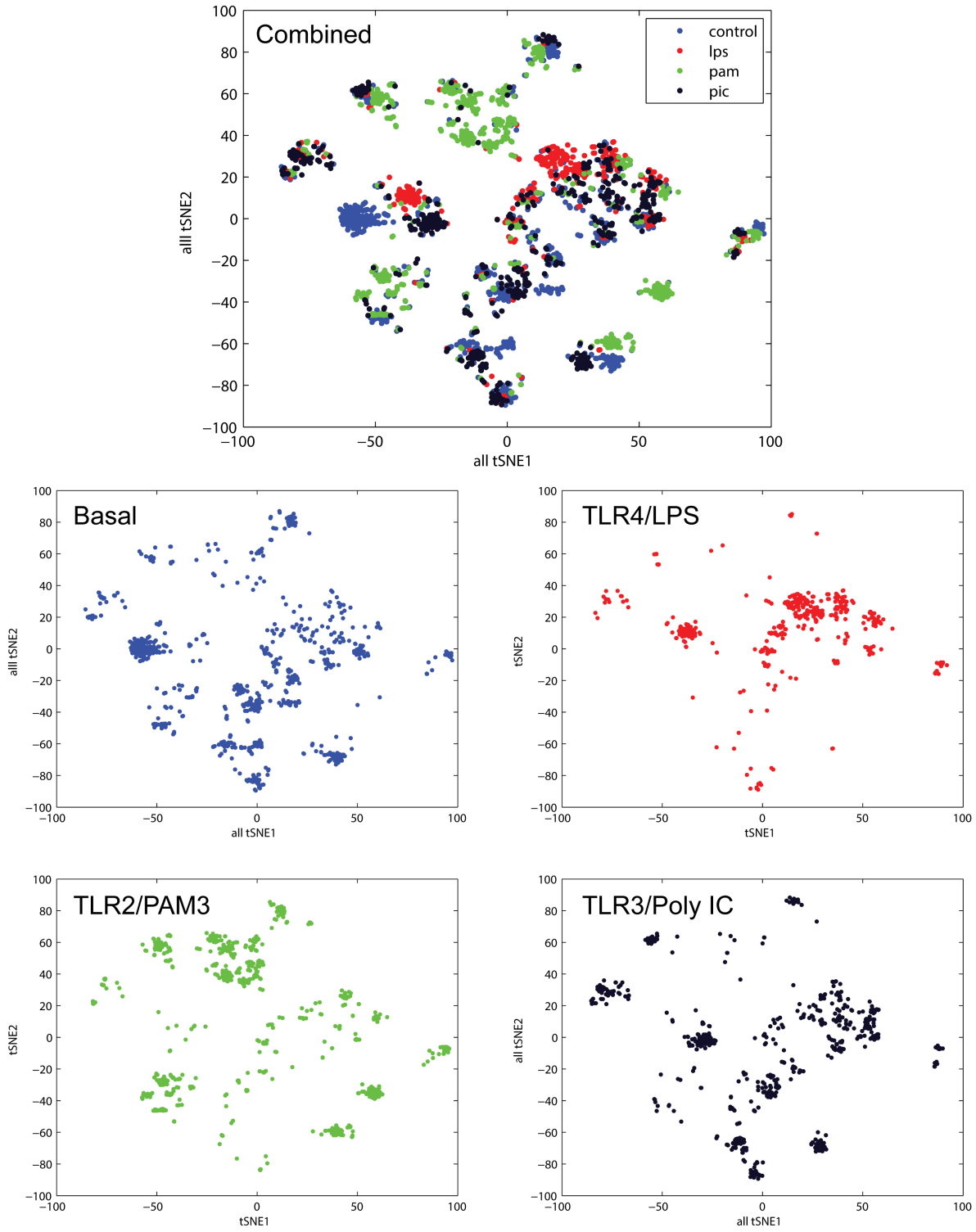

Fig. S21 viSNE maps for primary macrophage cells derived from a healthy donor. viSNE structure maps showing primary macrophage under the stimulation of different TLR ligands(basal, TLR4 by LPS, TLR2 by PAM3, TLR3 by poly IC).

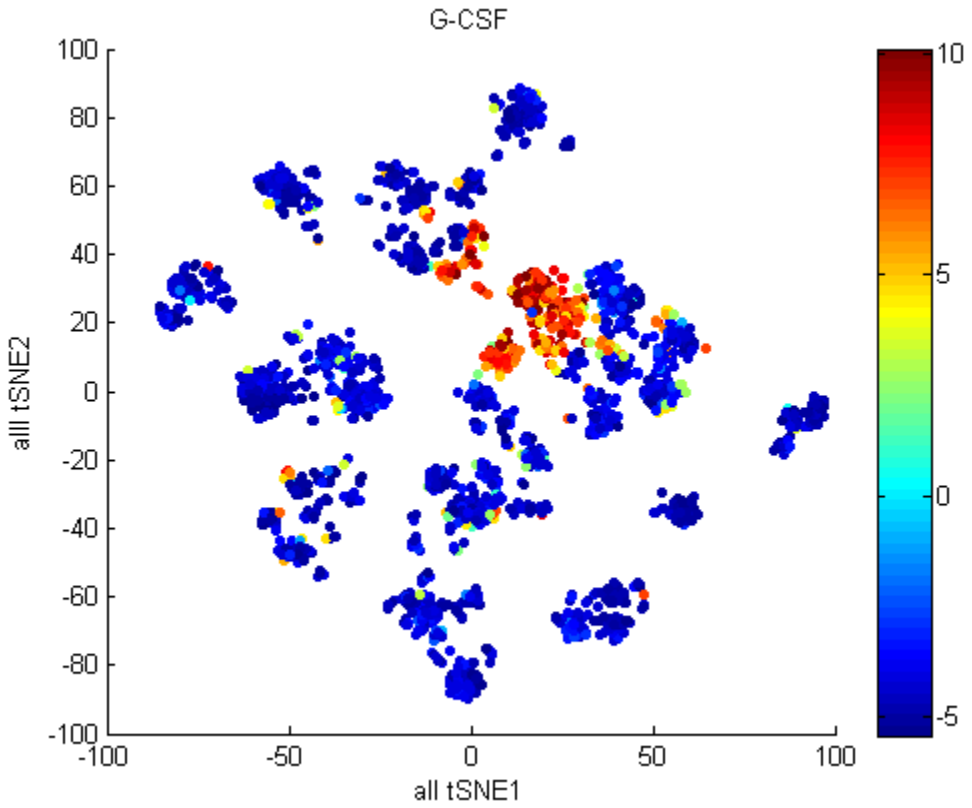
G-CSF
alll tSNE2
all tSNE1

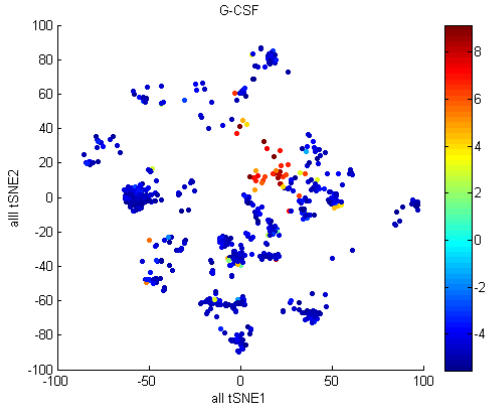
G-CSF
alll tSNE2
all tSNE1

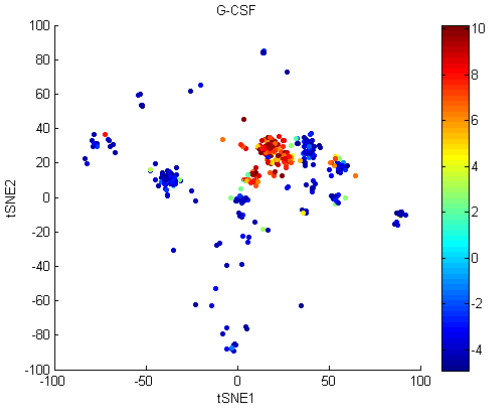
G-CSF
tSNE2
tSNE1

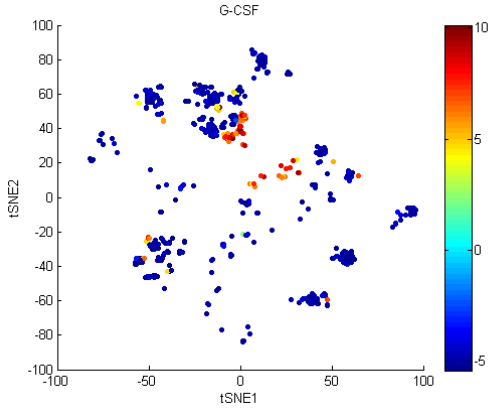
G-CSF
tSNE2
tSNE1

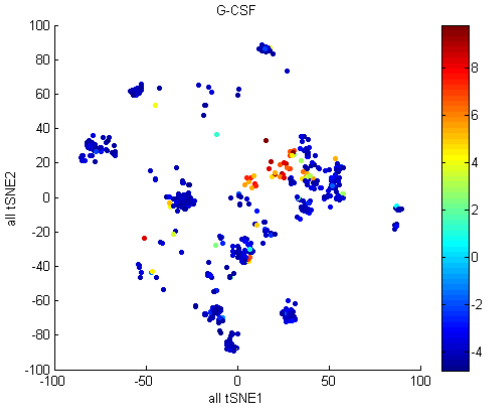
G-CSF
all tSNE2
all tSNE1

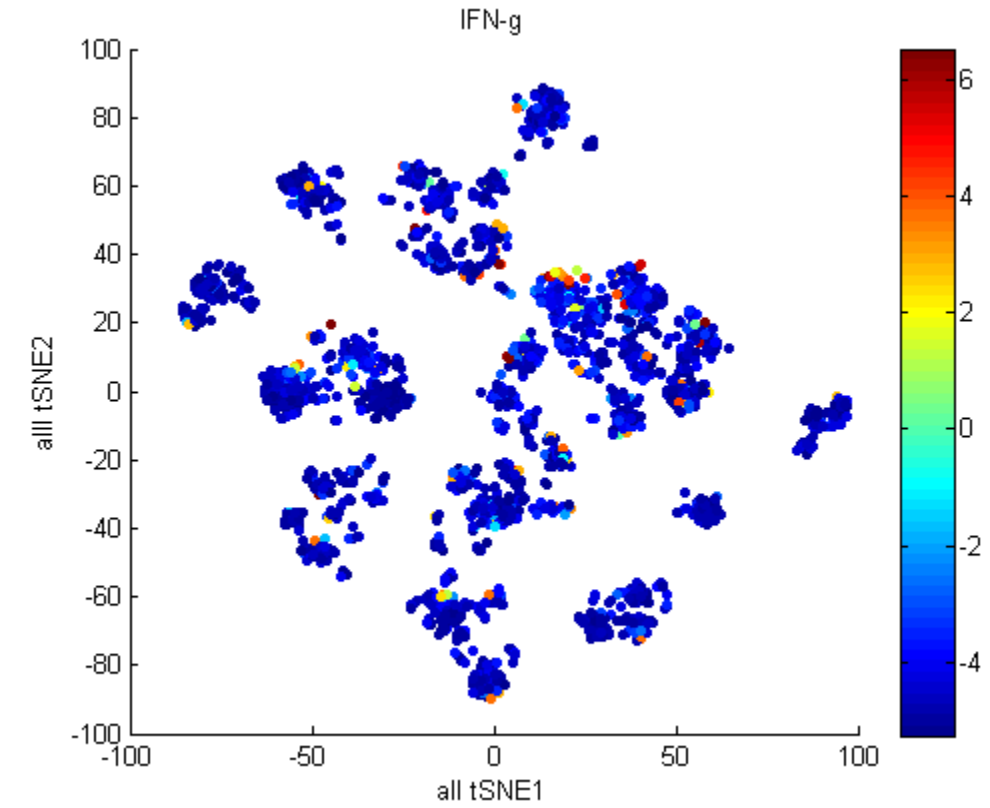
IFN-g
alll tSNE2
all tSNE1

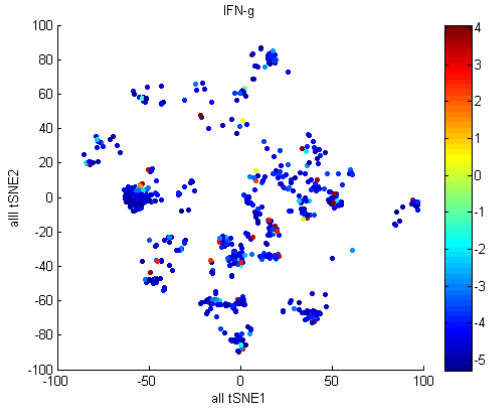
IFN-g
alll tSNE2
all tSNE1

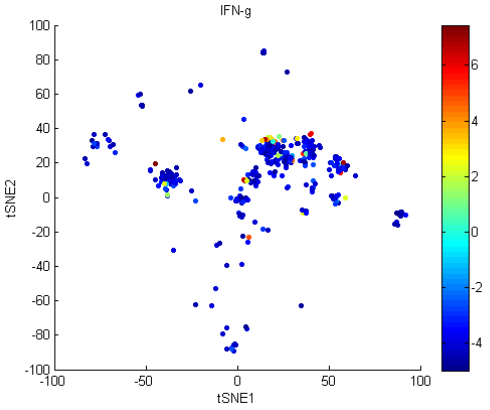
IFN-g
tSNE2
tSNE1

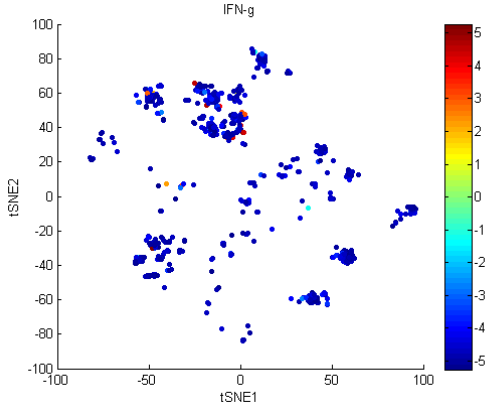
IFN-g
tSNE2
tSNE1

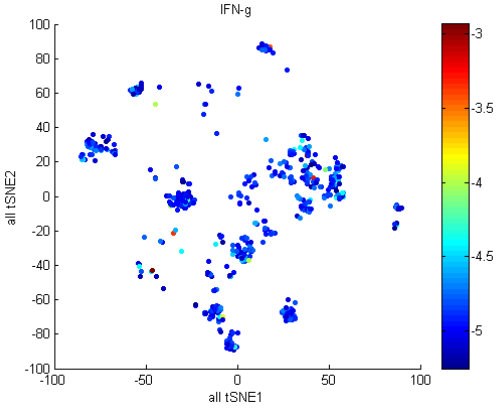
IFN-g
all tSNE2
all tSNE1

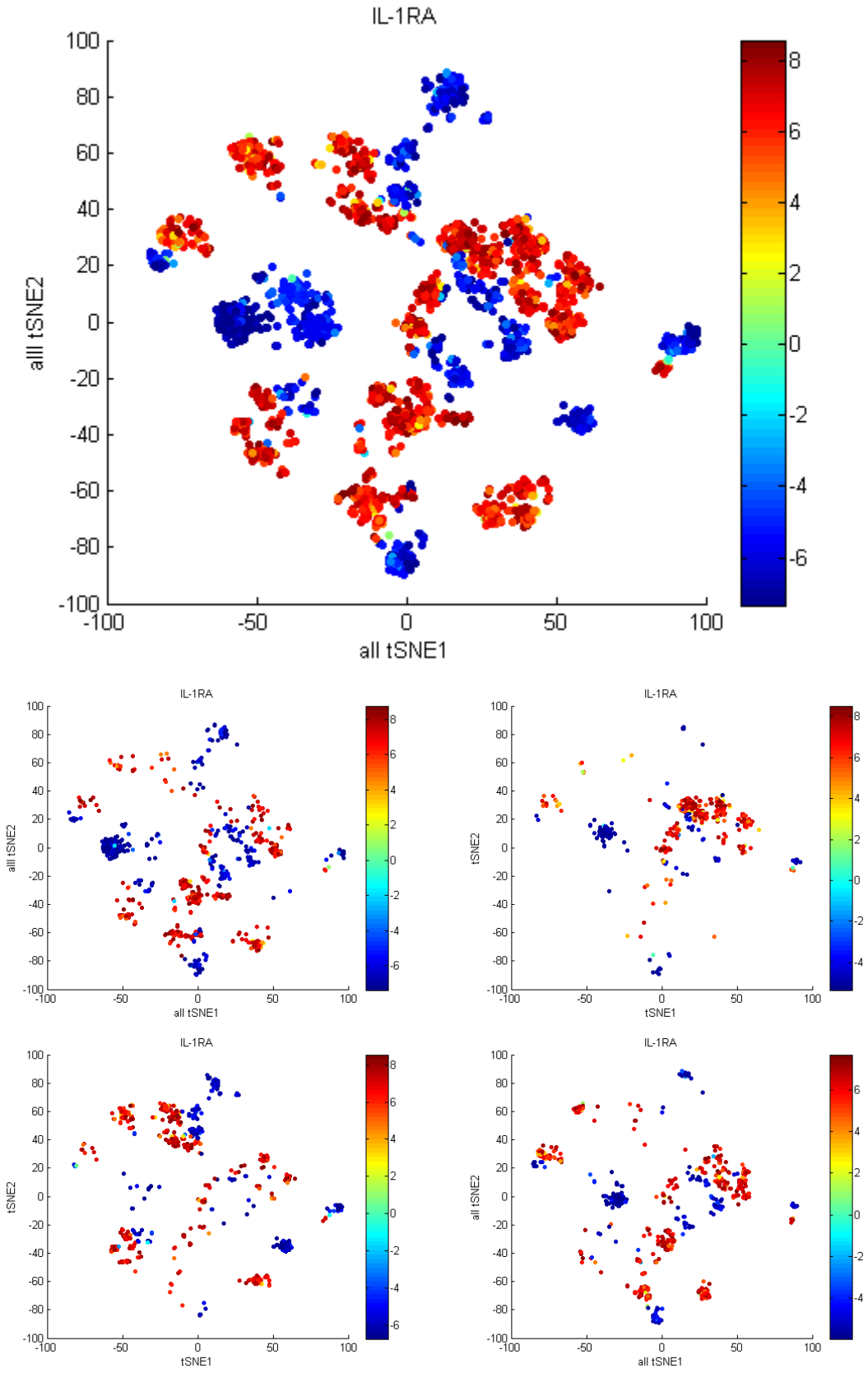
IL-1RA
alll tSNE2
all tSNE1
tSNE2
tSNE1

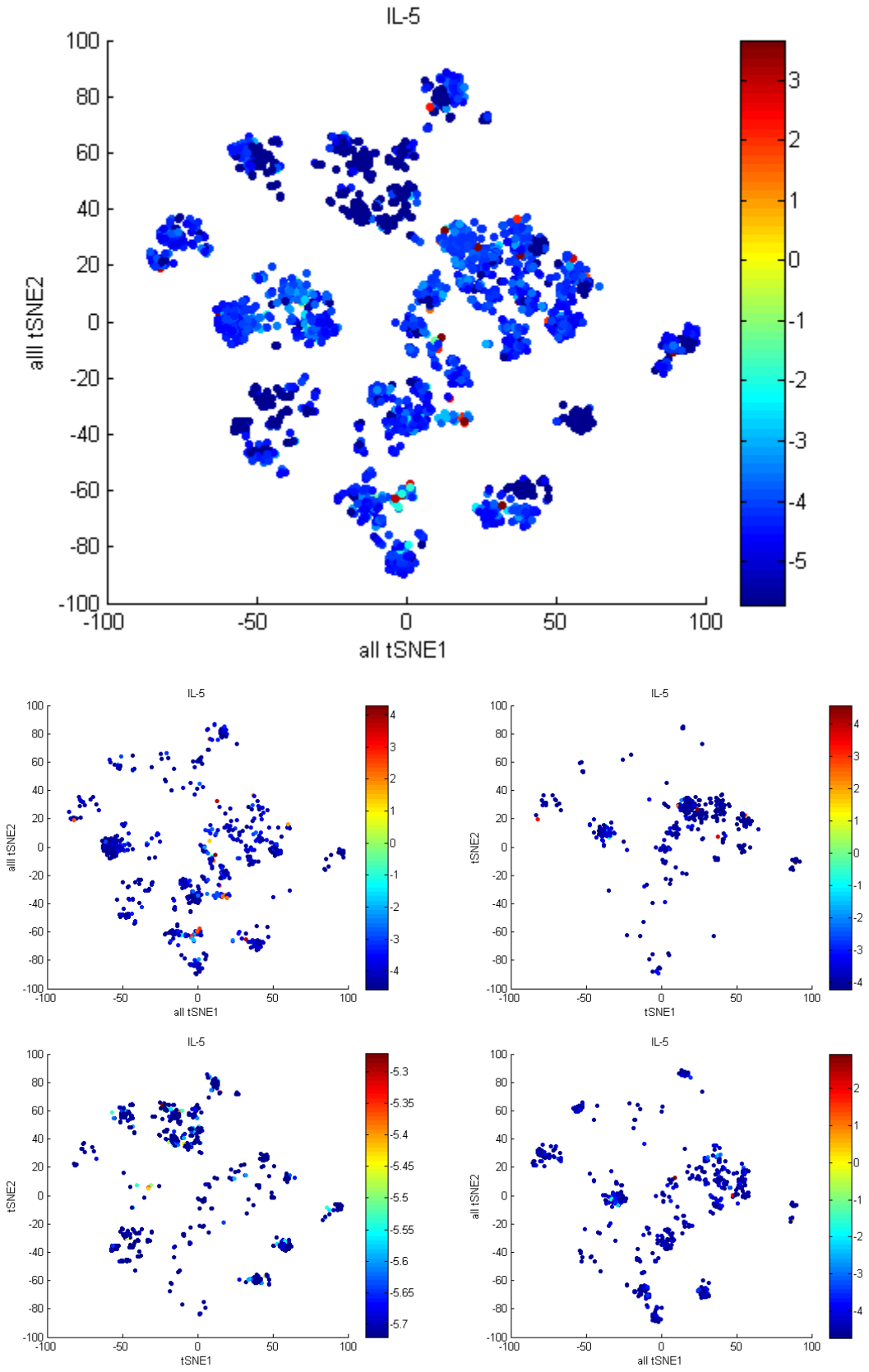
IL-5
alll tSNE2
all tSNE1
tSNE2
tSNE1

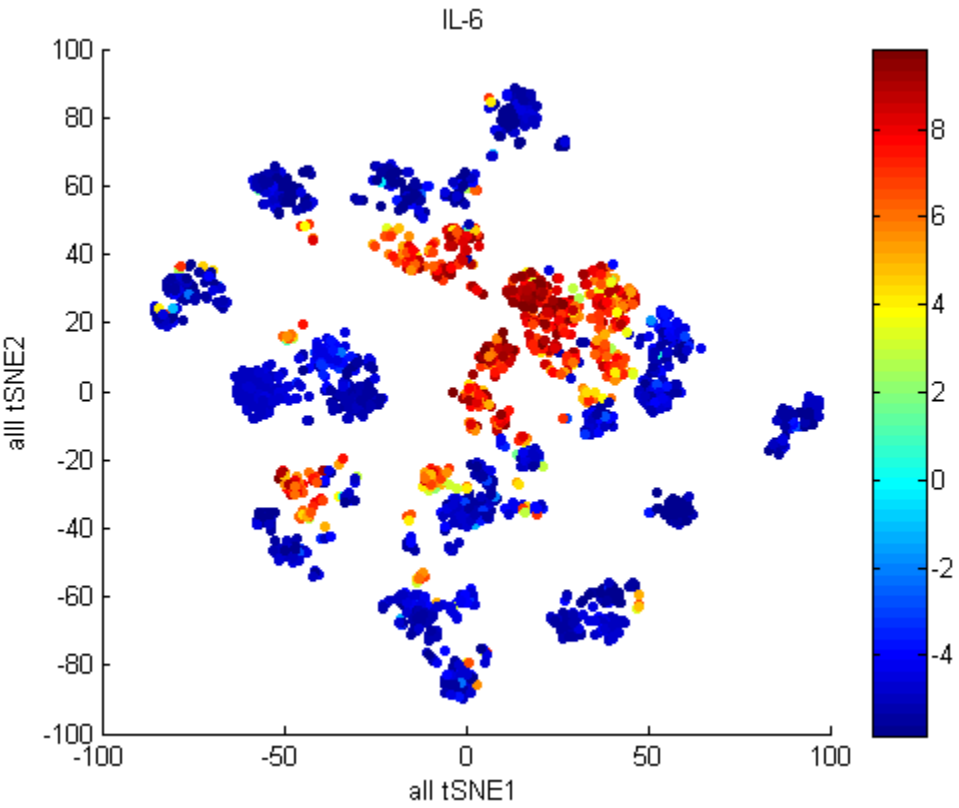
IL-6
alll tSNE2
all tSNE1

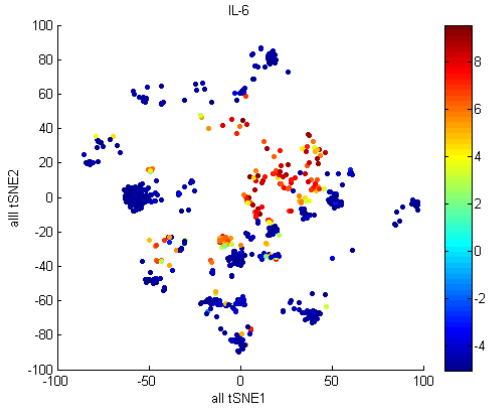
IL-6
alll tSNE2
all tSNE1

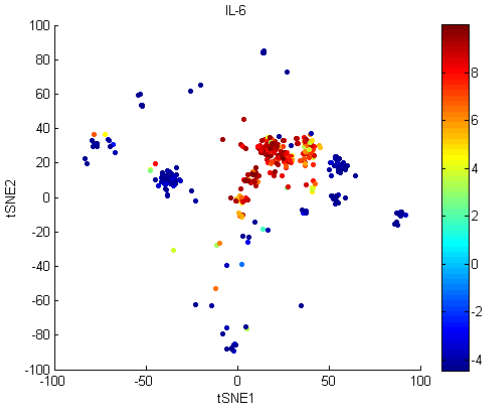
IL-6
tSNE2
tSNE1

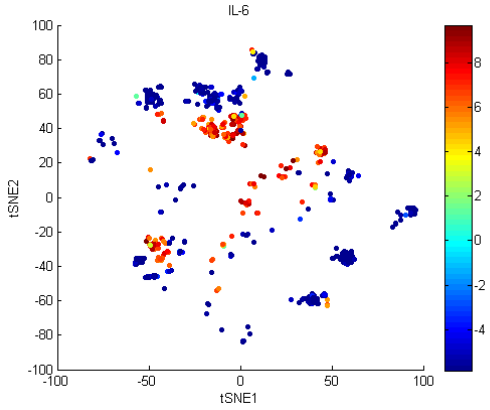
IL-6
tSNE2
tSNE1

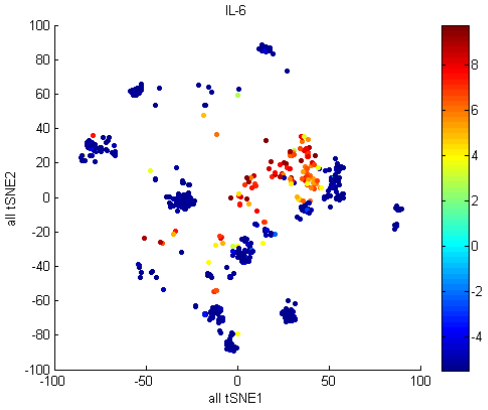
IL-6
all tSNE2
all tSNE1

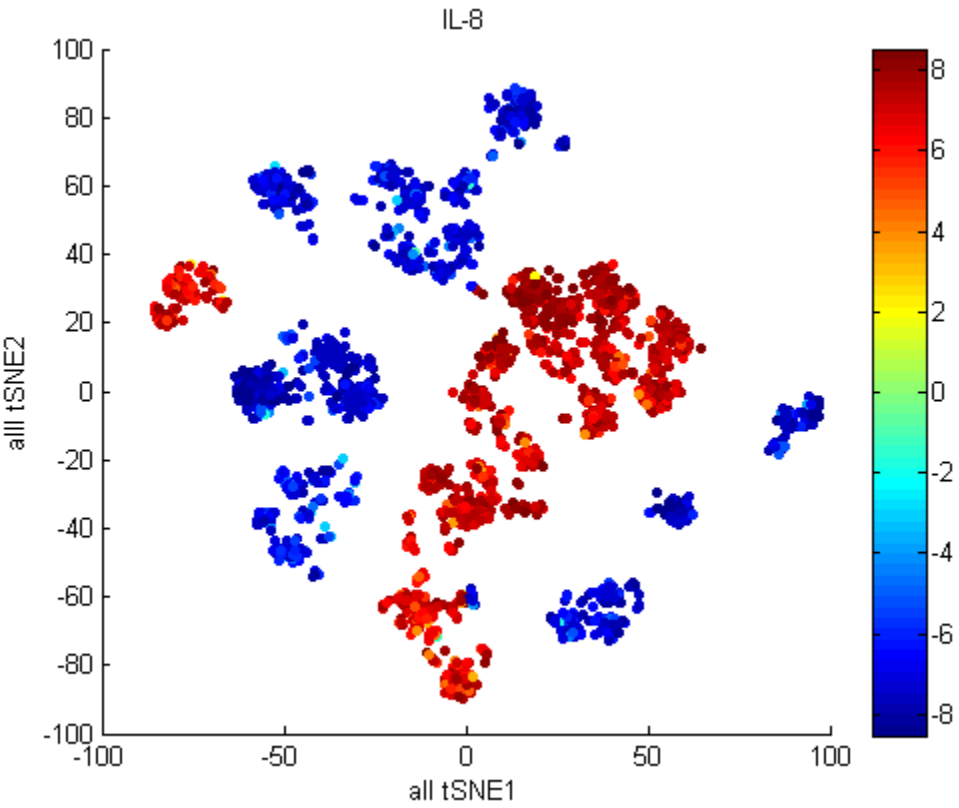
IL-8
alll tSNE2
all tSNE1

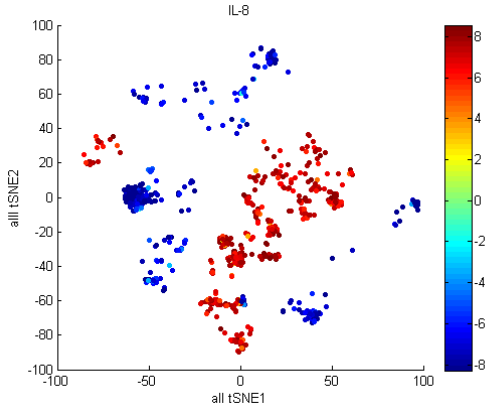
IL-8
alll tSNE2
all tSNE1

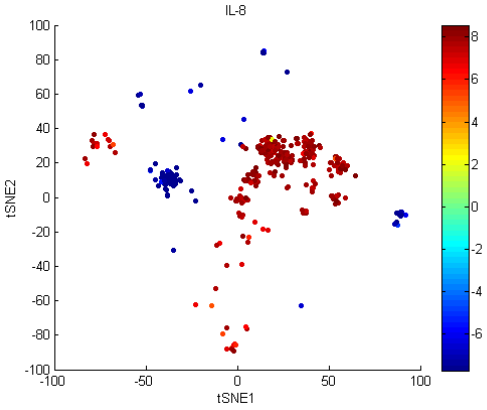
IL-8
tSNE2
tSNE1

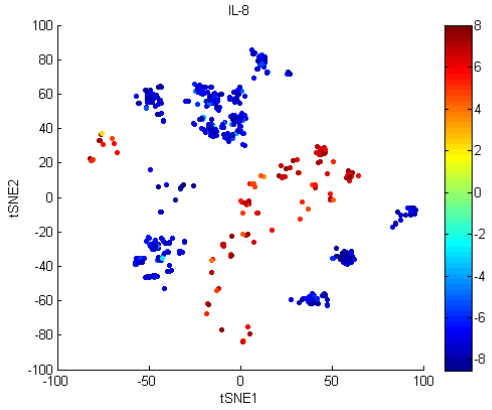
IL-8
tSNE2
tSNE1

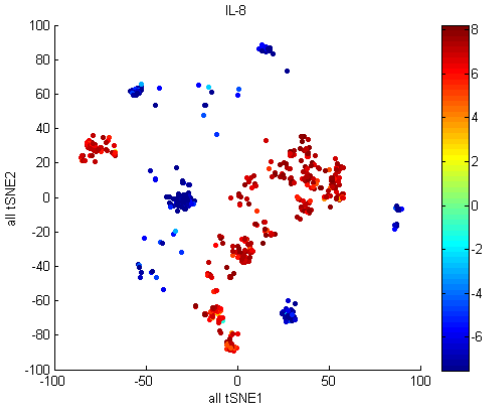
IL-8
all tSNE2
all tSNE1

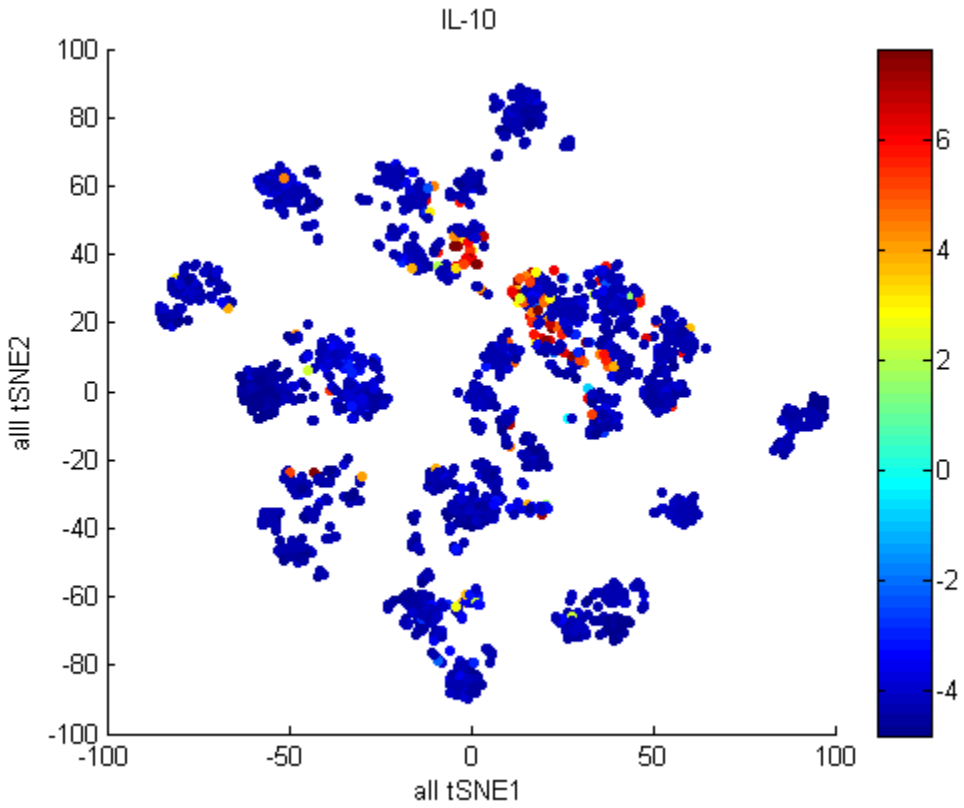
IL-10
alll tSNE2
all tSNE1

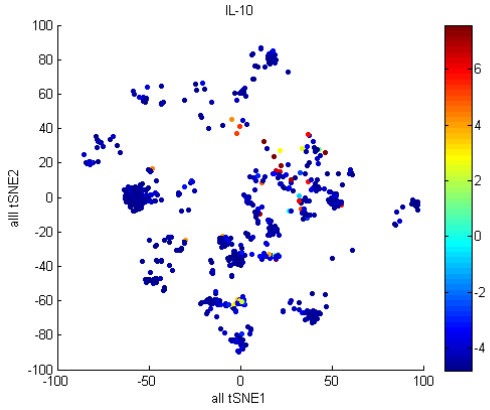
IL-10
alll tSNE2
all tSNE1

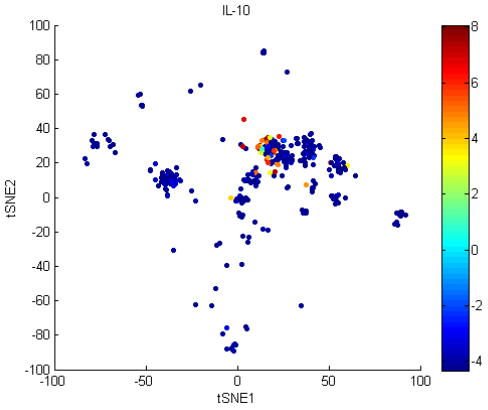
IL-10
tSNE2
tSNE1

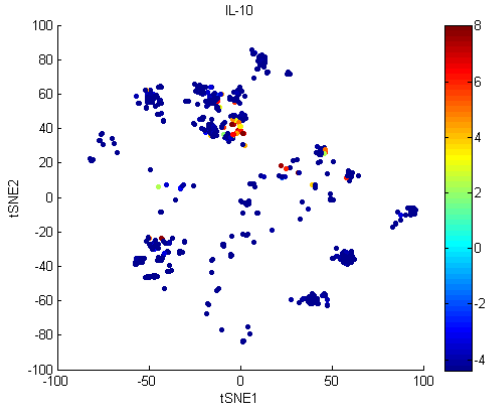
IL-10
tSNE2
tSNE1

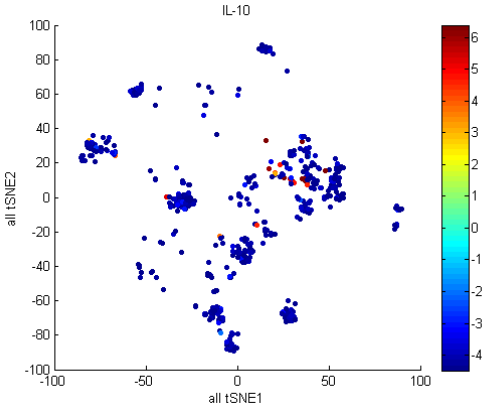
IL-10
all tSNE2
all tSNE1

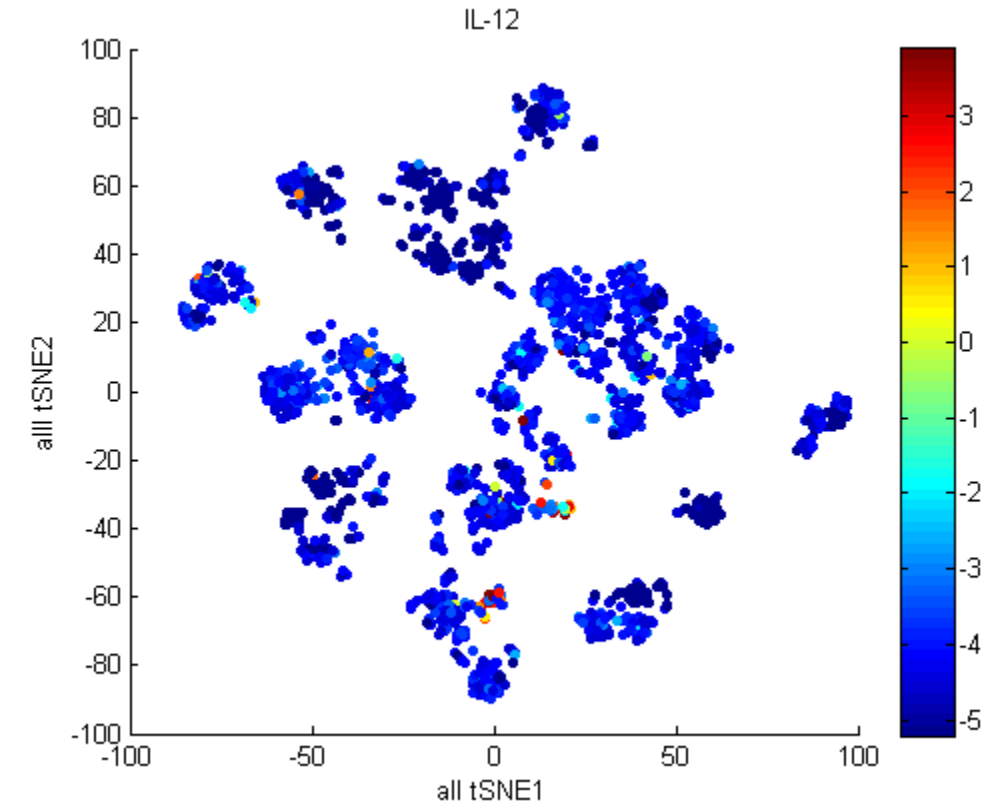
IL-12
alll tSNE2
all tSNE1

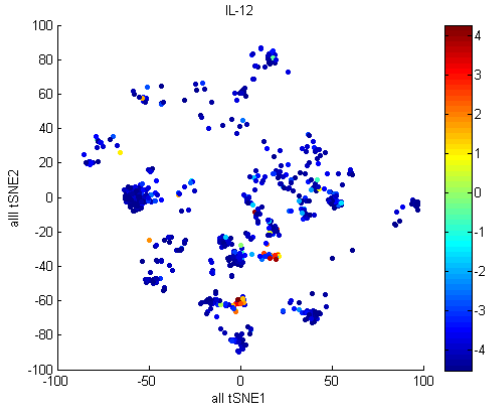
IL-12
alll tSNE2
all tSNE1

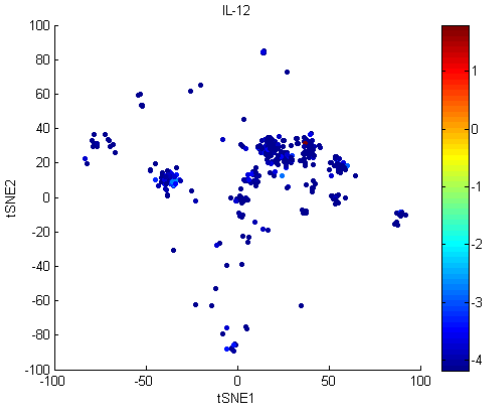
IL-12
tSNE2
tSNE1

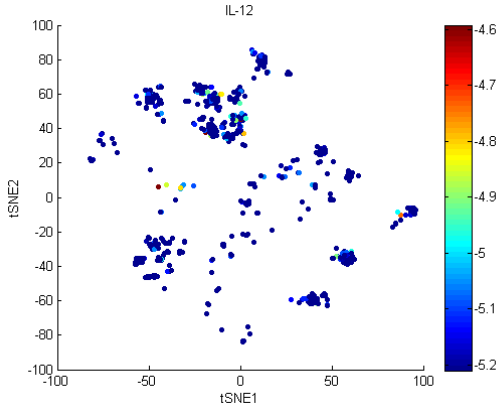
IL-12
tSNE2
tSNE1

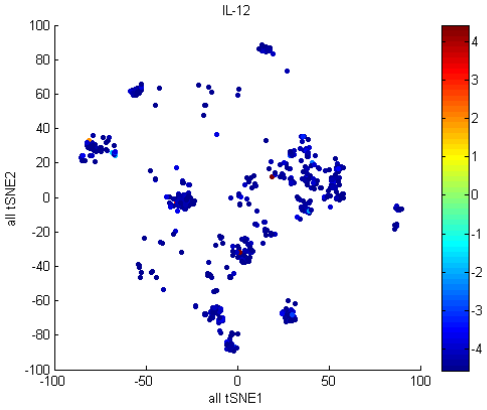
IL-12
all tSNE2
all tSNE1

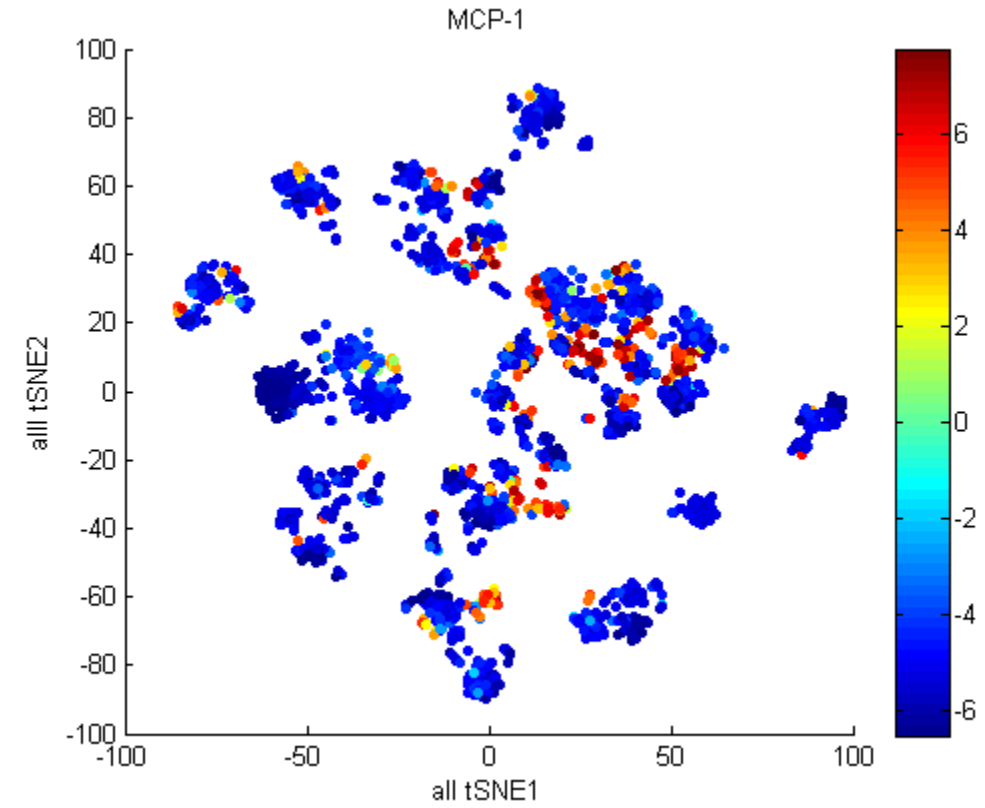
MCP-1
alll tSNE2
all tSNE1

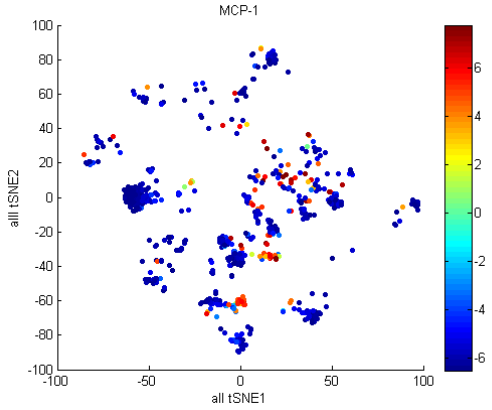
MCP-1
alll tSNE2
all tSNE1

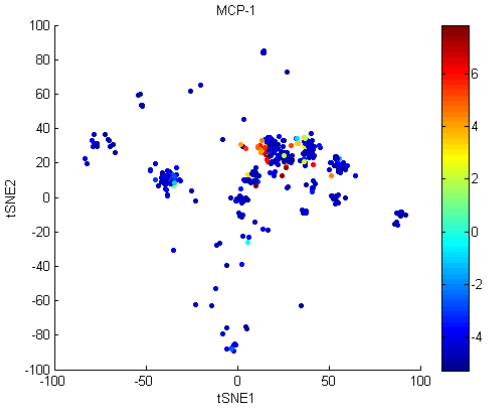
MCP-1
tSNE2
tSNE1

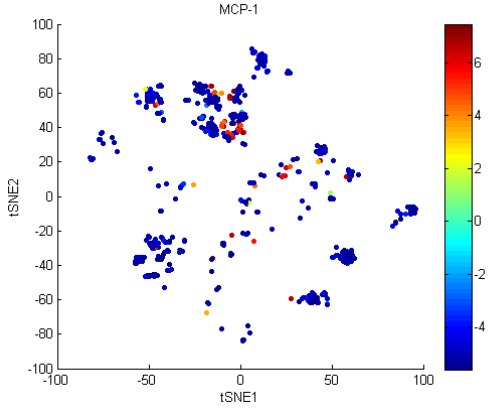
MCP-1
tSNE2
tSNE1

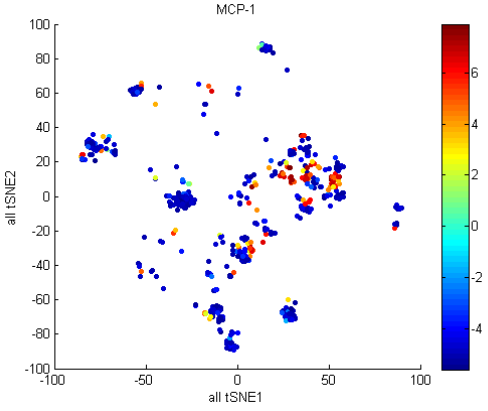
MCP-1
all tSNE2
all tSNE1

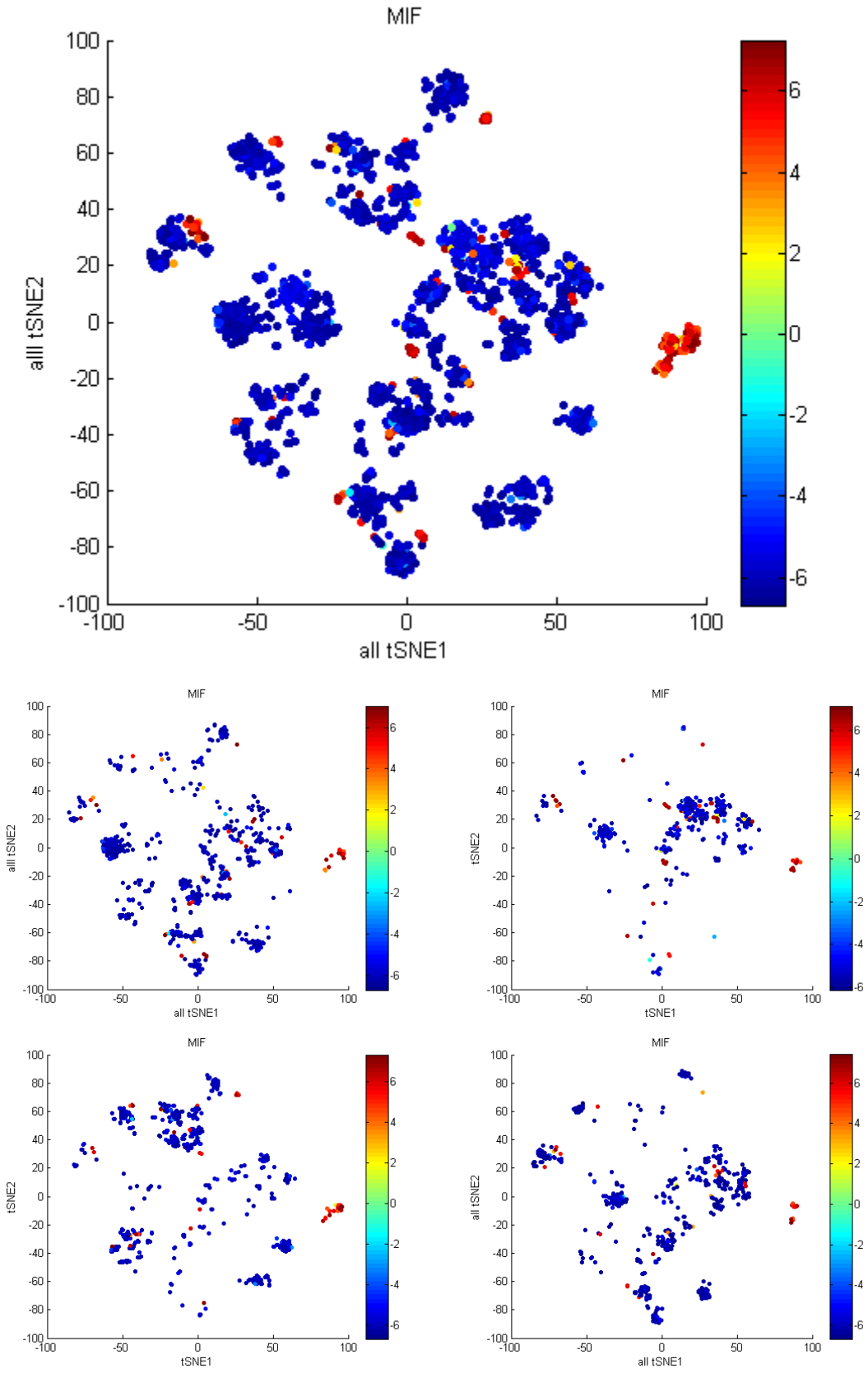
MIF
alll tSNE2
all tSNE1
tSNE2
tSNE1

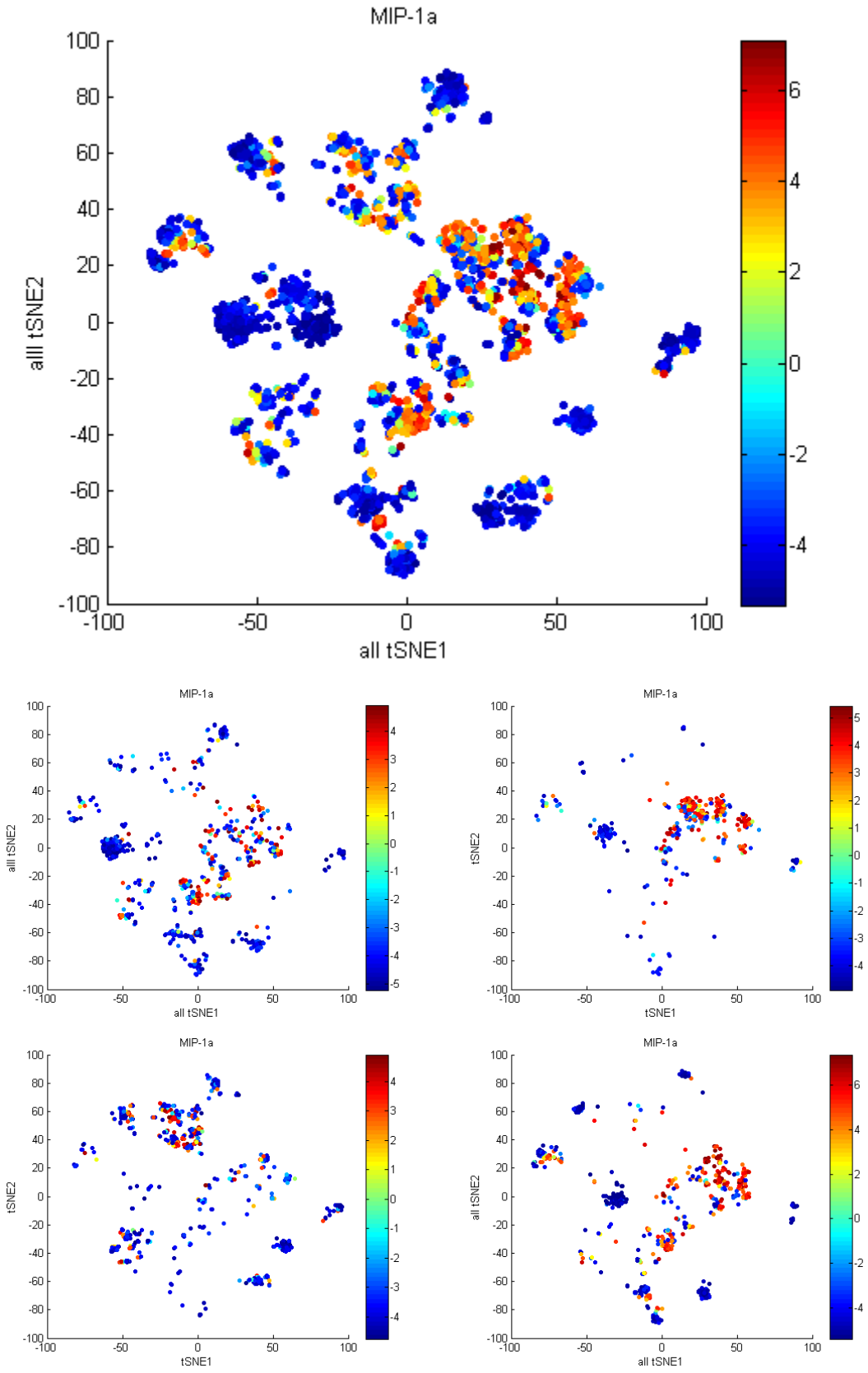
MIP-1a
alll tSNE2
all tSNE1
tSNE2
tSNE1

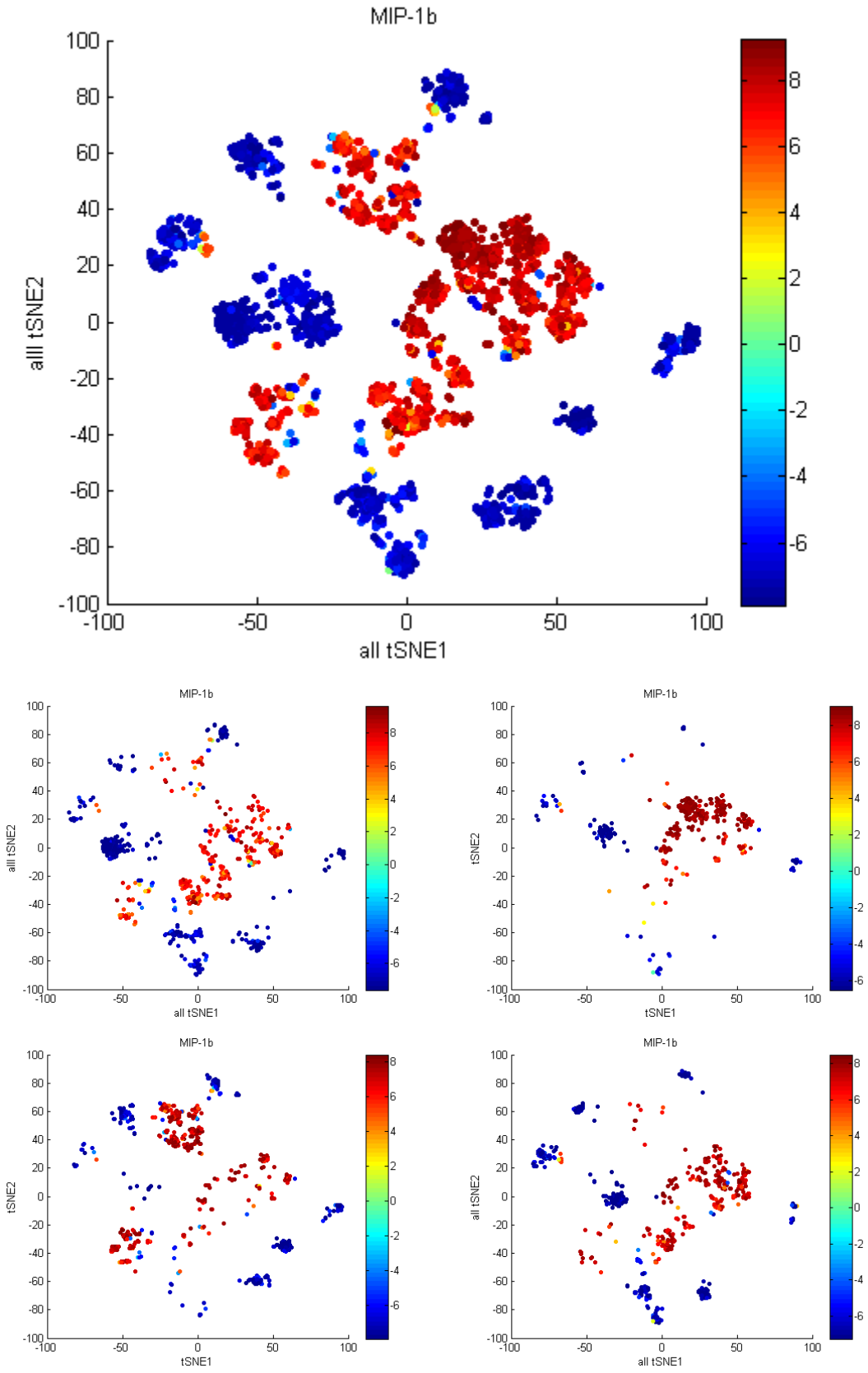
MIP-1b
alll tSNE2
all tSNE1
tSNE2
tSNE1

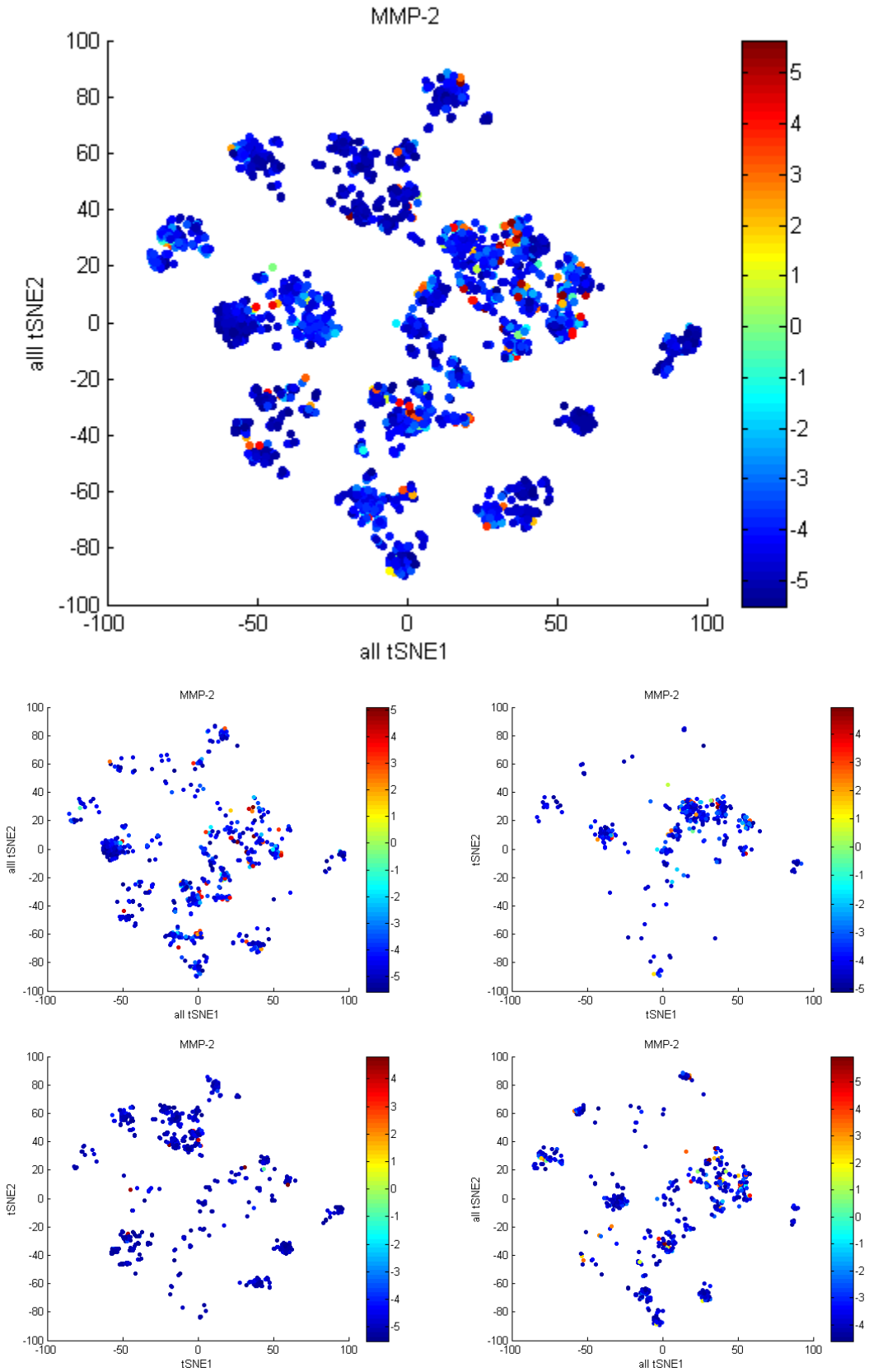
MMP-2
alll tSNE2
all tSNE1
MMP-2
alll tSNE2
all tSNE1
MMP-2
tSNE2
tSNE1
MMP-2
tSNE2
tSNE1
MMP-2
all tSNE2
all tSNE1

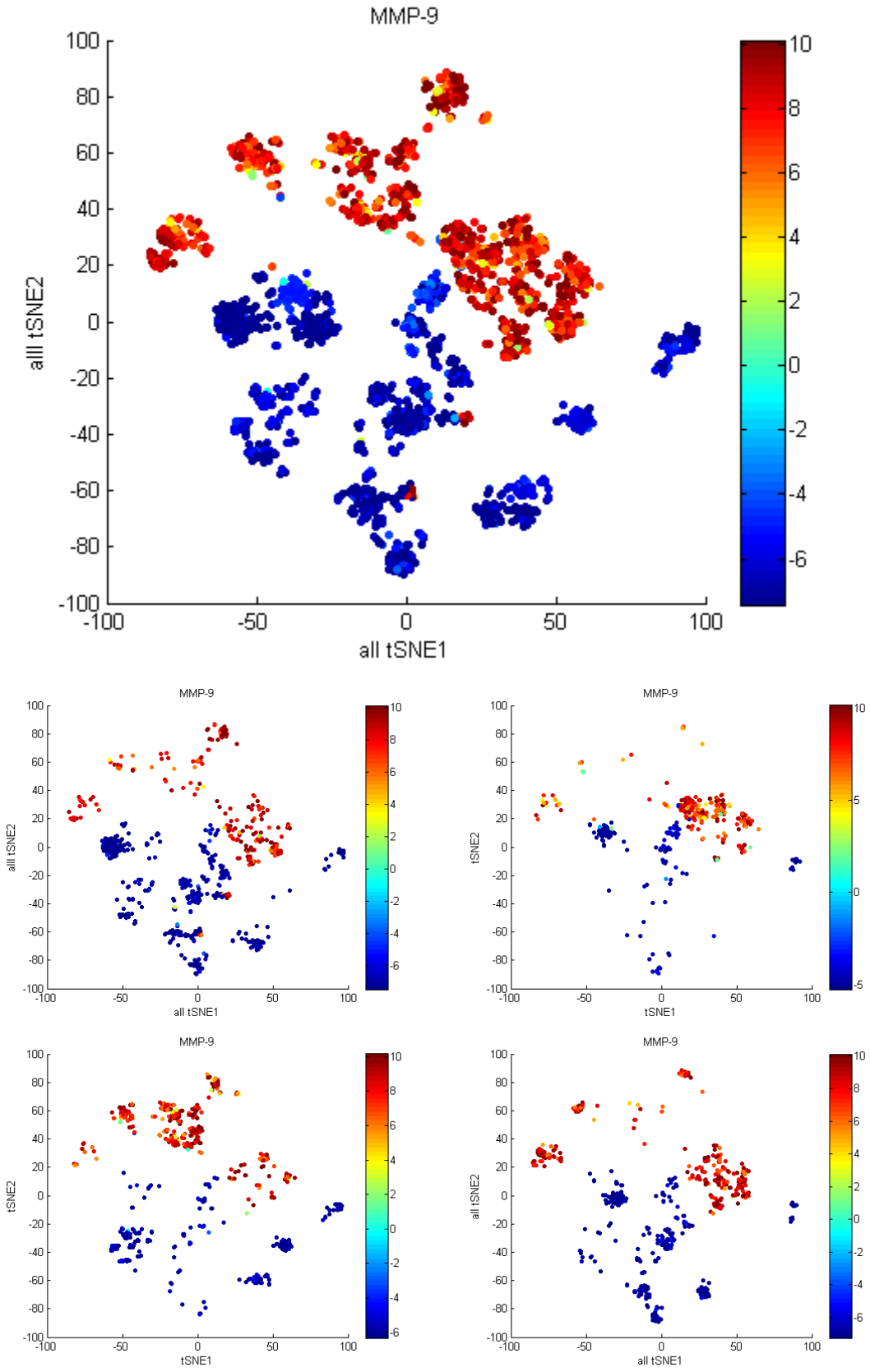
MMP-9
alll tSNE2
all tSNE1
tSNE2
tSNE1

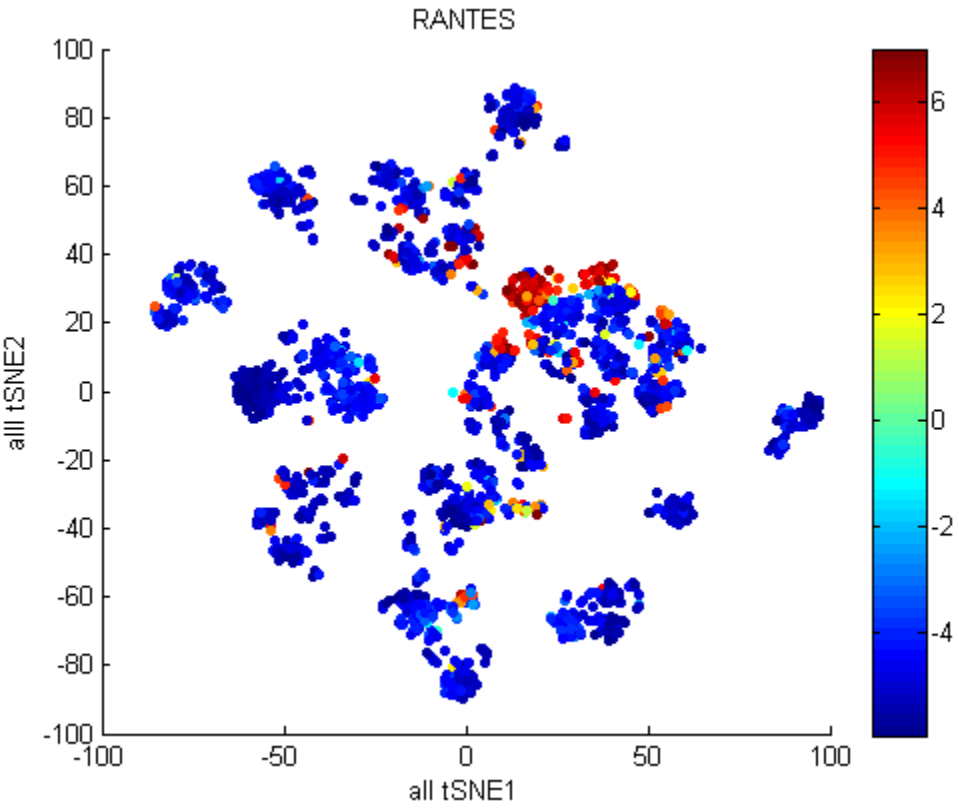
RANTES
alll tSNE2
all tSNE1

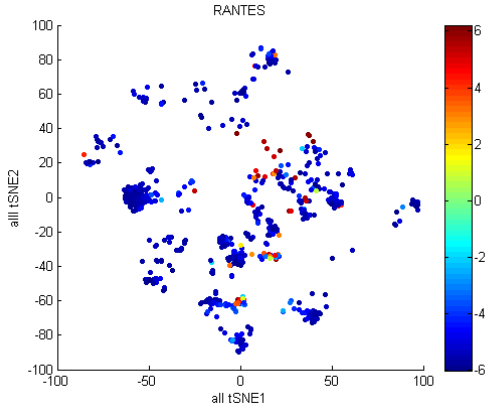
RANTES
alll tSNE2
all tSNE1

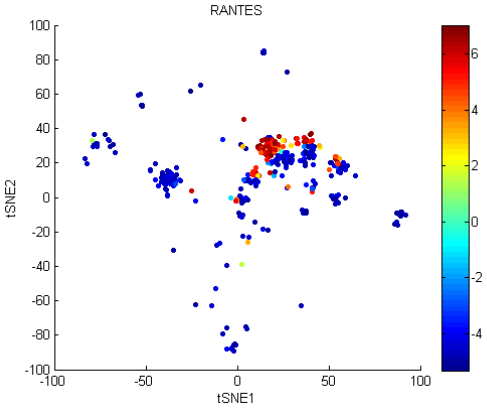
RANTES
tSNE2
tSNE1

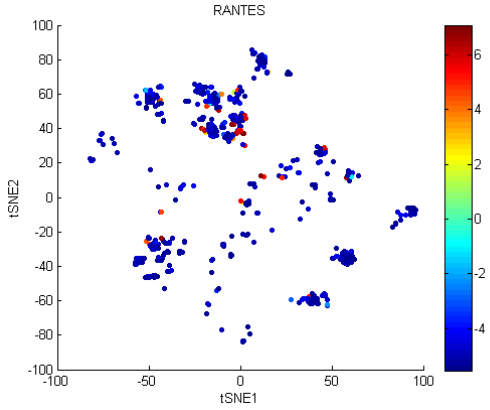
RANTES
tSNE2
tSNE1

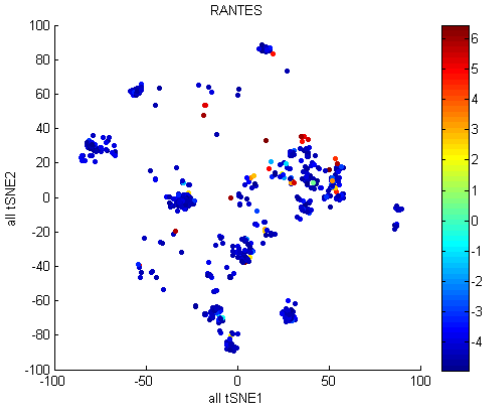
RANTES
all tSNE2
all tSNE1

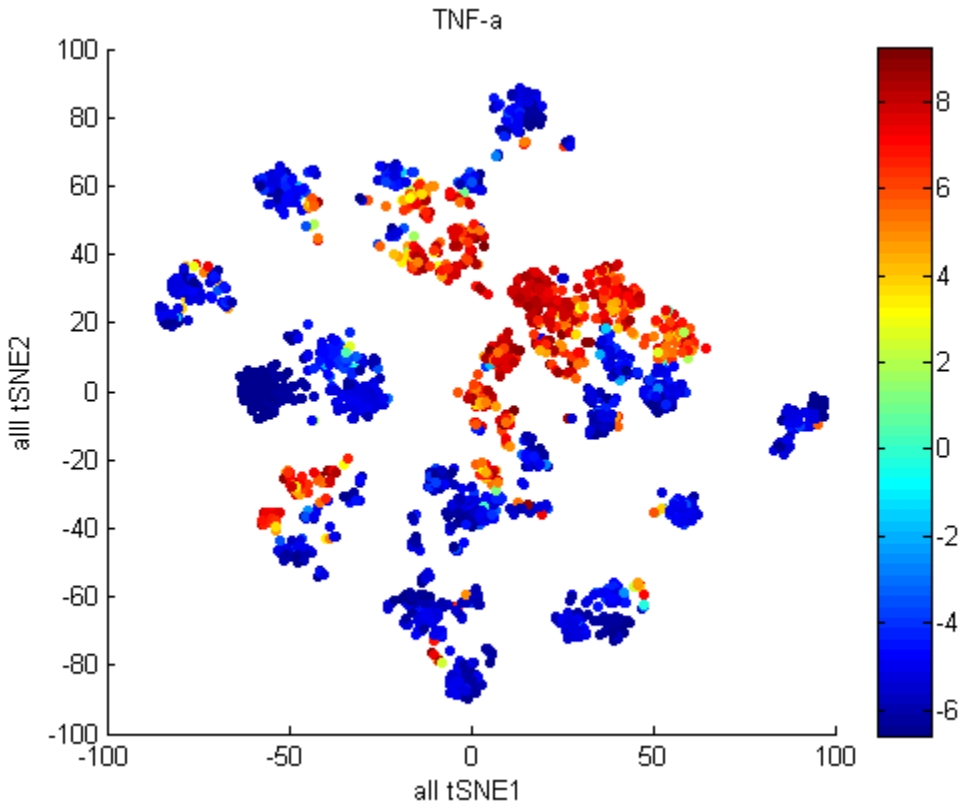
TNF-a
alll tSNE2
all tSNE1

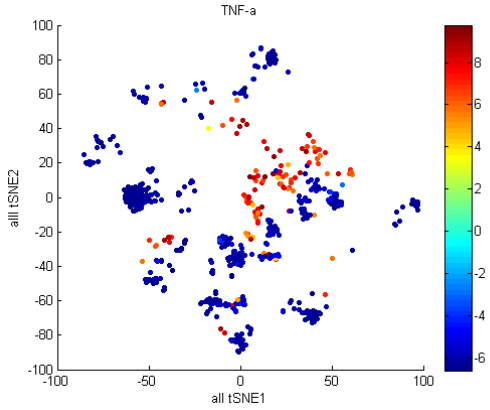
TNF-a
alll tSNE2
all tSNE1

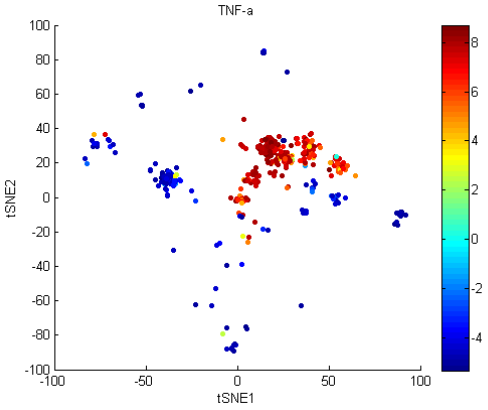
TNF-a
tSNE2
tSNE1

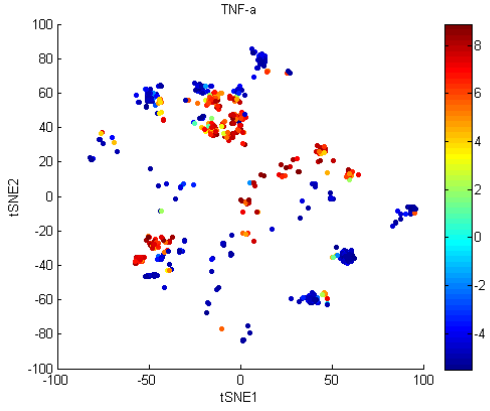
TNF-a
tSNE2
tSNE1

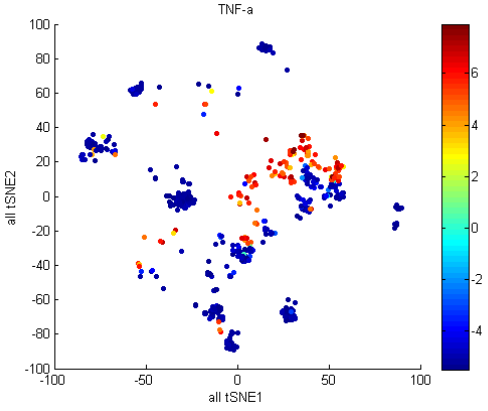
TNF-a
all tSNE2
all tSNE1

Fig. S22. Protein distribution in the viSNE maps for primary macrophages derived from a healthy donor. Cytokine functions in all primary macrophage subpopulations identified by the viSNE analysis. U937 derived macrophage under the stimulation of different TLR ligands (basal, TLR4 by LPS, TLR2 by PAM3, TLR3 by poly IC).

Table S1: Summary of antibodies (name, clone, company, catalog) used in this study (most are monoclonal antibodies).

Protein	Capture antibody Isotype/clone/vendor/catalog	Detection antibody Isotype/clone/vendor /catalog
IL-1a	Mouse IgG2A /4414/RD/MAB200	Mouse IgG1, κ /364-3B3-14/Biolegend/500104
IL-1b	Mouse IgG1 /JK1B-1/Biolegend/508202	Mouse IgG2b, κ /JK1B-2/Biolegend/508304
IL-3	Mouse IgG1 /653A10B1/Invitrogen/ AHC0832	Rat IgG1, κ /BVD8-3G11/Biolegend/500502
IL-4	Mouse IgG1, κ /8D4-8/Biolegend/ 500702	Rat IgG1, κ /MP4-25D2/Biolegend/ 500802
IL-5	Rat IgG2a, κ/JES1-39D10/Biolegend/500902	Rat IgG2a, κ /JES1-5A10/Biolegend/ 501006
IL-6	Rat IgG2a, κ /MQ2-39C3/Biolegend/501204	Rat IgG1, κ /MQ2-13A5/Biolegend/ 501102
IL-7	Rat IgG2a, κ /BVD10-11C10/Biolegend/506604	Rat IgG1, κ /BVD10-40F6/Biolegend/501302
IL-8	Mouse IgG1, κ /H8A5/Biolegend/511502	Mouse IgG1, κ /E8N1/Biolegend/ 511402
IL-10	Rat IgG2a, κ/JES3-12G8/Biolegend/ 501504	Rat IgG1, κ /JES3-9D7/Biolegend/ 501402
IL-12(p70)	Mouse IgG1/24945/RD/MAB611	Rat IgG1, κ /7B12/Biolegend/511002
IL-13	Mouse IgG1/32116/RD/MAB213	Rat IgG1, κ /JES10-5A2/Biolegend/ 501902
IL-15	Mouse IgG/RD duoset capture antibody/DY247	Mouse IgG1/AM00959PU-N/Acris/AM00959PU-N
IL-1RA	Mouse IgG1 /JK1RA-1/Biolegend/ 509902	Mouse IgG/RD duoset Capture antibody/DY280
MIF	Mouse IgG1 Kappa/2A10-4D3/Abnova/H00004282-M01	Mouse IgG1 Kappa/2A10-4D3/Abnova/H00004282-M01
IL-17A	Mouse IgG2a, κ /BL127/Biolegend/512603	Mouse IgG1, κ/BL23/Biolegend/512702
MCP-1	Mouse IgG1, κ /5D3-F7/Biolegend/502607	Armenian Hamster IgG /2H5/Biolegend/ 505902
Rantes	Mouse IgG2b kappa/VL1/Invitrogen/AHC1052	Mouse IgG1 /21418/RD/MAB678
TNF-a	Mouse IgG1, κ /Mab11/Biolegend /502902	Mouse IgG1, κ /MAb1/Biolegend/502802
TNF-b	Mouse IgG2A /5807/RD/MAB621	Mouse IgG1, κ /359-238-8/Biolegend/ 503002
IL-22	Rat IgG2a, kappaIL22JOP/Ebioscience/16-7222-85	Mouse IgG1 /142928/RD/MAB7821
MIP-1b	Mouse IgG1 kappa/A174E 18A7/Invitrogen/AHC6114	Mouse IgG2B /24006/RD/MAB271
SCF	Mouse IgG1 /J231/Peprotech/500-M44	Mouse IgG1/13302/RD/MAB655
M-CSF	Mouse IgG2b/AM09180PU-N/Acris/AM09180PU-N	Mouse IgG2A/ 21113/RD/MAB616
EGF	Mouse IgG1/AM09146PU-N/Acris/AM09146PU-N	Mouse IgG1 /10827/RD/MAB636
HGF	Mouse IgG1 /SBF5 C1.7/Novus/NB100-2696	Mouse IgG1 /24516/RD/MAB694
NGF-b	Mouse IgG1, κ /JKhNGF-1/biolegend/509602	Mouse IgG1, κ /JKmNGF-1/Biolegend/ 509702

PDGF	Rabbit IgG/ polyclonal/Acris/PP1061P2	Mouse IgG1 /108128/RD/MAB1739
VEGF	Mouse IgG1/A183C/Invitrogen/ AHG0114	Mouse IgG2B/26503/RD/MAB293
IL-2	Mouse IgG2A /5355/RD/MAB602	Goat IgG /RD duoset detection antibody/DY202
MIP-1a	Mouse IgG1/14D7 1G7/Invitrogen/AHC6034	Goat IgG /RD duoset detection antibody/DY270
TGF-a	Goat IgG /RD duoset capture antibody/DY239	Goat IgG /RD duoset detection antibody/ DY239
TGF-b	BD 559119	BD 559119
G-CSF	Mouse IgG1/3316/RD/MAB214	Goat IgG /polyclonal/RD/BAF214
IFN-g	Mouse IgG1, κ /MD-1/Biolegend/507502	Mouse IgG1, kappa/4S.B3/ebioscience/13-7319-85
GMCSF	Rat IgG2a, κ /BVD2-23B6/Biolegend/502202	Rat IgG2a, κ /BVD2-21C11/Biolegend/502304
IL-9	Ebioscience Ready sets go	Ebioscience Ready sets go
IL-23	Ebioscience Ready sets go	Ebioscience Ready sets go
MMP-2	Mouse IgG/RD duoset capture antibody/DY902	Mouse IgG/RD duoset detection antibody/DY902
MMP-9	Mouse IgG1 /36020/RD/MAB936	Goat IgG /polyclonal/RD/BAF911
IL-27	Ebioscience Ready sets go	Ebioscience Ready sets go
IL-29	Ebioscience Ready sets go	Ebioscience Ready sets go
TSLP	Ebioscience Ready sets go	Ebioscience Ready sets go
BSA -488 conjugated	488 conjugated BSA	
BSA-532 conjugated	532 conjugated BSA	
BSA-635 conjugated	635 conjugated BSA	

Table S2: List of all proteins(full name and their functions in human physiology) incorporated in the microchip assay platform.

Protein	Full name	Function
IL-1a	Interleukin-1 alpha	Inflammation, as well as the promotion of fever and sepsis
IL-1b	Interleukin-1 beta	Cell proliferation, differentiation, and apoptosis.
IL-3	Interleukin 3	Improve the body's natural response to disease
IL-4	Interleukin 4	Key regulator in humoral and adaptive immunity
IL-5	Interleukin 5	Stimulates B cell growth and increases immunoglobulin secretion

IL-6	Interleukin 6	Both a pro-inflammatory cytokine and an anti-inflammatory myokine
IL-7	Interleukin 7	T cell maturation
IL-8	Interleukin 8	Chemotaxis
IL-10	Interleukin 10	Inhibit synthesis of pro-inflammatory cytokine
IL-12(p70)	Interleukin 12 active heterodimer	Stimulate the growth and function of T cells
IL-13	Interleukin 13	Proliferation of natural killer cells
IL-15	Interleukin 15	Regulates T and natural killer (NK) cell activation and proliferation
IL-1RA	Interleukin-1 receptor antagonist	Modulates a variety of interleukin 1 related immune and inflammatory responses.
MIF	Macrophage migration inhibitory factor	Important regulator of innate immunity /Macrophage function
IL-17A	Interleukin 17A	Regulates the activities of NF-kappaB and mitogen-activated protein kinases
MCP-1	Monocyte chemotactic protein 1	Recruit monocytes, memory T cells, and dendritic cells to the sites of inflammation
Rantes	Chemokine (C-C motif) ligand 5	Chemotaxis
TNF-a	Tumor necrosis factor alpha	Acute phase reaction
TNF-b	Tumor Necrosis Factor Beta	Acute phase reaction
IL-22	Interleukin 22	Potent mediators of cellular inflammatory responses
MIP-1b	Macrophage inflammatory protein-1β	Chemoattractant for a variety of immune cells
SCF	Stem Cell Factor	Hematopoiesis (formation of blood cells), spermatogenesis, and melanogenesis
M-CSF	Macrophage colony-stimulating factor	Proliferation, differentiation, and survival of monocytes, macrophages, and bone marrow progenitor cells.
EGF	Epidermal growth factor	Cell growth, proliferation, differentiation
HGF	Hepatocyte growth factor	Mitogenesis, cell motility, matrix invasion
NGF-b	Nerve growth factor	Important for the growth, maintenance, and survival of certain target neurons
PDGF	Platelet-derived growth factor	Cell proliferation, cell migration, angiogenesis
VEGF	Vascular endothelial growth factor	Vasculogenesis, angiogenesis
IL-2	Interleukin 2	Growth and function of T cells
MIP-1a	Macrophage inflammatory protein-1α	Recruitment and activation of polymorphonuclear leukocytes
TGF-a	Transforming growth factor alpha	Epithelial development, neural cell proliferation

TGF-b	Transforming growth factor beta	Proliferation, cellular differentiation
G-CSF	Granulocyte colony-stimulating factor	Stimulates the survival, proliferation, differentiation, and function of neutrophil precursors and mature neutrophils
IFN-g	Interferon gamma	Macrophage activation
GMCSF	Granulocyte-macrophage colony-stimulating factor	Granulocyte and monocyte production
IL-9	Interleukin 9	Regulator of a variety of hematopoietic cells
IL-23	Interleukin 23	Inflammatory response against infection
MMP-2	Matrix metalloproteinase-2	Endometrial menstrual breakdown, regulation of vascularization and the inflammatory response
MMP-9	Matrix metallopeptidase 9	Breakdown of extracellular matrix in normal physiological processes
IL-27	Interleukin 27	Regulating the activity of B- and T-lymphocytes
IL-29	Interleukin 29	Defenses against microbes
TSLP	Thymic stromal lymphopoietin	Maturation of T cell populations

Table S3: Statistic analysis of protein signal measured in U937-derived human macrophage cells (basal vs LPS stimulation).

Protein	Detectable above background*	Detectable regulation by LPS**
EGF	Not detected	---
G-CSF	Low confidence	No difference
GMCSF	High confidence	Up-regulated
HGF	High confidence	Up-regulated
IFN-g	High confidence	No difference
IL-10	High confidence	Up-regulated
IL-12	Low confidence	No difference
IL-13	Low confidence	No difference
IL-15	Not detected	---
IL-17A	Not detected	---
IL-1RA	High confidence	No difference
IL-1a	Not detected	No difference
IL-1b	High confidence	No difference
IL-2	Not detected	---
IL-22	High confidence	No difference
IL-23	Low confidence	No difference
IL-27	Low confidence	No difference
IL-29	High confidence	No difference
IL-3	High confidence	No difference
IL-4	Not detected	---
IL-5	High confidence	No difference

IL-6	High confidence	Up-regulated
IL-7	Not detected	---
IL-8	High confidence	Up-regulated
IL-9	High confidence	No difference
MCP-1	High confidence	No difference
MCSF	Not detected	---
MIF	High confidence	No difference
MIP-1a	High confidence	Up-regulated
MIP-1b	High confidence	Up-regulated
MMP-2	Low confidence	No difference
MMP-9	High confidence	No difference
NGF-b	Not detected	---
PDGF	High confidence	No difference
RANTES	High confidence	No difference
SCF	High confidence	Up-regulated
TGF-a	High confidence	No difference
TGF-b	Low confidence	No difference
TNF-a	High confidence	Up-regulated
TNF-b	Not detected	---
TSLP	High confidence	Up-regulated
VEGF	High confidence	No difference

*Explanation of classifications:

High confidence: 3 out of 3 data sets of single cell intensities

Low confidence: 2 out of 3 data sets of single cell intensities

are statistically different to background intensities. Evaluation was done using bootstrapping and Wilcoxon-Mann-Whitney test with $\alpha = 0.0012$.

**Up-regulated: Intensities of up-regulated cytokines are significantly higher in LPS treated single cells as compared to non-treated single cells. Evaluation was performed using bootstrapping and Wilcoxon-Mann-Whitney test with $\alpha = 0.0012$.